62-1-3
NOX -3

NOLTR 61-75

THE PROPERTIES OF TiNi AND ASSOCIATED PHASES (U)

3 AUGUST 1961

NOL
UNITED STATES NAVAL ORDNANCE LABORATORY, WHITE OAK, MARYLAND

NOLTR 61-75

NOLTR 61-75

THE PROPERTIES OF TiNi AND ASSOCIATED PHASES

by

W. J. Buehler and R. C. Wiley

ABSTRACT: A new class of alloys based on the ductile intermetallic compound TiNi and associated phases Ti_2Ni, $TiNi_3$ was investigated. These alloys, referred to as the "Nitinol" series, are non-magnetic, corrosion resistant and hardenable (by suitable composition and treatment) up to 62 R_c.

The most phase-pure TiNi composition was found at about 54.5 percent nickel, by weight. This composition (body-centered cubic crystal structure) possessed good room temperature ductility and a moderately high melting point, about 1300°C. The room temperature mechanical properties of the pure TiNi phase (hot worked) indicated a maximum ductility of 15 percent tensile elongation and up to 28 ft-lbs impact strength. An ultimate tensile strength of 124,000 psi was also measured.

Hot hardness measurements revealed a secondary hardening peak, in the rapid cooled TiNi alloys, between 427-482°C. ~~Based upon these data~~ TiNi appears to have usable strength up to about 649°C.

TiNi-base alloys, with excess nickel added, were capable of being hardened by quenching. Quenched hardnesses as high as 62 R_c were obtained. They showed a marked improvement in hot hardness over the predominantly phase-pure TiNi at temperatures up to 482°C.

Investigations into the TiNi alloy containing 54.5 w/o Ni revealed some unusual mechanical vibration damping properties. At room temperature the alloy had a very high damping capacity, upon heating to temperatures slightly in excess of room temperature the damping capacity markedly decreases.

Magnetic susceptibility measurements over a wide temperature range showed the material to be paramagnetic with a permeability approaching unity (1.002).

U. S. NAVAL ORDNANCE LABORATORY
White Oak, Silver Spring, Maryland

This material offers a potential solution for many troublesome non-magnetic material applications where low permeability, strength, hardness, fabricability, and corrosion and abrasion resistance are a problem. It appears particularly useful as a material for non-magnetic tools in mine disposal applications and in various components of magnetometers, mine laying and servicing craft where the above characteristics are required. Its corrosion and abrasion resistance suggests its use in food and chemical processing industries. The improved low temperature (-80°C) impact strength values (43-79 percent increase over room temperature)suggest the use of TiNi-base alloys as cryogenic materials. The marked changes in damping characteristics with temperature indicates a possible application of TiNi in temperature sensing devices.

PUBLISHED AUGUST 1961

NOLTR 61-75 3 August 1961

This report describes the mechanical and physical properties of the intermetallic compound TiNi and TiNi-base alloys. This system was examined as a basis from which a high temperature material could be prepared. Investigative work in this direction was performed under PR-7 - Intermetallics, BuWeps Task Intermetallic Compounds - RRMA 02009/212 1/R007 06 001, and as a non-magnetic tool material for ordnance disposal under BuWeps Task RUUO-3-E-231/212 1/F008-12-002.

W. D. COLEMAN
Captain, USN
Commander

Louis R. Maxwell
L. R. MAXWELL
By direction

CONTENTS

TABLES AND ILLUSTRATIONS

THE PROPERTIES OF TiNi AND ASSOCIATED PHASES

INTRODUCTION

An "Intermetallic Compound" is a metallic alloy material quite difficult to define. The 8th edition of the Metals Handbook[1] defines an Intermetallic Compound generally as "An intermediate phase in an alloy system, having a narrow range of homogeneity and relatively simple stoichiometric proportions, in which the nature of the atomic binding can vary from metallic to ionic." Others[2,3] have indicated that to classify intermediate phases as intermetallic compounds requires that identical kinds of atoms occupy identical points on the lattice. Further, on the point of a narrow homogeneity range, one author[3] states that in many alloy systems intermediate phases are found in which the composition varies over such a narrow range that no difference can be detected experimentally; such phases are usually called intermetallic compounds. Compounds of this latter type generally correspond with a reasonably simple whole number ratio of constituent atoms. It should be noted, however, that in a great majority of cases the formulas of intermetallic compounds do not agree with those to be expected from the normal valency principles.

In order to study intermetallic compounds for structural applications the subject investigators have adopted a slightly modified and less rigid definition of an intermetallic compound. Like Westbrook[4] this investigation considers "all intermediate phases in binary and higher order metal systems whether ordered or disordered." With this flexibility in definition systems for study were chosen where the compound exists over a range of chemical composition, such as TiNi, NiAl, TiAl, etc.

Intermetallic compound alloys have for some time been recognized to possess certain unusual physical and mechanical properties; examples are the ability of some to act as semiconductors and others to resist losing their strength at high homologous temperatures (T/Tm.p.).

During the past ten years a tremendous amount of research has been conducted on various intermetallic compounds for use as semiconductors. In this application it is important to create a near perfect covalent bond between the atoms of the two elements used. Many of the semiconducting compounds are formed by combining elements from Group III of the periodic table (three valence electrons) with elements from Group V (five valence

electrons). The resultant compound will then have an "average" of four electrons per atom, and it can be expected to have semiconducting properties.

Although many compounds maintain their strength to high homologous temperatures, extreme brittleness at room temperature has limited their structural usefulness to a role of minor strengthening constituents in a more ductile matrix metal or alloy. Because of this brittleness problem little attention was given to intermetallic compound-base materials for structural use until recent years. At this time a number of investigators[4,5,6,7,8] began looking at the structural potential of intermetallic compounds in general and NiAl in particular. The latter compound was considered seriously for application in the hot turbine section of gas turbine aircraft engines.

This present investigation was initiated because second-generation missiles and spacecraft are expected to require materials of higher strength and lighter weight capable of operating at very high temperatures. Initially the program was oriented in the direction of uncovering or developing intermetallic compounds or intermetallic compound-base materials with suitable room temperature ductility. Toward this end a binary alloy constitution investigation[9] and some preliminary alloying experiments were performed. The results of this work showed that the compound TiNi possessed unusual ductility at room temperature for a compound with a moderately high melting point. A program was then initiated to investigate the Ti-Ni alloys in the TiNi homogeneity range. As a result of this study a series of new engineering alloys based on the TiNi phase composition were uncovered showing many remarkable and unusual mechanical and physical properties as shown in Table I. The report that follows describes in detail the studies performed on TiNi and the related compounds of Ti_2Ni and $TiNi_3$.

PRIOR WORK ON TiNi COMPOUND ALLOYS

Much of the prior investigative study on Ti-Ni alloys, in the equi-atomic composition range, was concerned with determining the constitution of these alloys. The original and alternative constitution diagrams for the Ti-Ni alloys are given by Hansen[9]. The major disagreement between these diagrams occurs in the TiNi phase field. These areas of major disagreement are shown in Fig. 1.

Duwez and Taylor[10] investigated intermediate phases in alloys of titanium with iron, cobalt, and nickel. In these studies they confirmed the existence of a CsCl type cubic structure in the equi-atomic alloys,

TABLE I
SUMMARY OF PROPERTIES OF TiNi PHASE ALLOYS

PHYSICAL (55.1 w/o Ni-Ti)

Density (25°C), gr/cm^3	6.45
* Melting Point, °C	1240-1310
* Melting Point, °F	2264-2390
* Crystal Structure	Cs Cl (B.C.C.)
* Lattice Parameter, Å	3.015
Electrical Resistivity (25°C), microhm-cm	~80
Electrical Resistivity (900°C), microhm-cm	~132
Linear Coef. of Expansion (24-900°C), per °C	10.4 x 10^{-6}
Recrystallization Temperature, °C	550 - 650
Magnetic Permeability	<1.002
Magnetic Susceptibility (mass, χ , -196 to 550°C)	5.-9. x 10^{-6}

MECHANICAL

	54.5 w/o Ni	55.1 w/o Ni
Ultimate Tensile Str., psi	110,000 - 124,000	82,000 - 140,000
Yield Str., psi	40,000 - 55,000	33,000 - 81,400
Young's Modulus, psi	11.2 - 11.8 x 10^6	up to 11.8 x 10^6
Tensile Elongation, %	up to 15.5	up to 10
Reduction in Area, %	up to 16	-
Hardness, Rockwell-A	42-52	65-68
Impact Str., ft-lbs		
24°C (room temp.)	28	24
-80°C	40	43
Modulus of Rupture, psi	-	216,000
Mod. of Elas. (Trans. Bend),psi	-	11.3 x 10^6
Hot Hardness**, D.P.H.		
25°C (room temp.)	230	330
260°C	215	230
463°C	230	295
593°C	65	95
649°C	45	50

TABLE I (continued)

ENVIRONMENTAL

Oxidation Resistance (sample wt. ~ 6.5 grams)	
wt gain, in air, 10 hrs at 600°C	0.0015 grams
wt gain, in air, 10 hrs at 800°C	0.023 grams
wt gain, in air, 10 hrs at 1000°C	0.10 grams
Corrosion Resistance	
Salt spray (20% soln, 95°F, 96 hrs)	faint whitish deposit
Sea water	Nil
Normal air atmosphere	Nil
Normal handling	Nil

Ni-RICH TiNi (60 w/o Ni-Ti)

Hardness, Rockwell-C	
quenched	62
furnace cooled, from 900°C	35
from 800°C	38
from 700°C	40
from 600°C	59

* Data obtained from published literature

** Specimens rapidly cooled prior to testing

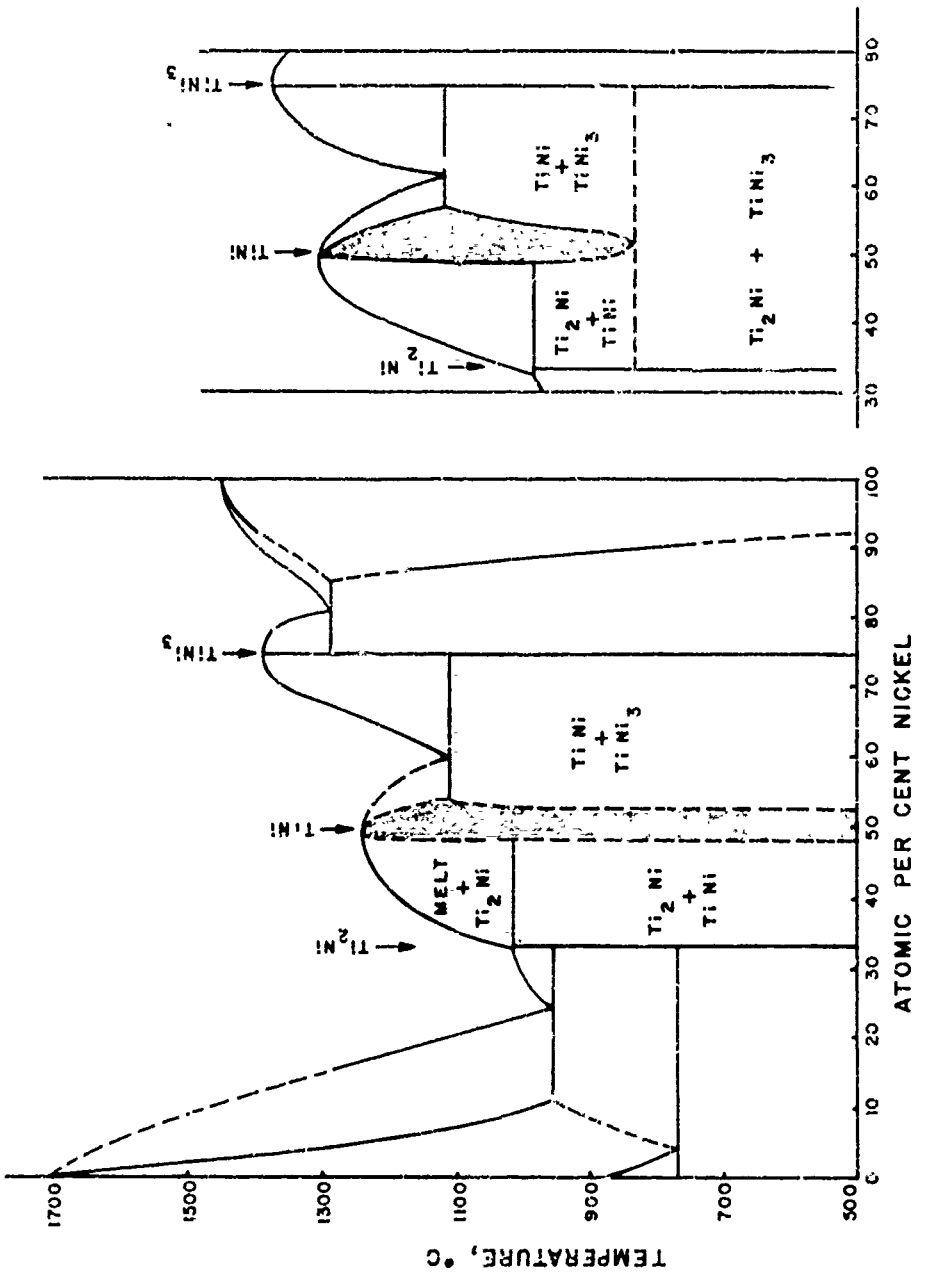

FIG. 1 TWO VERSIONS OF THE NICKEL-TITANIUM CONSTITUTION DIAGRAM

through X-ray diffraction measurements. Most significant was the discovery that prolonged heating (10 days), at both 800°C and 650°C, of powdered TiNi alloy in a sealed evacuated quartz tube resulted in the TiNi phase decomposing into Ti_2Ni and $TiNi_3$. From this, the TiNi phase was considered by Duwez and Taylor to be stable only at high temperatures, with the critical decomposition temperature being about 800°C.

Based upon X-ray diffractometer scans made on heated TiNi alloy filings, Poole and Hume-Rothery[11] were in agreement with Duwez and Taylor that TiNi was an unstable low temperature phase and would decompose into Ti_2Ni and $TiNi_3$ if heated for a prolonged period of time at about 600°C. Short-time treatments only served to yield a diffuse X-ray pattern of the CsCl type, probably due to a partially decomposed TiNi phase.

Margolin et al[12] working with arc-melted alloy buttons of the TiNi alloy composition in lieu of powdered samples were unable to detect the decomposition of the TiNi phase even when heated above and below 800°C. This contradictory finding left the ambient temperature existence and stability of the TiNi phase somewhat in doubt.

In addition to the phase equilibria work done by the above investigators, Philip and Beck[13] investigated the ordering into a CsCl structure of alloys composed of the transition elements. In addition to TiNi the equi-atomic compound alloys of TiCo and TiFe were studied by X-ray diffraction techniques. It was found that the lattice parameter of TiFe (2.976 ± 0.001 Å) was smaller than that of TiNi (3.015 ± 0.001 Å) with TiCo (2.991 ± 0.001 Å) falling between the two. In accordance with the usual atomic radii of the elements concerned, Philip and Beck expected the lattice parameter of TiNi to be smallest, with TiFe possessing the largest lattice parameter. This anomaly caused the investigators[13] to conclude that the A-B bond in TiFe is stronger than that in TiNi, with the bond strength of TiCo falling between these extremities. In connection with the above bonding behavior TiFe was outwardly hard and brittle, while the TiNi material was noticeably softer and less brittle.

Further corroboration of the ordered nature of TiNi at ambient temperatures was obtained by Pietrokowsky and Youngkin[14]. In their work they observed only one diffraction maxima (100) associated with long range order in TiNi. However, they considered the order structure evidence strong since Ti_2Ni and $TiNi_3$ do not produce constructive interference at the (100) angle of the TiNi.

Ti-Ni CONSTITUTION STUDIES

Recognizing the uncertainty existing concerning the constitution of the titanium-nickel system in the TiNi area and having found that alloys of TiNi intermetallic composition were ductile at ambient temperatures stimulated further investigation into the constitution of this system. Alloys of the TiNi composition (55.06 w/o Ni) left several unanswered questions, the main one being whether TiNi is a stable room temperature phase or does it in fact decompose into Ti_2Ni and $TiNi_3$ at temperatures below about 830°C. From preliminary work on these individual latter phases, they were found to be hard, abrasion resistant, and brittle at room temperature. Therefore, the problem to solve was whether the stoichiometric TiNi phase was ductile or whether the product produced by the coexistence of the two known hard and brittle phases of Ti_2Ni and $TiNi_3$ was in fact responsible for the ductile behavior.

With this as background a constitution investigation was begun dealing with the Ti-Ni alloys from 33 to 75 a/o Ni, with special interest focused upon the TiNi phase homogeneity range (about 48 to 52 a/o Ni). Several approaches were employed: These include X-ray diffraction, internal friction, metallography, electrical resistivity, hardness, magnetic susceptibility, etc. Since the findings of these various research studies are closely inter-related, each study will be first described as a separate entity, then the salient features of these data will be discussed as they apply to a more complete understanding of the overall Ni-Ti alloy phase equilibria picture.

1. X-ray Diffraction Studies on 50 to 60 w/o Ni-Ti Alloys

Initially, in this portion of the investigation, it was of paramount importance to determine what phase existed at room temperature for the stoichiometric TiNi composition, calculated to be 55.06 w/o Ni. To this end an arc-melted and hot swaged rod of the TiNi composition was prepared. To obtain a suitable X-ray specimen the rod was filed to produce moderately fine particles. These particles were annealed in dry argon gas at about 1000°C for 15 minutes. This heat treatment was designed to eliminate stresses introduced during filing. The above sampling technique is similar to that used by Philip and Beck[13] and Poole and Hume-Rothery[11]. X-ray diffractometer scans were made at room temperature as described in detail in Section I of the Appendix. The resultant X-ray pattern revealed an almost completely two-phase material containing Ti_2Ni and $TiNi_3$ in about the propor proportions to satisfy the alternative phase diagram given in Fig. 1.

Recognising the adverse effects of the filing operation upon the above X-ray results, there was still doubt about the identity of the true room temperature phase. Subsequent metallography (Figs. 2 and 3) and mechanical property studies cast further doubt on the validity of powder specimen X-ray results for this alloy.

A series of new 15 gram Ni-Ti alloys were prepared as described in Section II of the Appendix. These alloys varied in composition from 50 to 60 w/o Ni at about 2% increments. X-ray diffraction scans were made on the carefully prepared flat bottom surface of these alloy buttons. X-ray diffraction data pertaining to phase and quantity of phase were obtained on the alloys in the "as cast" and four other heat treated conditions. The entire assemblage of data is presented in Fig. 4. From observing Fig. 4, two things are immediately apparent; first, the most phase-pure composition appears to fall slightly below 55.1 w/o Ni (calculated stoichiometric TiNi alloy), secondly, in the alloys containing in excess of about 54 w/o Ni the three phases TiNi, Ti_2Ni and $TiNi_3$ can coexist, contradicting the "phase rule" for equilibrium alloy systems. Prolonged heating at 750 and 800°C seems to have little effect in stimulating more equilibrium status to these higher nickel alloys. These data of Fig. 4 are further plotted in Fig. 5 as "average quantity of coexisting phases in percent" as a function of "weight percent nickel." From a close comparison of the phase equilibria existing in these alloys with the two versions of the Ni-Ti constitution diagram (top Fig. 5) it can be seen that the Ti-rich alloys, those containing less than 52 w/o Ni, appear to follow the version showing the TiNi dissociating into Ti_2Ni and $TiNi_3$ at the lower temperatures. On the other hand, the alloys containing Ni in excess of 54 w/o tend to verify the existence of the TiNi phase at room temperature. As the nickel content increases there is an expected increase in the amount of $TiNi_3$ phase.

The X-ray diffraction studies on arc-melted monolithic specimens corroborates the findings of Margolin et al[12] and Pietrokowsky and Youngkin[14]. The TiNi phase can exist in a stable or metastable form at room temperature. In the case of the filed particles, work is apparently introduced which affects the energy balance and with the aid of the high temperature anneal promotes the TiNi phase decomposition.

Concurrently with the X-ray diffraction studies on the Ni-Ti alloys it was found principally through hardness and vibration damping that the alloy containing 54.5 w/o Ni-Ti possessed some unusual properties. The nature of these property anomalies will be described in more detail in their respective sections of this report. In view of the above findings some X-ray diffraction studies were initiated on the 54.5 w/o

FIG. 2 PHOTOMICROGRAPH SHOWING THE SUPERFICIAL LAYER OF MARTENSITIC STRUCTURE FORMED UPON THE SURFACE DURING ABRASIVE CUTTING OF THE SAMPLE. 500 X

FIG. 3 PHOTOMICROGRAPH SHOWING A PORTION OF THE MARTENSITIC LAYER REMOVED BY CAREFUL SURFACE PREPARATION. LOWER PART OF PHOTO SHOWS TRUE BASE STRUCTURE – UPPER PART IS MASKED BY REMAINING OVERLAY OF MARTENSITE. 500 X

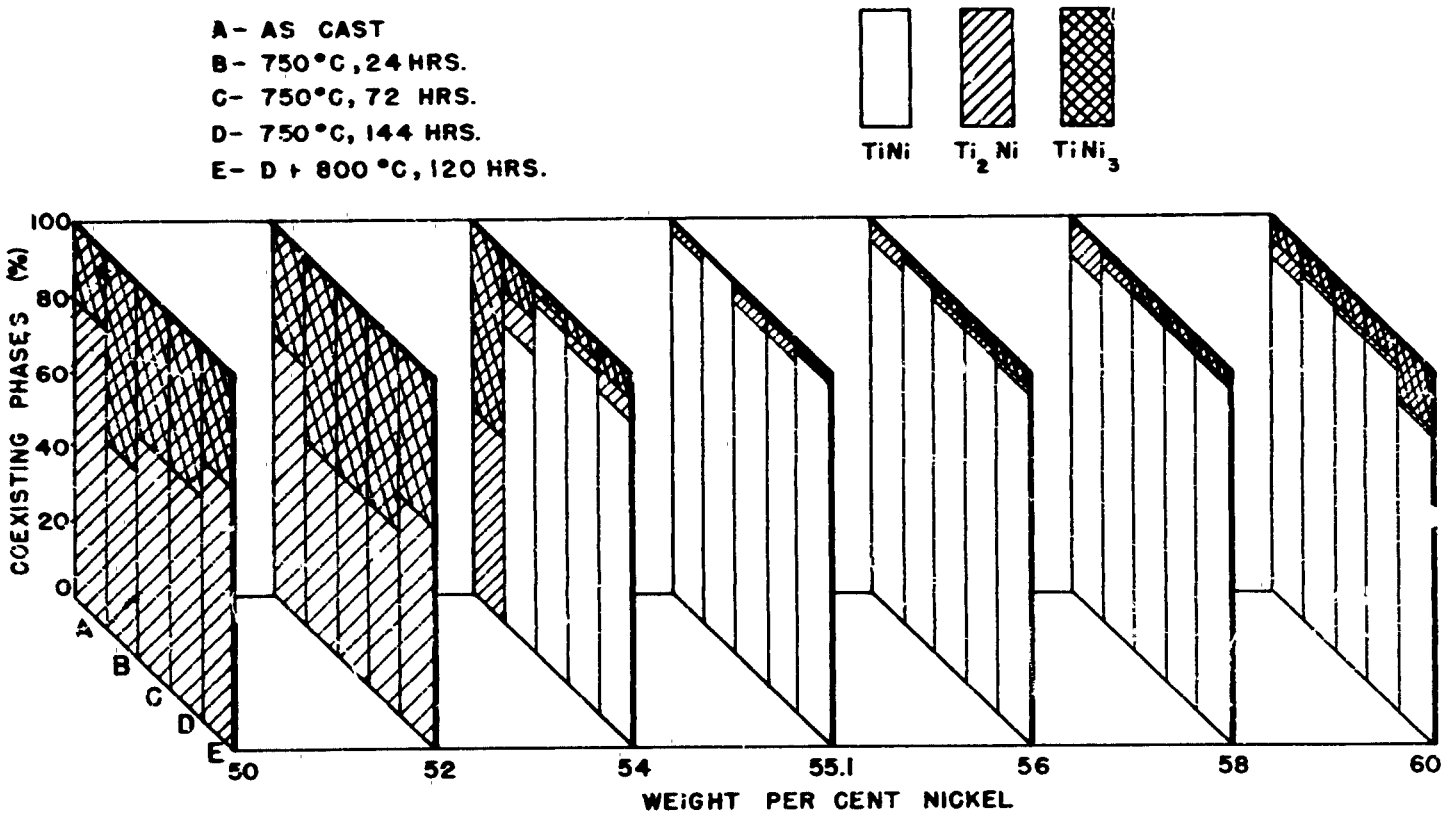

FIG. 4 SHOWS PHASES EXISTING IN SEVERAL Ni-Ti ALLOYS FROM 50 TO 60 % Ni. ALSO SHOWN ARE THE CHANGES IN THE QUANTITIES OF THE PHASES WITH THERMAL TREATMENT.

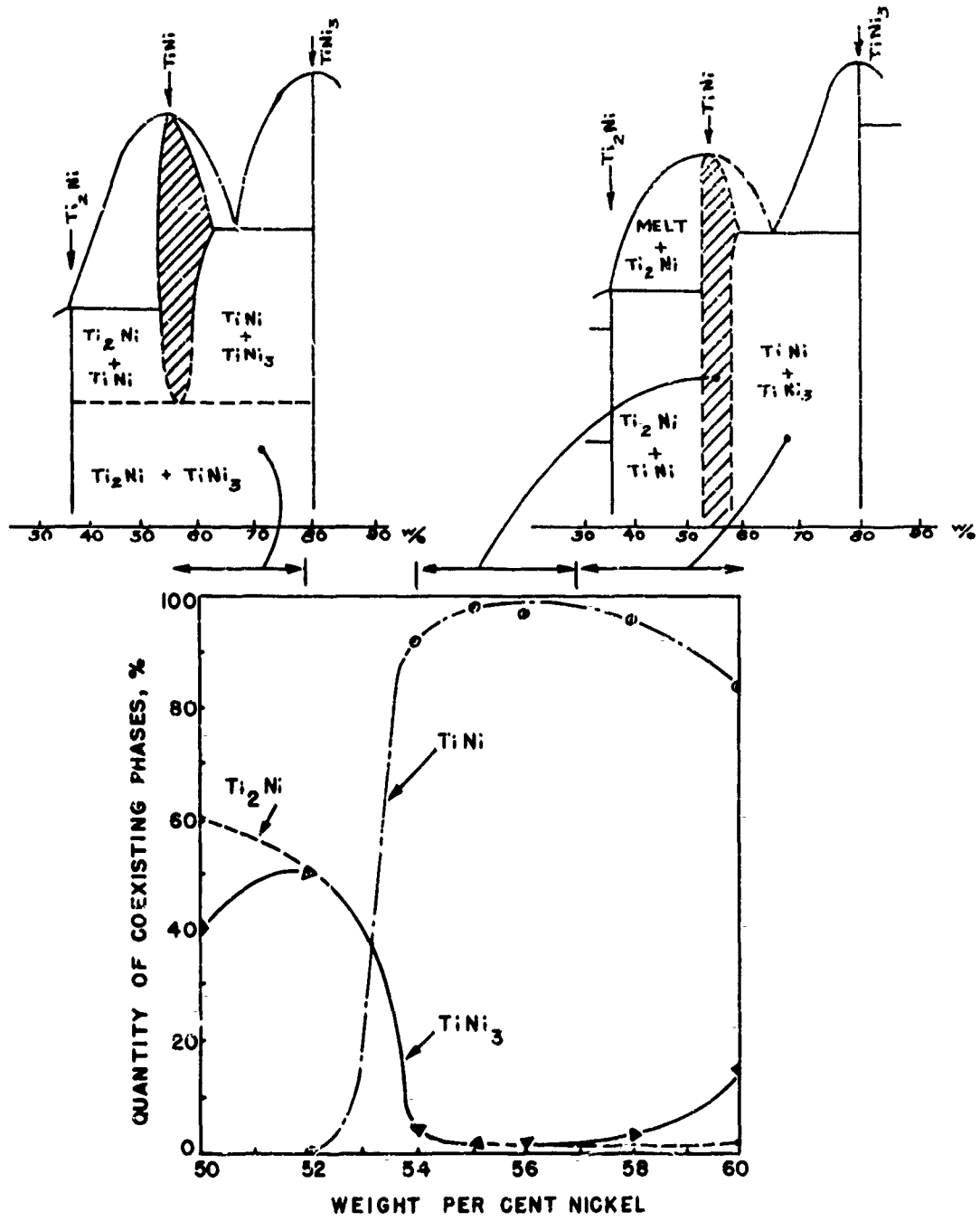

FIG. 5 ROOM TEMPERATURE PHASE RELATIONSHIP OF NICKEL-TITANIUM ALLOYS FROM 50 TO 60 % Ni.

Ni-Ti alloy. Fig. 6 shows a series of diffractometer scans made on the 54.5 w/o Ni alloy when given various temperature treatments. The diffractometer patterns in this figure encompass the principal TiNi phase reflections and were scaled to make the main TiNi peak equivalent height. Through careful observation of the series it can be seen that at room temperature (panel A) only a very minor amount of excess phase(s) exists in an alloy of this composition, indicating that the stoichiometric TiNi composition may lie closer to 54.5 w/o Ni than the calculated 55.06 w/o Ni composition. Indications of some existing excess phase(s) are shown as minor peaks at about the 26.5 and 20.5° angles. In panels B and C of Fig. 6 the alloy is heated. With the increased temperature these extraneous peaks are lessened to the point of almost complete elimination. As a result, it can be seen that with very minor temperature increases the TiNi phase is made more phase-pure. This is accomplished at the expense of eliminating the extraneous phase(s). Precisely what the other phase(s) are remains in some doubt due to the reflection interferences produced.

Following the heating studies, the same 54.5 w/o Ni-Ti alloy button was cooled below room temperature. Fig. 6, panels D, E and F, show the resultant strengthening of the extraneous phase(s). After being at -10°C the sample was warmed rapidly to room temperature. Panel G shows the alloy maintaining much of the -10°C phase equilibria upon its return to room temperature. In order to return to the normal room temperature phase equilibria the sample was placed a short time in boiling water. Upon cooling to room temperature the diffractometer scan shown in panel H resulted. This pattern is very similar to the original room temperature pattern (panel A). Cooling in liquid nitrogen at -196°C and returning to room temperature produced the pattern in panel I. Here the extraneous phase(s) are becoming very pronounced. Again, as before, this low temperature phase equilibria is removed by boiling in water as shown in panel J.

In preparing the 54.5 w/o Ni arc-melted button X-ray sample, polishing followed by deep etching was tried in order to minimize orientation effects. This treatment produced the extremely unusual results shown in Fig. 6, panel K. The deep etching alone or in combination with the surface polishing caused a partial dissociation of the TiNi into Ti_2Ni + $TiNi_3$. Calculations based upon X-ray power input, wave length, etc., revealed that the depth of penetration was between 0.0015 and 0.0075 inches. Thus, in the surface of the specimen, to a depth of 0.0075 inches, much of the TiNi phase was dissociated by the localized effect of the etchant, in this case a solution of HNO_3 and HF acids. It is the belief of the investigators that this example of TiNi decomposition and that

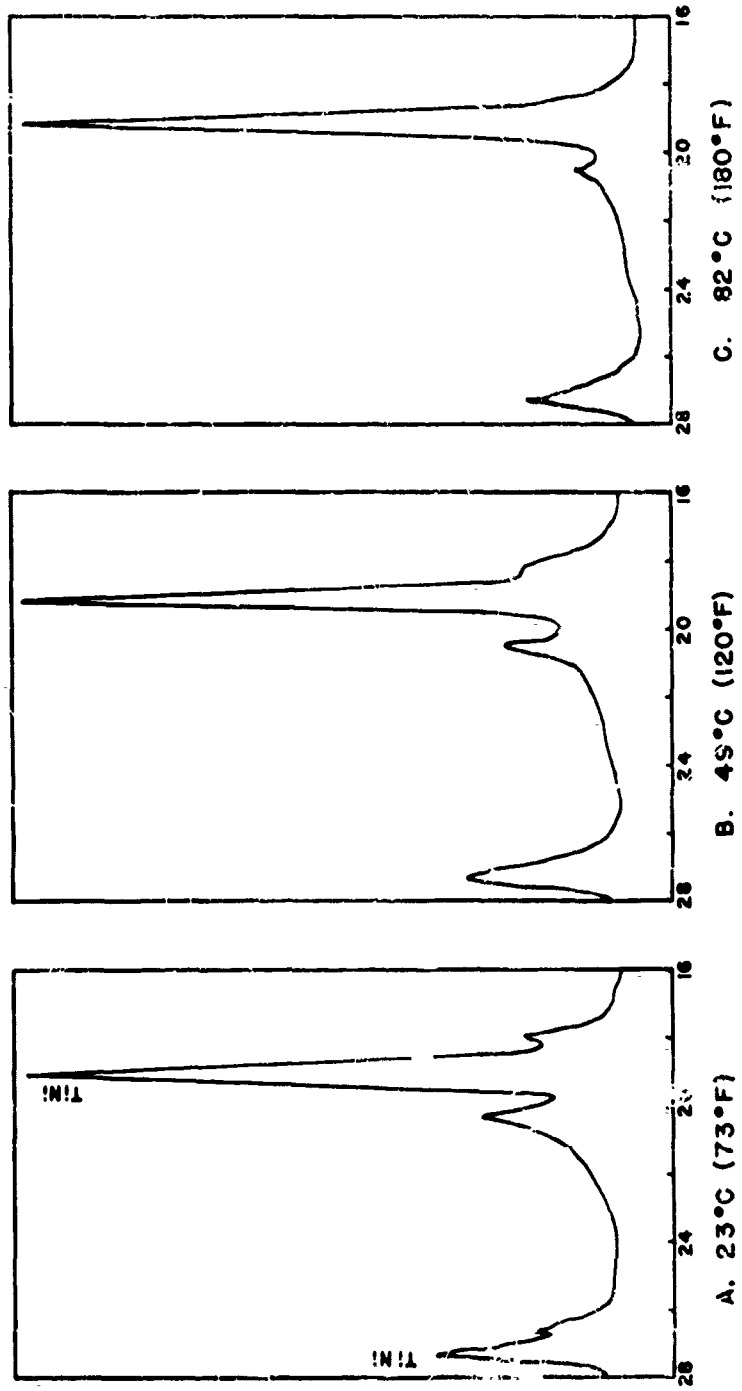

FIG. 6 X-RAY DIFFRACTOMETER SCANS MADE ON A 54.5 % Ni – Ti ALLOY UNDER VARYING CONDITIONS

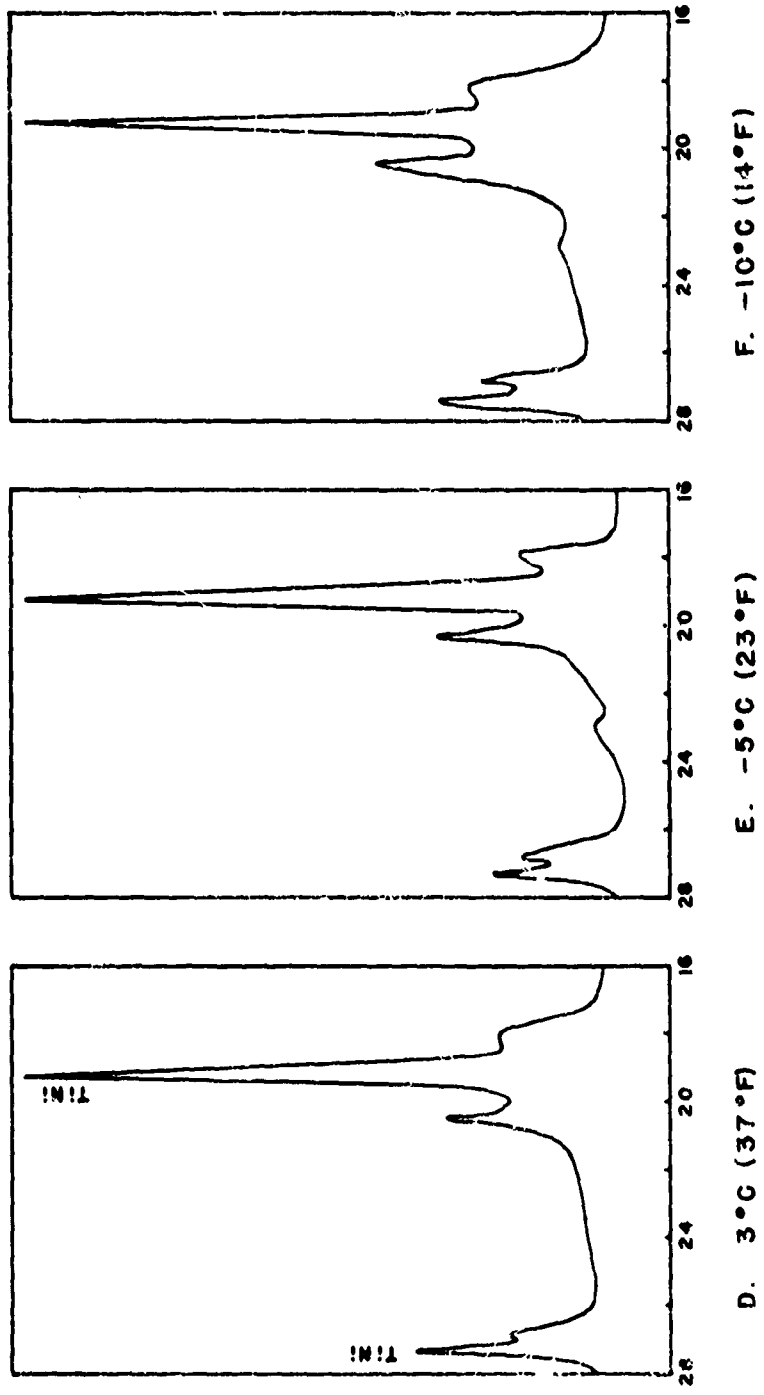

FIGURE 6 (CONTINUED)

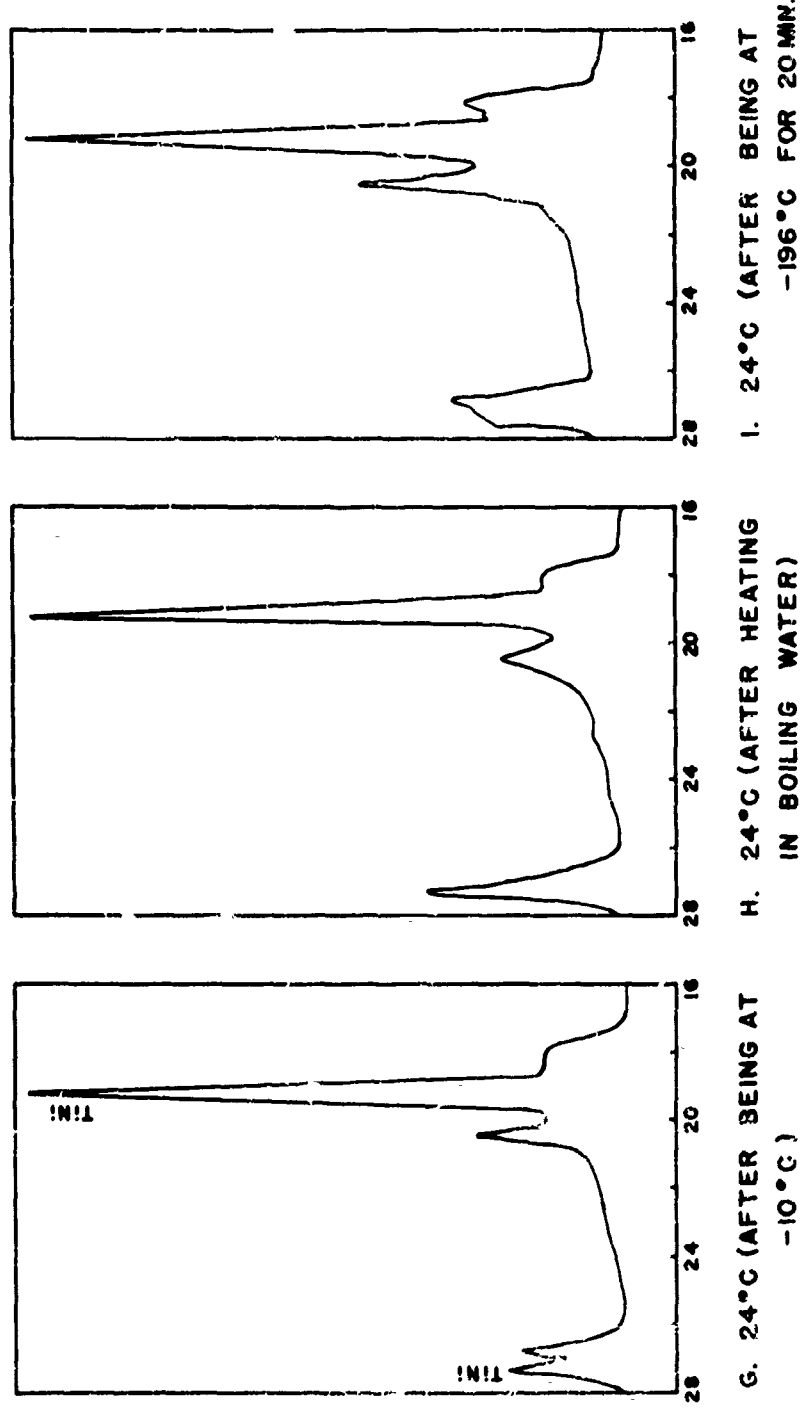

FIGURE 6 (CONTINUED)

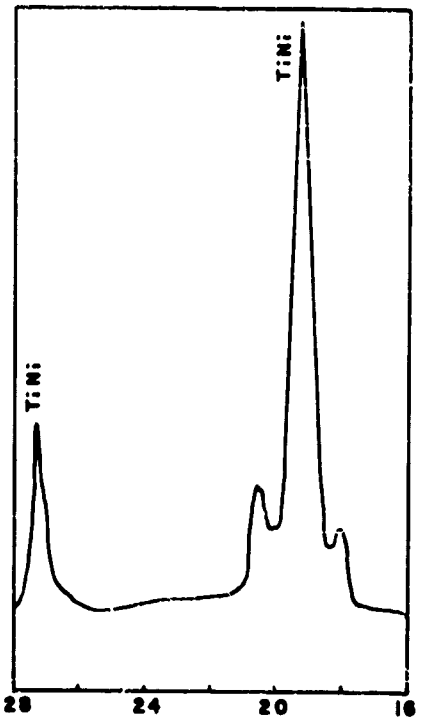

J. 24°C (-196°C FOLLOWED BY HEATING IN BOILING WATER)

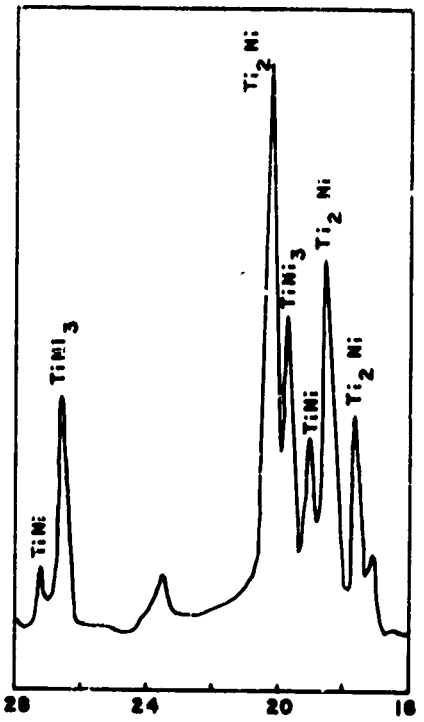

K. 24°C (ARC-CAST ALLOY POLISHED AND DEEP-ETCHED)

FIGURE 6 (CONTINUED)

produced in the aforementioned annealed TiNi X-ray filings and the martensite-like structure seen in Figs. 2 and 3 are all related to the same structural mechanism. However, limited investigation precludes further discussion on how or why the TiNi decomposition occurs under the above stimuli.

The above transformation, due to polishing and deep etching or etching alone, may point up some practical engineering applications. Since Ti_2Ni, one of the major phases produced by the TiNi transformation, has an ambient temperature hardness of about 611 D.P.H. (about 55 R_c) its presence in the outer surface would act as a surface hardener. TiNi and $TiNi_3$ both possess hardnesses in the thirties on the R_c hardness scale. As a result, the above may be a potential method of preferentially hardening all or parts of the surface of a softer and tougher core TiNi material without subjecting any part of the TiNi material to heating.

2. Internal Friction (Qualitative Studies)

During the arc-melting of thin cylindrical bars of the 54.5 w/o Ni alloy (employing commercially-pure titanium melting stock) it was noted that when these bars were cooled to room temperature and suspended freely upon a string they yielded nothing more than a dull thumping noise when struck by a hardened steel bar. The same bars when warmed slightly (about 120 to 130°F) and similarly suspended rang when struck. When the temperature in the TiNi bar was increased to a value in excess of 160°F (71°C) and the bar struck, it rang brilliantly. This initial experience with the temperature-sensitive mechanical vibration damping of the TiNi-base alloys opened the way for additional internal friction studies.

Initially, the vibration damping was studied by the qualitative acoustical technique of striking the freely suspended bar specimens. Ni-Ti alloy bars varying from 52.5 to 58 w/o Ni, with special emphasis on compositions in the 54.5 w/o Ni range, were arc-melted. The resultant alloy bars were tested over a temperature range from about -80°F to 350°F (-62 to 177°C). The sound produced by striking was categorized into five groups. These data were plotted in Fig. 7. In this figure tentative boundaries were established. The most significant fact is the narrow and distinct transition temperature range in the 54.5 w/o Ni alloy. Increasing or decreasing the nickel content widens this temperature range.

Subsequent acoustical studies performed on 54.5 w/o Ni alloys, prepared from titanium melting stock of varying purity, produced markedly different results. It was found that iron additions up to about 0.1 w/o tended to maintain the damping to non-damping transition closer to room

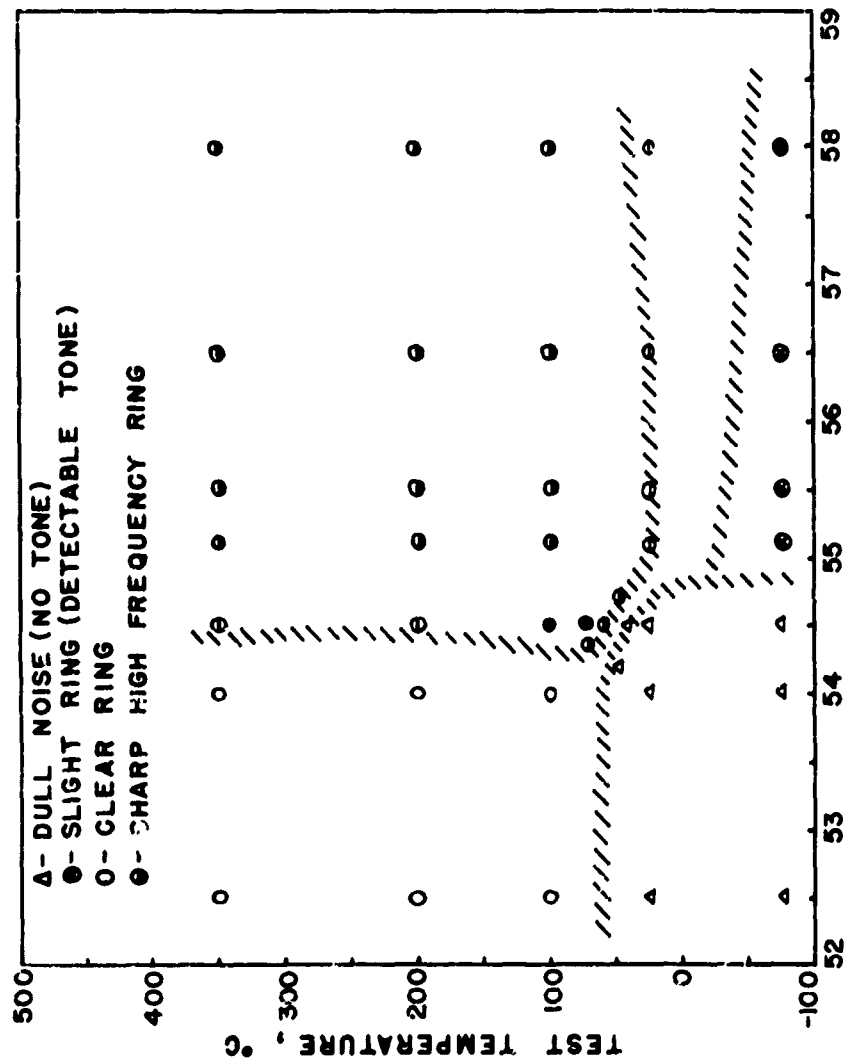

FIG. 7 SHOWS VARIATIONS IN THE SOUND PRODUCED BY STRIKING SUSPENDED ARC-CAST BARS (APPROX. 9/16" DIA. x 4" LONG) OF VARYING COMPOSITION AND AT DIFFERENT TEMPERATURES. NOTE SUDDEN SOUND TRANSITION WITH TEMPERATURE FOR ALLOYS CONTAINING ABOUT 54.5 % Ni.

temperature.

Some of the same alloys 54, 54.5 and 55.1 w/o Ni were hot swaged at 900°C into uniform but smaller diameter bars. As in the case of the arc-cast bars, these wrought bars were suspended and struck at various temperature levels. The resulting data are presented in Fig. 8. Comparing Figs. 7 and 8, it is apparent that hot working the arc-cast bars has served to widen the transition temperature range from high to low damping. Preliminary neutron diffraction studies revealed that in the course of hot working some additional extraneous phase(s) were precipitated in the TiNi matrix, indicating some relationship between TiNi phase purity and the resultant damping properties. Another possible cause of the transition temperature change may be explained by VanBueren[15], quoting others, who have noted grain boundary relaxation effects that were traceable to changes in grain size.

Some interesting relaxation effects were discovered in cooled arc-cast bars containing 54.65 and 54.8 w/o Ni. As above, the sound produced by striking was used as a criteria to determine the existing internal friction in the materials at various temperatures. It was found that a 54.8 w/o Ni alloy rang brilliantly at room temperature. Upon cooling to -15°C any trace of a ring had disappeared. With warming to room temperature (25°C) the ring was of considerably lower quality than originally experienced at this temperature. Continuing to heat to 45°C restored the brilliant ring which remained upon cooling back to room temperature. Similar effects were noted in the 54.65 w/o Ni alloy.

Suspecting the relaxation behavior may be time-dependent, the 54.8 w/o Ni alloy bar was again cooled down to -76°C and then warmed to room temperature. Ninety-two hours at room temperature were required for the 54.8 w/o Ni bar to recover its equilibrium sound behavior.

3. Internal Friction (Quantitative Studies)

Internal friction or mechanical damping is the capacity of a solid to convert the mechanical energy of vibration into heat even though the energy losses to its surroundings are negligible. If a metal were able to follow a perfectly elastic behavior, thus obeying Hooke's Law, it would be able to vibrate or be subjected to stress cycles within its elastic limit without any loss of energy except to the surrounding atmosphere. In this scheme there would be no conversion of the energy of vibration into heat within the metal and consequently no internal friction. The fact that vibrations are damped out in a metal more rapidly than the external loss of energy could possibly account for, indicates the non-elastic behavior of

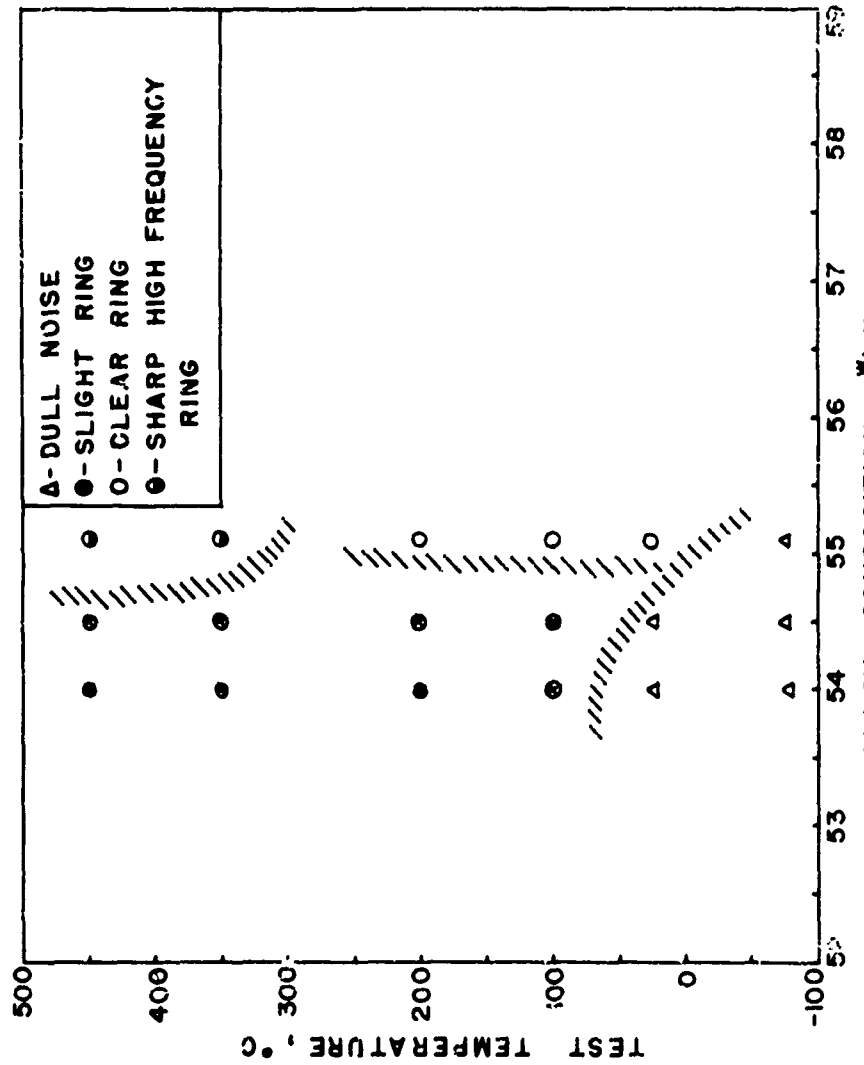

FIG. 8 SHOWS VARIATIONS IN THE SOUND PRODUCED BY STRIKING SUSPENDED HOT-SWAGED (900°C) BARS (0.5" DIA. x 5.5" LONG) OF VARYING COMPOSITION AND AT DIFFERENT TEMPERATURES.

metals rather than a true elastic one. Of the many processes responsible for internal friction, all generally relate to a phase lag between the applied stress and the resulting strain. This phase lag may be caused by plastic deformation, or if the stress is too low for this to occur, thermal, magnetic, or atomic effects may be responsible. As the damping properties of a metal are particularly sensitive to the presence of physical imperfections and to the interaction between them, the study of internal friction is quite often applied towards a better understanding of the effect and properties of lattice imperfections in crystalline solids.

Of the many known methods for measuring internal friction the simplest to understand and easiest to set up is the "Torsion Pendulum" method. A schematic drawing of the torsion pendulum apparatus used is shown in Fig. 9. A wire sample 20 cm long is held on each end by pin vices. The upper vice is mounted stationary while the lower vice is equipped with inertial weights which cause it to act as a torsion pendulum. Forces tending to promote swinging of the wire were minimized by using a steel tipped plum bob and the magnetic field of a permanent magnet. The latter also served to damp out extraneous vibrations. The entire assembly was mounted on a vibration damping material. To initiate torsional movement one of the steel inertial weights was attracted by pulsing an electromagnet mounted adjacent to the weight. The amplitude of each torsional swing was measured by observing a reflected beam of light upon a translucent scale. This method is suitable for frequencies from 0.1 to 10 c/sec. Although the method is not extremely sensitive, the interpretation of results is aided by its simplicity.

Figures 10 through 13 show the data obtained by the torsion pendulum method when 54.5 and 55.1 w/o Ni composition specimens were employed. The decrement is obtained by plotting the natural logrithm of the amplitude against the number of cycles of vibration. The internal friction in all cases was independent of amplitude as straight line curves were obtained. The slope of the line gives the decrement directly. Tests were performed on annealed wires having diameters of 0.0206 and .0360", drawn by a technique described in Section II of the Appendix. The frequency was approximately 0.4 c/sec in all instances with a constant length between the pin vise grips of 20 cm. To avoid disturbances from air currents the apparatus was fully enclosed in a plexiglass case.

Fig. 10 shows only a very minor change in the decrement between room temperature and 200°F for the 55.1 w/o Ni alloy wire specimen. Fig. 11 shows the large decrement change obtained for two wire diameters of the 54.5 w/o Ni alloy at room temperature and 200°F. In this instance there is a pronounced decrease in the amount of internal friction present as the temperature is raised from R.T. to 200°F. For the 0.036" diameter wire

A – PIN VICES
B – MIRROR
C – PLUMB BOB (steel tipped)
D – PERMANENT MAGNET
E – INERTIAL WEIGHTS
F – COPPER HEATER LINER
G – CERAMIC TUBE
H – HEATER ELEMENT
I – THERMOCOUPLE
J – COLLIMATED LIGHT BEAM
K – TRANSLUCENT SCALE
L – TORQUE INITIATING MAGNET
M – NYLON THREAD
N – WIRE SPECIMEN

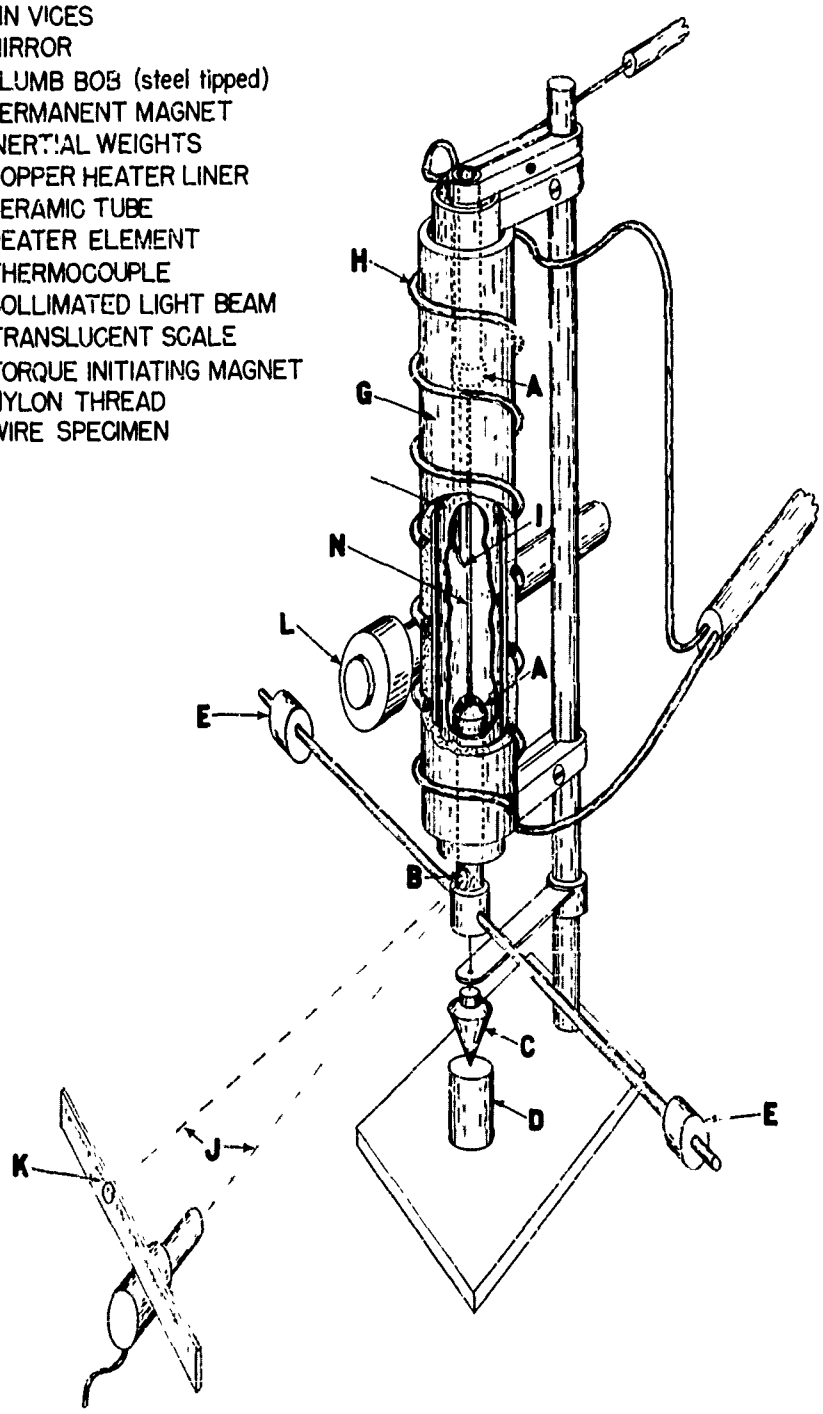

FIG. 9 SCHEMATIC DRAWING OF TORSION PENDULUM APPARATUS FOR MEASURING INTERNAL FRICTION

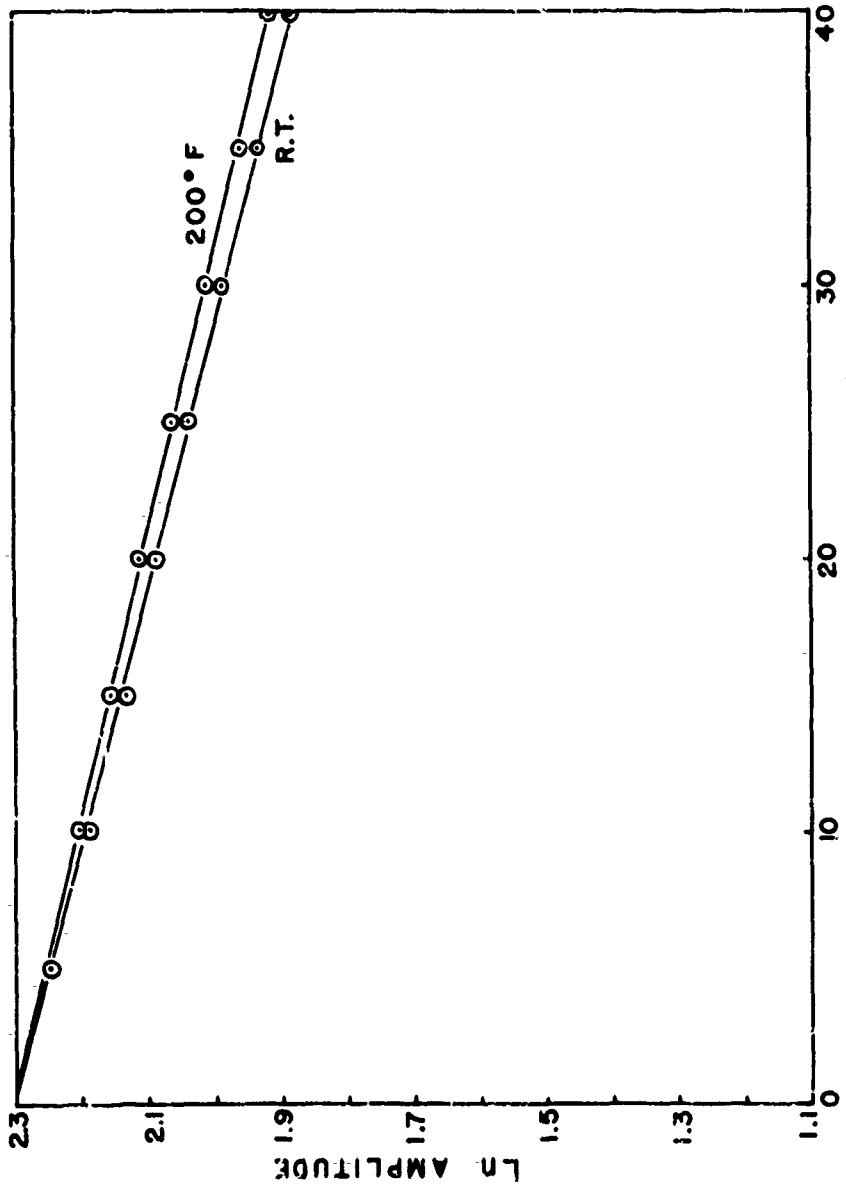

FIG. 10 SHOWS THE DECAY IN TORSIONAL VIBRATION AS A FUNCTION OF NUMBER OF CYCLES AND TEMPERATURE FOR 55.1 % Ni-Ti ALLOY WIRE 0.0206" DIA.. AVERAGE FREQUENCY = 0.408 CYCLES/ SECOND.

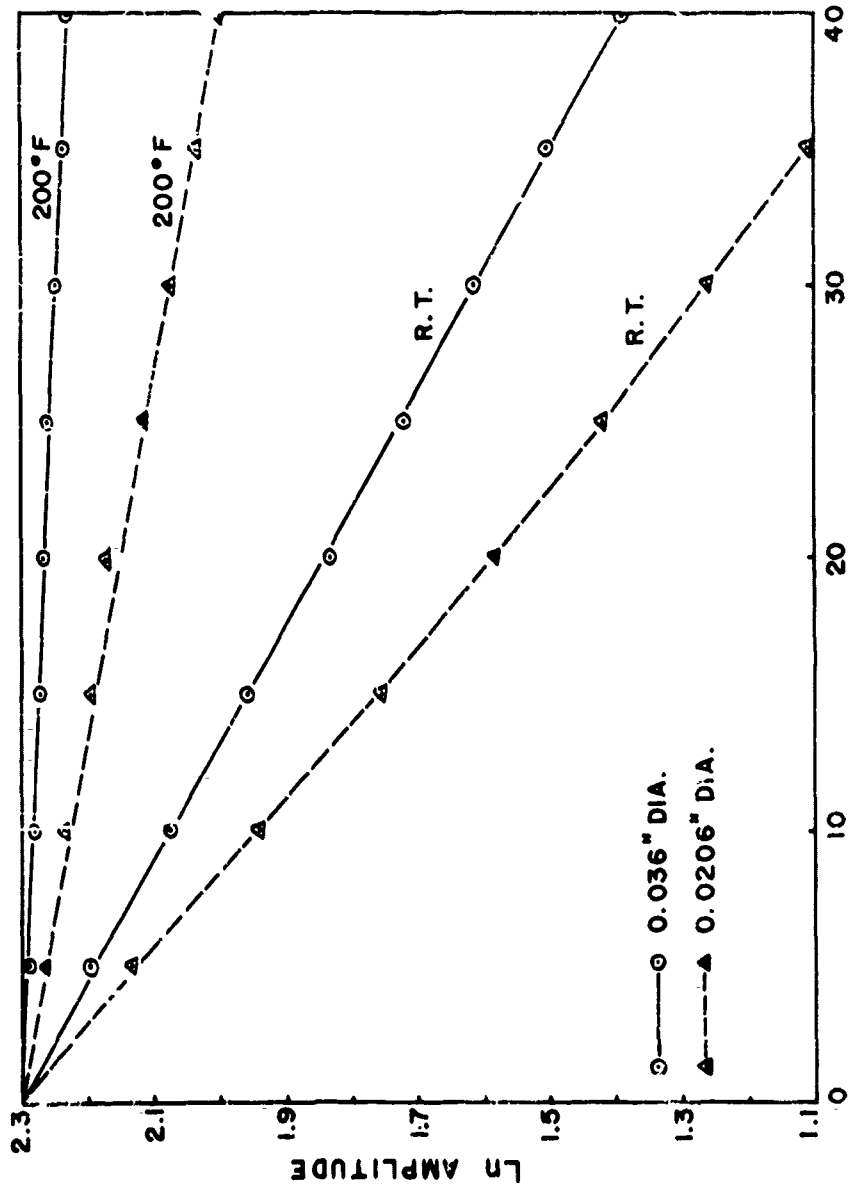

FIG. 11 SHOWS THE DECAY IN TORSIONAL VIBRATION AS A FUNCTION OF NUMBER OF CYCLES AND TEMPERATURE FOR 54.5 % Ni-Ti ALLOY WIRES. THE AVERAGE TORSIONAL FREQUENCY WAS 0.400 CYCLES/ SECOND FOR THE 0.036" DIA. WIRE AND 0.440 CYCLES/ SECOND FOR THE 0.0206" DIA. WIRE.

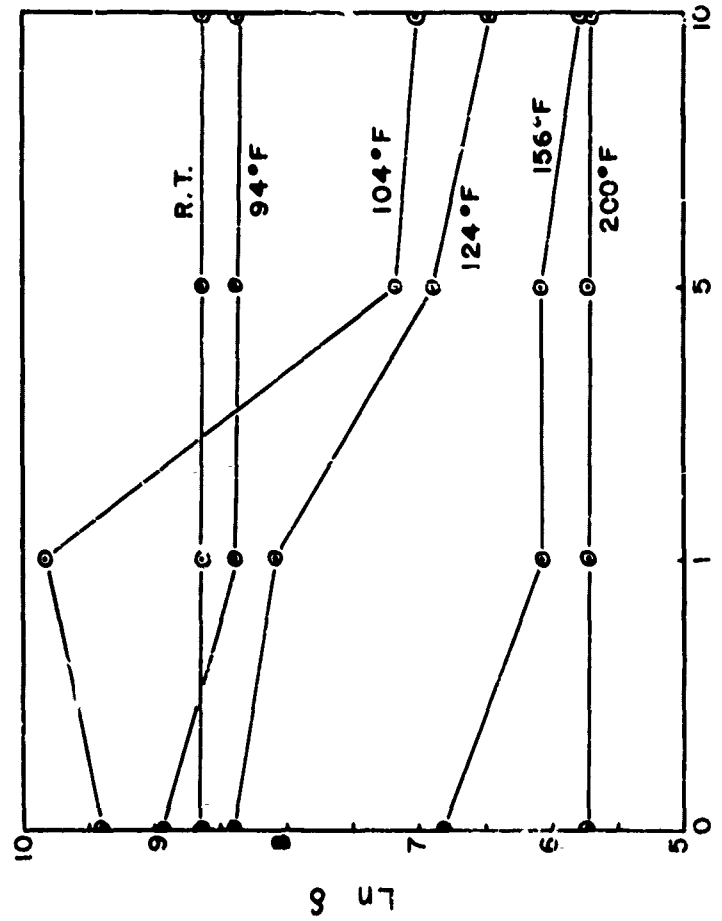

FIG.12 SHOWS A TIME-DEPENDENT EFFECT IN THE DAMPING OF A 54.5 % Ni-Ti ALLOY AT INTERMEDIATE TEMPERATURES. WIRE DIAMETER = 0.036". AVERAGE FREQUENCY OF TORSION VIBRATION = 0.40 CYCLES/SECOND.

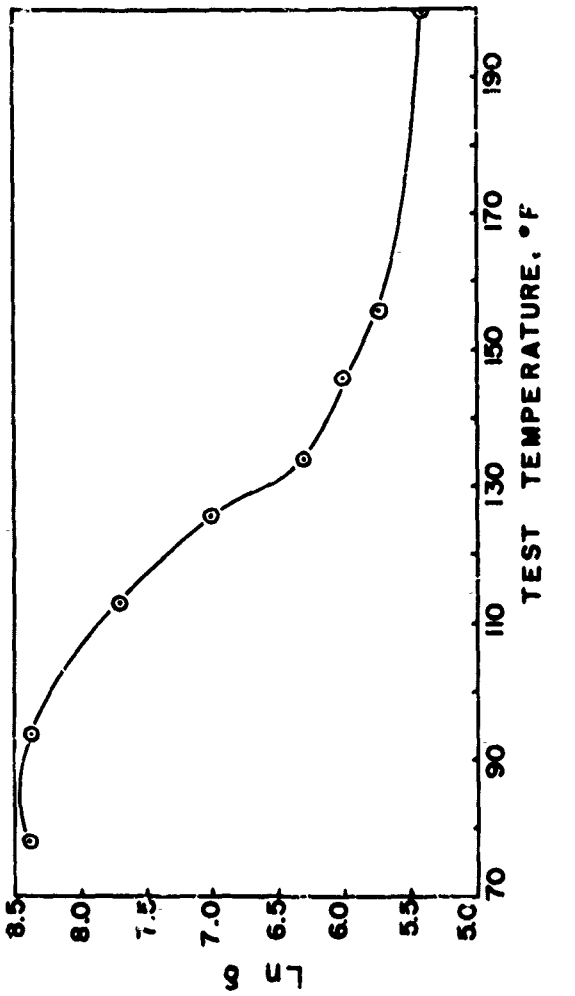

FIG. 13 SHOWS THE DECREASE IN DAMPING OF A 54.5 % Ni-Ti ALLOY WIRE WITH INCREASED TEMPERATURE. WIRE DIAMETER = 0.036". AVERAGE FREQUENCY OF TORSION VIBRATION = 0.40 CYCLES / SECOND.

only a slight change in frequency (< 2%) was measured between R.T. and 200°F. It was observed during this test that increasing the frequency to above 2.0 cycles/sec resulted in no observable change in the degree of damping between R.T. and 200°F. The degree of damping therefore appears to have a frequency dependence associated with relaxation type internal friction.

Fig. 12 illustrates the effect of time at temperature on the degree of damping. At the temperatures, as shown on the graph, between ambient and 200°F, pronounced changes in the decrement were observed. The five minute time period appeared to be critical for the transition to occur. Also of interest is the sudden increase in damping after one minute at 104°F. The damping rate appears to stabilize after ten minutes at temperature and is progressively lowered with increasing temperature.

Fig. 13 illustrates the effect of temperature upon the degree of damping as shown by the change in the decrement. At 200°F, the damping rate is noticeably less than at room temperature. The most pronounced change in the damping rate is evidenced between 94°F and 134°F. This shows a marked similarity to the data obtained on the material in the as-cast condition, as tested acoustically.

4. Electrical Resistivity

The relationship of the flow of electricity with the existing structures and temperatures has been fairly well established by previous investigators.[16] Electrical resistivity measurements provide a sensitive means of studying atomic structural changes occurring within a metallic system. This technique was applied to the investigations of the TiNi alloys (54.5 and 55.1 w/o Ni). A complete description of the polycrystalline specimens used and testing apparatus is given in Section III of the Appendix.

Through electrical resistivity studies it was hoped that information would be obtained that would shed some added light on the existing phase-equilibria and the long-range ordering of this alloy system. Since resistance to the flow of electricity is dependent upon the scattering of conduction electrons, it follows that a more perfect lattice of an ordered, single phase, homogeneous, stoichiometric alloy would provide the least resistance to electron movement. With this thought in mind, three separate electrical resistivity measurements were made. These were:

a. Electrical resistivity as a function of test temperature, over the range from -70°F to 210°F (-57 to 99°C)

b. Electrical resistivity as a function of test temperature, from room temperature to 900°C

c. Electrical resistivity (at room temperature) as a function of quenching temperature.

Electrical resistivity data, for a hot rolled and air annealed 54.5 w/o Ni alloy at test temperatures between about -70 and 210°F is given in both Fig. 14 and Table II. Observing Fig. 14 it becomes apparent that there is a hysteresis effect produced by cycling the temperature from the starting point of 72°F (22°C) to 210°F (99°C) down to a temperature below -60°F (-51°C) and back to room temperature. The greatest resistivity change occurs upon cooling in excess of -60°F (-51°C) and warming to room temperature. This result is not surprising in view of the X-ray diffraction detection of extraneous phases precipitating at sub-ambient temperatures, shown in Fig. 6. Table II is given in addition to Fig. 14 to indicate the time periods involved in measuring the resistivity values.

It can be seen that while eight hours was used in going from -60°F (-51°C) back to ambient, in this comparatively short warming time the extraneous (low temperature) precipitating phases had insufficient opportunity to revert back to the metastable TiNi form. It can also be seen in Fig. 14 that the change in phase-equilibria is accompanied by a general decrease in the slope of the warming curve from -60°F (-51°C) to room temperature. As room temperature is approached, following cooling, reversion of the extraneous phases back to the TiNi form take place. This is corroborated by the reversion of the sub-ambient temperature X-ray diffraction patterns to the normal room temperature X-ray pattern when the specimen was warmed slightly, see Fig. 6, parts F, G,H, I, and J.

Fig. 15 and Table III give resistivity data on the 55.1 w/o Ni alloy when heated in an inert atmosphere at temperatures up to 900°C (1652°F). The data were too scattered to be capable of interpretation. About all that could be concluded from Fig. 15 is the resistivity increases with increased temperature and at 900°C is about 138 microhm-cm.

The last attempt at using electrical resistivity measurements to divulge information about the TiNi system was done at room temperature on quenched specimens. The idea behind quenching TiNi strip specimens heated to various temperatures was to arrest or preserve the dynamic equilibria existing at the quenching temperature between order and disorder, and measure this quantitatively at room temperature. Strips of the 55.1 w/o Ni composition were used. Four strips in all were used, two furnace cooled from 593°C (1100°F) and two others in an air cooled condition from hot rolling at 700°C (1292°F). With these initial

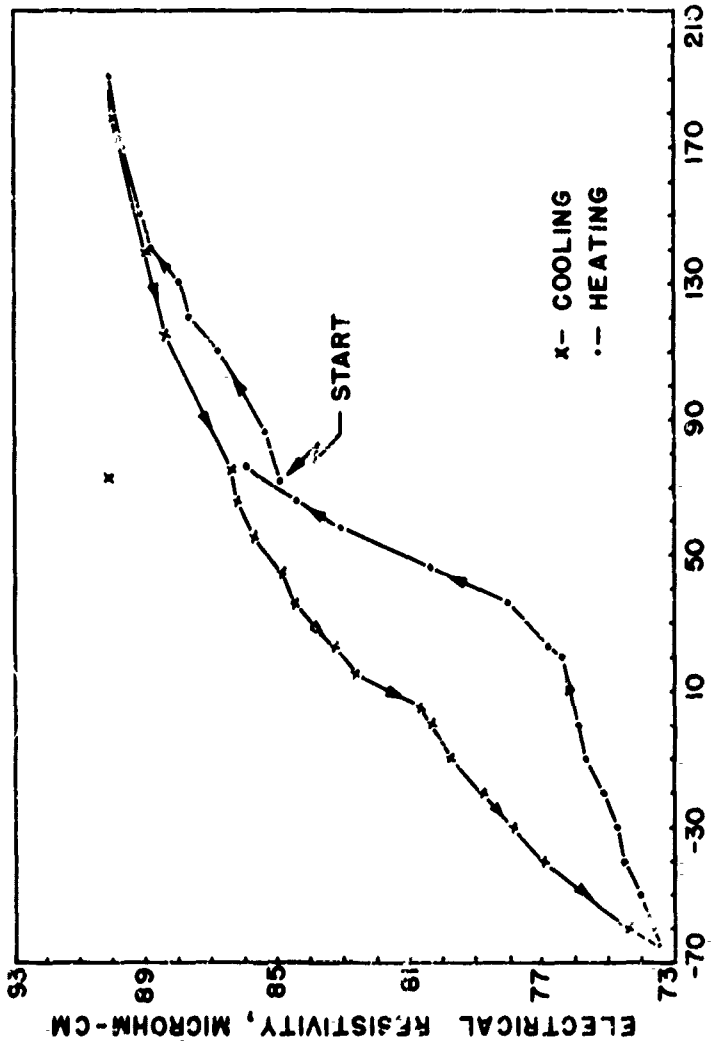

FIG. 14 ELECTRICAL RESISTIVITY AS A FUNCTION OF TEMPERATURE FOR A 54.5 % Ni-Ti ALLOY.

TABLE II

ELECTRICAL RESISTIVITY DATA FOR HOT ROLLED* 54.5 w/o Ni-Ti ALLOY AT TEMPERATURES AROUND ROOM TEMPERATURE

Test Temperature, °F	Resistivity Microhm-cm	Approximate Test Time, Hr.	Remarks
72 (22°C)	84.96	0	
86 (30°C)	85.40		
110 (43°C)	86.86		
120 (49°C)	87.61		
130 (54°C)	87.94		
140 (60°C)	88.88		
150 (65°C)	89.17		
170 (76°C)	89.69	8	
191 (88°C)	90.62	24	
210 (99°C)	91.26		
178 (81°C)	89.99		
139 (59°C)	88.95		
115 (46°C)	88.46		
72 (22°C)	89.99	32	←ρ curiously high at room temp.
75 (24°C)	86.45	48	←ρ after standing overnight more in line with other data
66 (19°C)	86.28		
55 (13°C)	85.78		
45 (7°C)	84.90		
35 (2°C)	84.57		
23 (-5°C)	83.20		
15 (-9°C)	82.76		
5 (-15°C)	80.76		
0 (-18°C)	80.30		
-10 (-23°C)	79.82		
-20 (-29°C)	78.81		
-30 (-34°C)	77.94		
-40 (-40°C)	76.99	56	
-60 (-51°C)	74.41	72	
-60+(-51°C)	---		
-60 (-51°C)	73.60		
-50 (-45°C)	74.06		
-40 (-40°C)	74.59		
-30 (-34°C)	74.67		
-20 (-29°C)	75.11		
-10 (-23°C)	75.66		
0 (-18°C)	75.90		
15 (-9°C)	76.43		
23 (-5°C)	76.85		
36 (2°C)	78.01		
46 (8°C)	80.42		
58 (14°C	83.11		
66 (19°C)	84.41	76	
76 (24°C)	86.01	92	

* Hot rolled at 900 and 700°C. Heat treatment: 1 hour at 300°C, followed by a furnace cool. Inert atmosphere used during heat treatment.

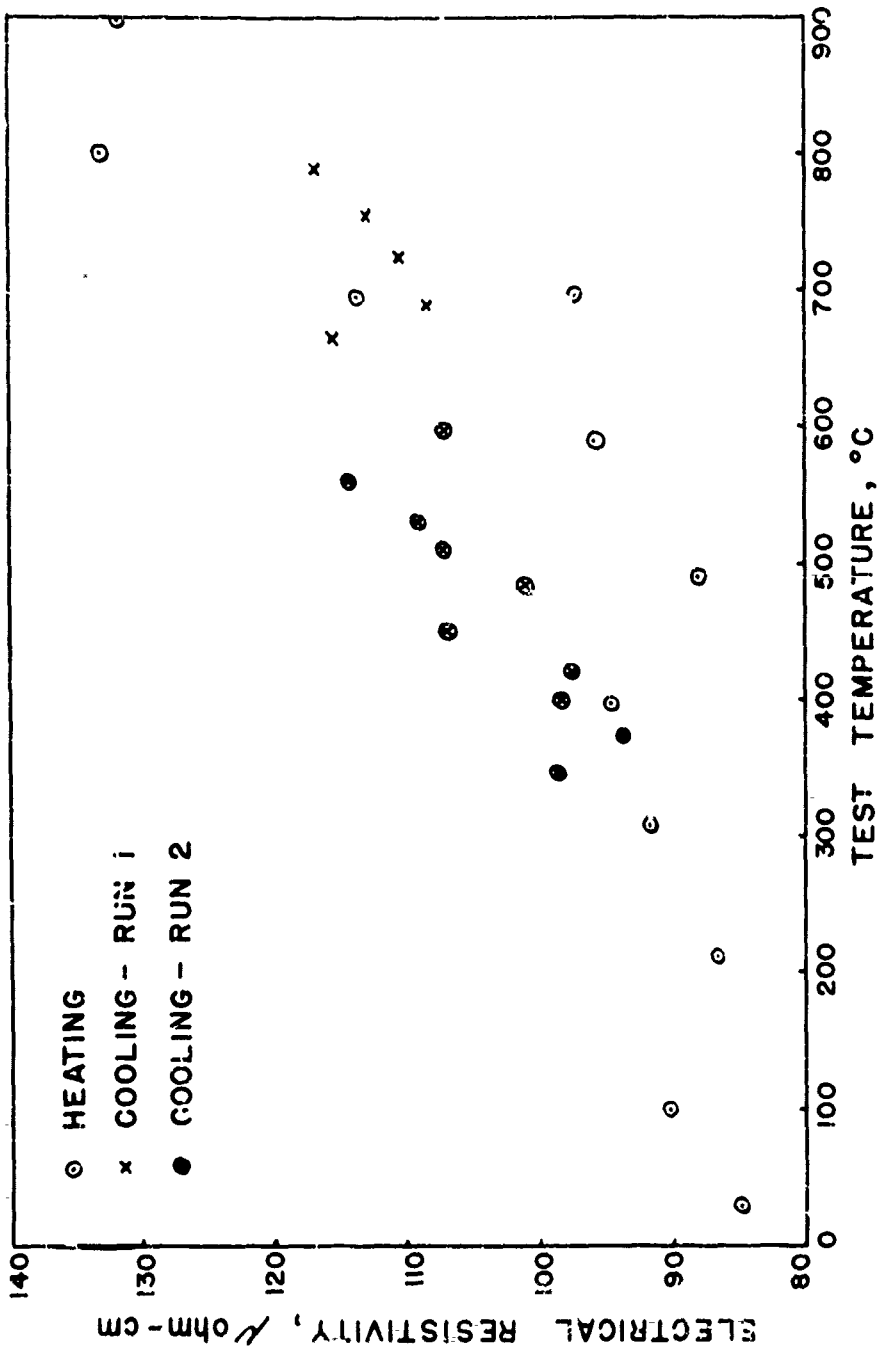

FIG. 15 DATA POINTS SHOWING CHANGES IN ELECTRICAL RESISTIVITY OF TiNi MATERIAL (55.1 W% Ni-Ti) AS A FUNCTION OF TEMPERATURE.

TABLE III

DATA EMPLOYED IN COMPUTING THE ELECTRICAL RESISTIVITY OF TiNi COMPOSITION (55.1 w/o Ni) AT VARIOUS TEMPERATURES

Temp. °C	I m.a.	E_{drop} m.v.	E_{therm} m.v.	$E_D - E_T$ m.v.	R_T ohms	ρ μ ohm-cm	Remarks
29°	6.9511	.257	.0155	.2415	.03474	84.71	Data taken during heating
100°	6.950	.2214	-.0332	.2573	.03702	90.27	
212°	6.950	.2152	-.0320	.2472	.03557	86.73	
307°	6.9511	.1882	-.0735	.2617	.03765	91.80	
396°	6.950	.1272	-.1430	.2702	.03888	94.80	
490°	6.935	.0780	-.1725	.2505	.03612	88.08	
590°	6.934	-.0580	-.3332	.2752	.03969	95.98	
695°	6.934	-.2073	-.5308	.3235	.04665	113.75	
697°	6.9277	-.1470	-.4230	.2760	.03984	97.15	
802°	6.9277	-.1608	-.5390	.3782	.05459	133.11	
900°	6.9287	-.2260	-.6000	.3740	.05398	131.62	
788°	7.009	-.0182	-.3544	.3362	.04797	116.97	Data taken during cooling - Run #1
754°	7.0064	.0905	-.2338	.3243	.04629	112.87	
725°	7.0074	.0700	-.2475	.3175	.04531	110.48	
690°	7.0040	.1084	-.2030	.3114	.04446	108.41	
640°	7.0022	.0159	-.3156	.3315	.04734	115.43	
599°	6.986	-.0425	-.350	.3075	.04402	107.34	Data taken during cooling - Run #2
558°	6.986	.0565	-.2705	.3270	.04681	114.15	
530°	6.986	.0957	-.2150	.3127	.04476	109.16	
510°	6.986	.119	-.1882	.3072	.04397	107.24	
482°	6.986	.045	-.185	.2895	.04144	101.06	
451°	6.986	.140	-.1665	.3065	.04387	106.99	
421°	6.9916	.154	-.126	.280	.04005	97.67	
399°	6.990	.140	-.142	.282	.04034	98.39	
373°	6.991	.1495	-.119	.2685	.03841	93.66	
345°	6.992	.212	-.0715	.2835	.04055	98.80	

histories the four strips were heated to various temperatures and quenched. Electrical resistivity measurements were made following each quenching treatment. The resultant data are presented graphically in Figs. 16 and 17. Observing these figures it can be seen in each case the electrical resistivity reaches a peak at about 800°F (427°C) and drops sharply to a minimum value at about 900°F (482°C). Following this drop the resistivity again climbs with increased temperature. The fact that four separate samples yielded the same result and that the gross change in resistivity amounted to about 10 microhm-cm supports the fact that a real change of some type occurs between 800°F (427°C) and 900°F (482°C). There still is doubt[16] whether the order-disorder transformation is continuous over a range of temperatures or abrupt. The resistivity data given in Figs. 16 and 17 would indicate an abrupt transformation; however, this is contradicted by the X-ray data of Pietrokowsky and Youngkin[14] and the present investigators who detect (100) ordering reflections from all samples of TiNi.

Since the ordered structure should provide the least resistance to current flow it would appear that minor ordering, perhaps short range ordering (or anti-phase domains), occurs at all temperature levels from below room temperature to about 800°F (427°C), thus producing the ordered reflections in the X-ray diffraction scans. However, between about 800°F (427°C) and 1000°F (538°C) a sharp transition to long range order may be occurring. Later in the report it will be seen that a secondary-hardening peak occurs in the hot hardness curve of a quenched 55.1 w/o Ni alloy specimen at 865°F (463°C), placing this phenomena in the same temperature range as the above marked resistivity change.

5. Metallography

The initial metallographic investigations into the essentially stoichiometric TiNi alloys were quite startling. In every case the polished and etched specimens revealed a martensite-like structure similar to that shown in Fig. 2. This martensite-like structure was particularly prevalent in the wrought materials. Following the misleading X-ray diffraction results obtained from TiNi filings, which showed this phase completely dissociated into Ti_2Ni and $TiNi_3$, the present investigators were willing initially to concede that the structure shown in Fig. 2 (with minor variations) may be the true structure. However, about this same time other mechanical and physical property indications made necessary further investigation into the polishing and etching techniques. Knowing from prior experience that the TiNi-type alloy work hardened readily, great care was exercised in the surface polishing procedure. To accomplish this, diamond polishing was used. These carefully polished specimens were then etched using an etchant containing concentrated HNO_3 and HF in varying proportions with water. More HF was used on the higher

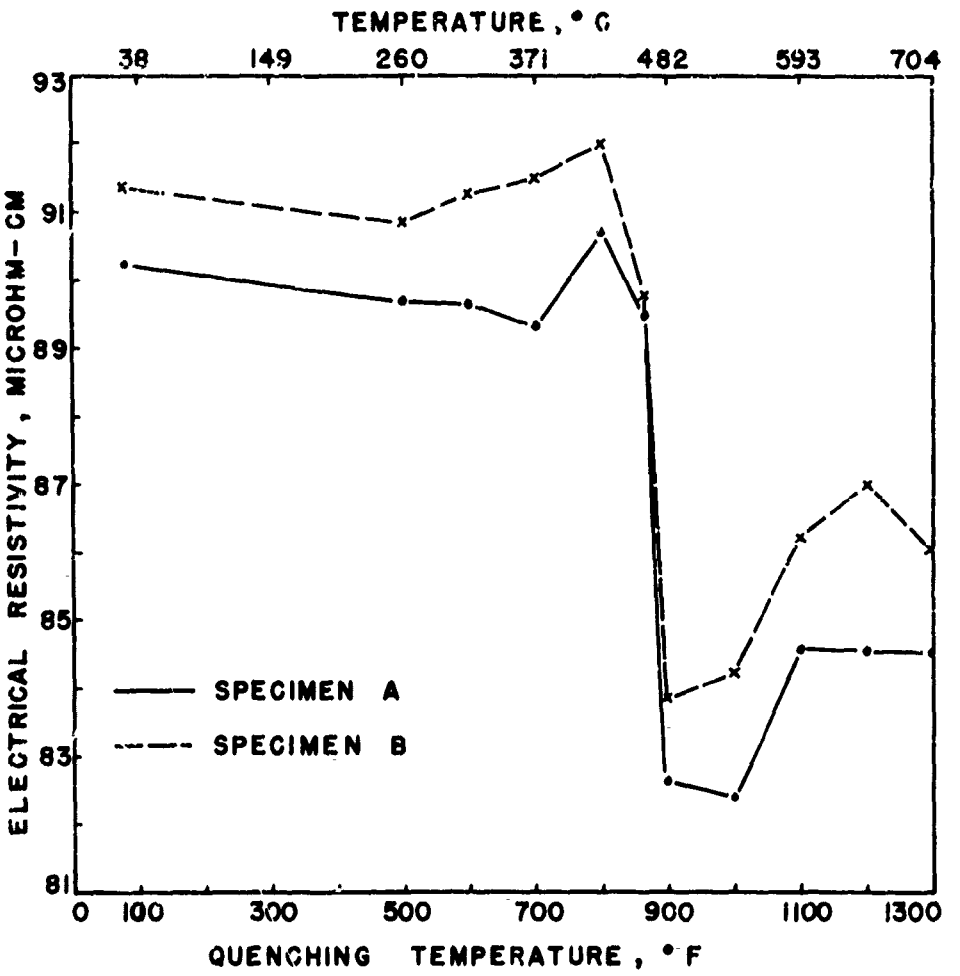

FIG. 16 CURVES SHOWING ROOM TEMPERATURE ELECTRICAL RESISTIVITY OBTAINED FROM STRIP TiNi MATERIAL (55.1 Wt% Ni-Ti) HEATED TO VARIOUS TEMPERATURES AND QUENCHED. INITIAL CONDITION OF SPECIMENS: FURNACE COOLED FROM 593 °C (1100°F).

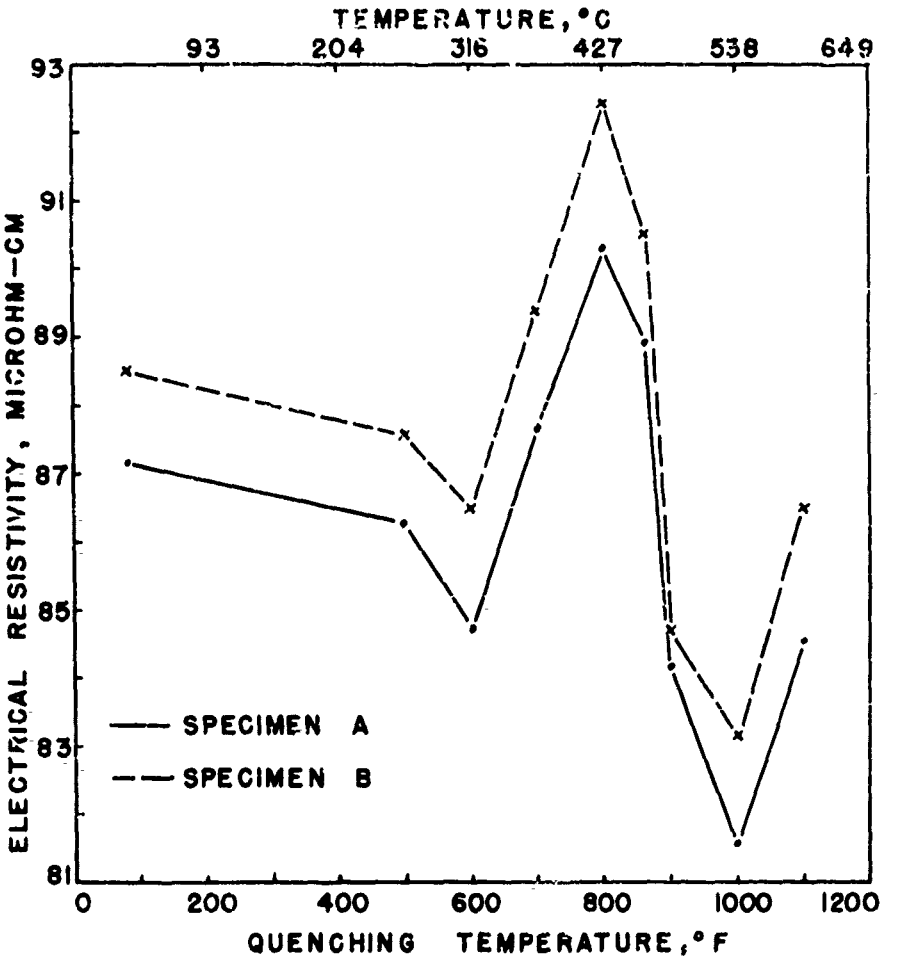

FIG. 17 CURVES SHOWING ROOM TEMPERATURE ELECTRICAL RESISTIVITY OBTAINED FROM STRIP TiNi MATERIAL (55.1 W% Ni-Ti) HEATED TO VARIOUS TEMPERATURES AND QUENCHED. INITIAL CONDITION OF SPECIMENS: HOT ROLLED TO 0.020" AT 700°C.

titanium alloys. This procedure resulted in revealing the true structure of these alloys. Fig. 3 is a photomicrograph showing the true base structure with the martensite-like worked material covering part of the surface.

Employing the new-found techniques of sample preparation other metallography investigations were performed. Fig. 18 shows the cast, hot rolled, and cold rolled structures obtained in a 55.1 w/o Ni alloy. The "as cast" structure of this figure greatly resembles the cast structure of 8 to 12 w/o Si-Al alloys given in the literature[17]. However, in the case of these Si-Al alloys they are two-phased (Al solid solution + silicon) and X-ray diffraction scans on the 55.1 w/o Ni specimen indicates a predominantly TiNi phase material with minor quantities of Ti_2Ni and $TiNi_3$ present. As a result, in spite of the similarity between "as cast" TiNi and the two-phase Al-Si eutectic, it must be concluded the TiNi structure is probably due to dendritic segregation or coring. Hot working this cast 55.1 w/o Ni alloy at increasingly higher temperatures shows conclusively the predominance of the TiNi phase. This confirms the X-ray diffraction findings given in Figs. 4 and 5. The extraneous phases, shown as rounded particles after rolling at 1100°C (2012°F), are Ti_2Ni and $TiNi_3$. Observing the 700°C (1292°F) structure reveals the gradual elimination of the dendritic-type structure. Cold rolling (about 33% thickness reduction) shown in Fig. 18 tends to give the material a typical fibred structure with the aligning of the excess phase particles.

The "as cast" structures of the phases bracketing TiNi, namely Ti_2Ni and $TiNi_3$ are shown in Figs. 19 and 20. Lower magnifications of 100X were employed to reveal the typical cored or dendritic structures. Since these phases are incapable of hot or cold working, no further metallographic studies were made.

Fig. 21 shows the result obtained by heating a titanium-rich TiNi alloy (about 52 w/o Ni) above the solidus temperature line separating the areas TiNi + liquid and TiNi + Ti_2Ni. This solidus temperature is variously reported as 984°C and 1015°C. Observing Fig. 21 it can be seen that the base alloy was partially fused and islands of the TiNi phase were separated and suspended in a matrix of the Ti_2Ni phase. Identification of the phases was accomplished by microhardness testing. In this experiment whole masses of the predominantly Ti_2Ni phase material flowed from cracks in the arc-melted button. The original button did not noticeably shrink with the loss of the Ti_2Ni phase.

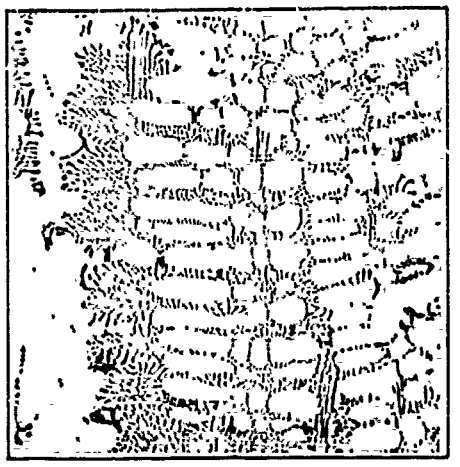

AS CAST, 500 X

HOT ROLLED AT 700°C , 500 X

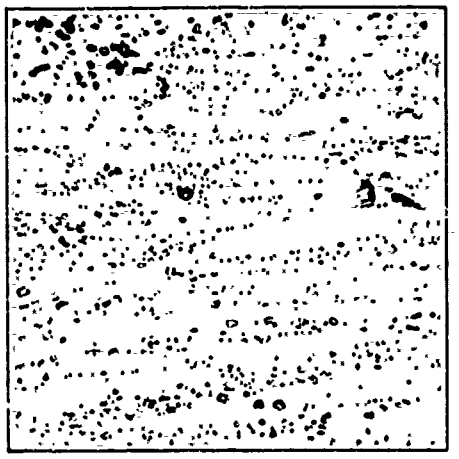

HOT ROLLED AT 1100°C, 500X

HOT ROLLED AT 700°C TO 0.021", COLD ROLLED AT ROOM TEMPERATURE TO 0.013", 250 X

FIG. 18 PHOTOMICROGRAPHS OF THE TiNi COMPOSITION ALLOY CONTAINING 55.1 % Ni-Ti

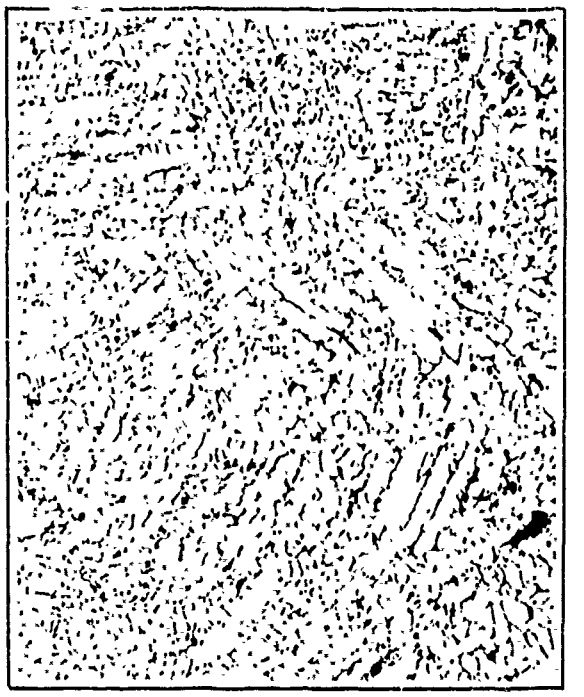

FIG. 19 "AS CAST" Ti_2Ni STRUCTURE. 100 MAG.

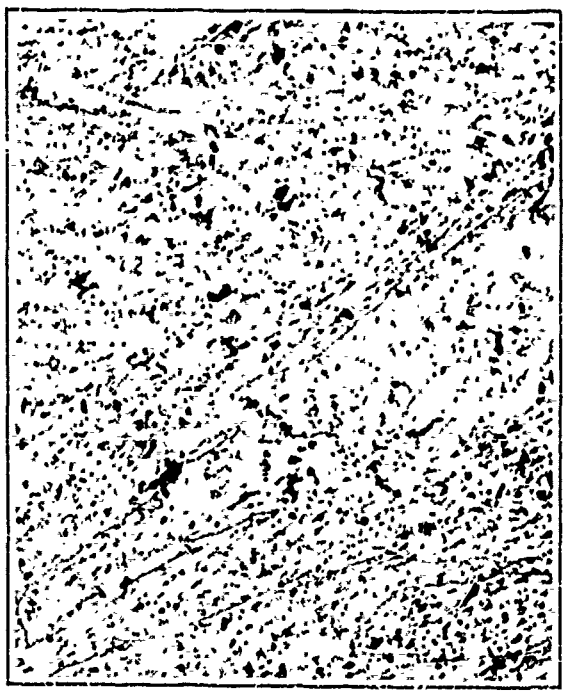

FIG. 20 "AS CAST" $TiNi_3$ STRUCTURE. 100 MAG.

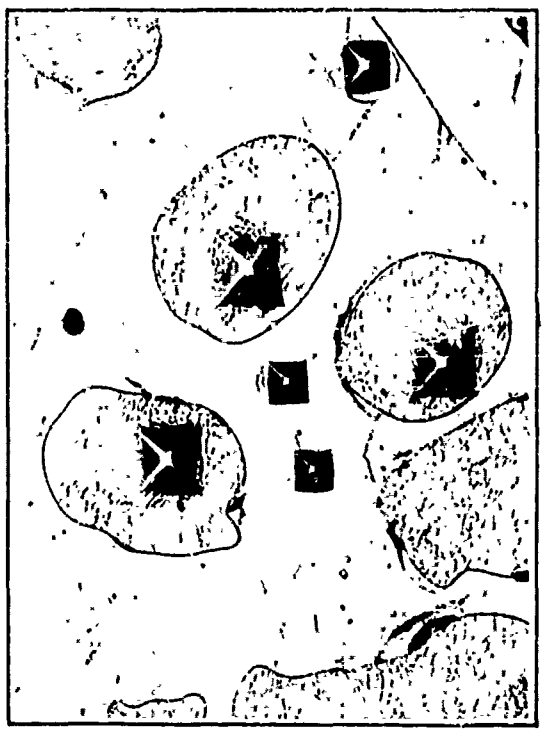

FIG. 21 TWO PHOTOMICROGRAPHS SHOWING Ti-RICH TiNi INTERMETALLIC COMPOUND AFTER HEATING ABOVE THE SOLIDUS INTO THE TiNi + LIQUID REGION. VARIATION IN MICROHARDNESS INDICATES PRESENCE OF TWO DISTINCT CONSTITUENTS TiNi (SOFT), Ti_2Ni (HARD MATRIX).

5. Magnetic Susceptibility

Susceptibility measurements were made on the 54.5 and 55.1 w/o Ni alloys for two reasons: First, to detect any changes in the magnetic properties of the material as a function of test temperature and secondly, to determine the extent and stability of paramagnetism in these alloys of the TiNi type over a wide temperature range. The data obtained from these tests are shown graphically in Fig. 22. Both alloys were cooled initially from room temperature to -196°C (liquid N_2) and then heated to temperatures in excess of ambient. The 54.5 w/o Ni alloy showed almost no change in mass susceptibility with temperature. The 55.1 w/o Ni alloy showed more indication of susceptibility change with temperature (particularly between -150 and 200°C). However, variations of up to 3×10^{-6} may be attributed to experimental error and the susceptibility of both alloys should be considered temperature independent.

By definition[18], a "paramagnetic material" is one which exhibits a small and positive susceptibility (K) value. Since permeability (μ) equals $1 + 4\pi K$ it can be seen that the expected permeability for these alloys should be very close to unity. Actual permeability measurements made on variously treated bar specimens of 55.1 w/o Ni alloy corroborated these findings. The measured μ values were less than 1.01 in every case.

From the above findings it would appear that the known changes occurring in phase equilibria with temperature, ($TiNi \rightleftharpoons Ti_2Ni + TiNi_3$) discussed earlier in the report, have almost negligible effect on the magnetic susceptibility and permeability. The latter consideration being important in possible non-magnetic applications of these materials.

SUMMARY OF CONSTITUTION STUDIES

Careful observation of the data obtained through the physical property studies and the unusual experiences encountered in preparing X-ray diffraction specimens, lead the present investigators to the general conclusion that the TiNi phase does in fact exist at room temperature (and even below) but that it can best be described as a "metastable" phase. The term "metastable" refers to systems that often exist for long periods of time in states which are not the equilibrium ones as defined by lowest free energy.

The existence of TiNi in its most phase-pure condition appears to occur at about 54.5 w/o Ni instead of the calculated stoichiometric 55.06 w/o Ni. It was found virtually impossible to isolate the TiNi phase, as either Ti_2Ni or $TiNi_3$, or both, are almost always present. This can be seen in the X-ray data given in Figs. 4, 5 and 6 and the photomicrographs

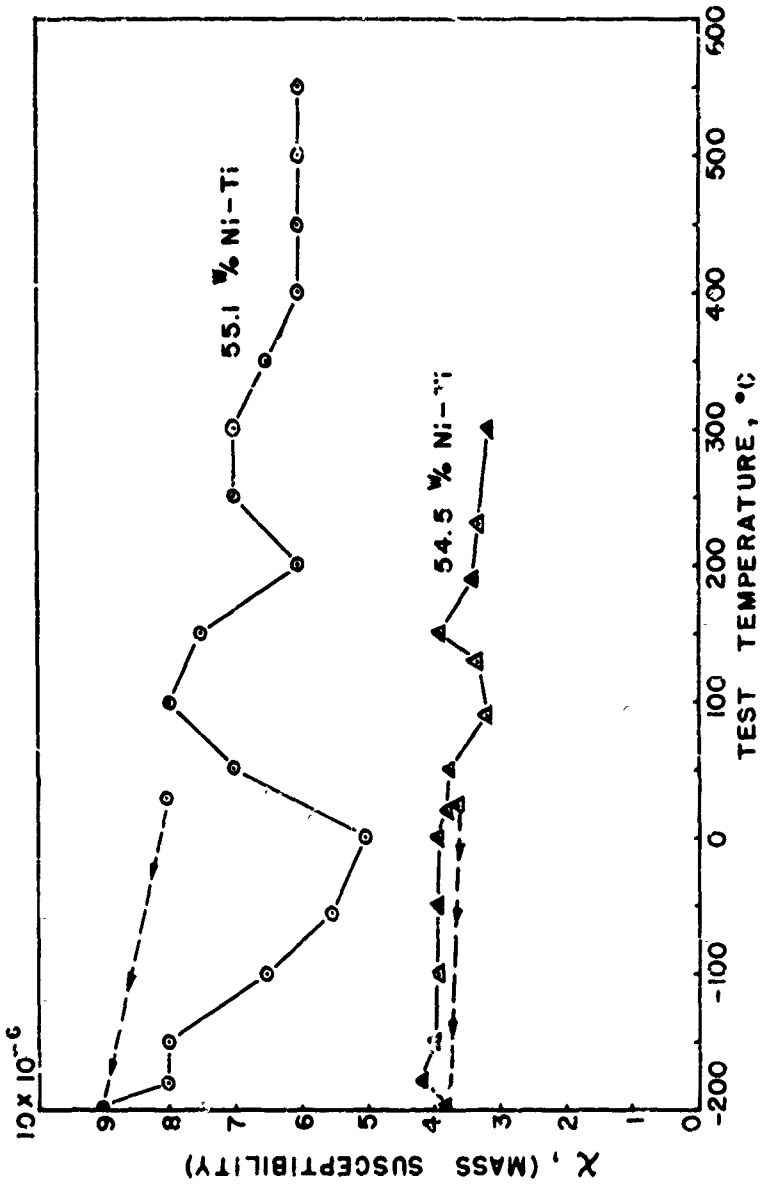

FIG. 22 MAGNETIC SUSCEPTIBILITY OF TWO Ni-Ti ALLOYS AS A FUNCTION OF TEMPERATURE.

given in Fig. 18. It is interesting to note, in the various parts of Fig. 6, that the quantity of these extraneous phases varies with temperature. The damping phenomena, as measured by low frequency internal friction measurements and qualitative high frequency sound tests, confirms this finding.

The damping phenomena as observed in the 54.5 w/o Ni alloy appears to be most closely associated with the general category of damping due to solute atoms or more specifically, transformation-type damping. As indicated by the X-ray diffraction studies, there is a change in phase-equilibria in this alloy as the temperature is raised from ambient. Heating to the 120 through 180°F (49-82°C) range appears to produce a more phase-pure TiNi structure. This phase purity seems to be further enhanced by the presence of iron up to 0.1 w/o which tends to stabilize the TiNi phase at lower temperature levels. At first it appeared that if a phase pure TiNi material existed the damping capacity would be very low. However, this idea is contradicted by the poor damping capacity of a 54.8 w/o Ni alloy and higher Ni alloys at room temperature, these alloys being far less TiNi phase pure than the 54.5 w/o Ni-Ti alloy. Based upon these observations it appears that the damping capacity of the TiNi phase alloys are drastically affected by the Ti_2Ni phase or impurity phases. This is confirmed by the fact that departing from stoichiometry on the nickel-rich side (increasing the presence of $TiNi_3$ phase) produces a low damping capacity around ambient temperatures. Conversely, going to the titanium-rich side of TiNi (increasing the presence of Ti_2Ni phase), causes these alloys to dampen vibrations readily around ambient temperatures.

X-ray diffraction scans on the 54.5 w/o Ni alloy, at varying temperatures, were able to depict a change in phase-equilibria but were unable to tell which phase(s) (possibly Ti_2Ni or $TiNi_3$) was changing in magnitude. This X-ray diffraction limitation was due to the constructive interference produced by the reflections from the Ti_2Ni and $TiNi_3$, making it virtually impossible to be certain which of the extraneous phases has changed.

The major differences that exist in the damping characteristics of the arc-cast and hot worked alloys, shown in Figs. 7 and 8, may be due in part to precipitation of extraneous phase(s) with hot work and the added effects of grain boundary internal friction.

While investigating the difference in damping characteristics between arc-melted and hot worked material, residual casting stresses in the arc-melted bars were considered as a possible cause of the difference. The stress-dependent idea was eliminated by annealing arc-cast bars for prolonged periods of time at 900°C in an argon atmosphere followed by furnace cooling. These stress-relieved bars were tested and found to possess the

same damping characteristics as the "as cast" unrelieved bars.

On the basis of the torsion pendulum tests supplemented by X-ray diffraction, hardness, and electrical resistivity data, it appears that a major portion of the damping phenomena is directly associated with the phase-equilibria existing in the alloy at a given temperature. Other internal friction mechanisms may contribute to a lesser degree. Some of these mechanisms which may be pertinent are dissolved interstitial atoms and their effect on dislocation movement, and degree of atomic ordering present in the system - more complete order providing for easier dislocation movement. Damping has been found by previous investigators to be inversely proportional to degree of order, the highly ordered materials being less capable of attenuating mechanical vibration.

In summary, it must be agreed that the constitution of alloys in the composition range of TiNi is not a simple relation [9,21]. This is especially true at the lower temperatures, both above and below ambient. In this temperature range minor variations in temperature cause proportional changes in the existing phase-equilibria[21]. Some of these phase transformations require a time of relaxation or like most chemical processes are capable of being expedited by slight increases in temperature.

One important fact uncovered in the present investigation was the conclusive evidence of the existence of the TiNi phase at room temperature and below. Some form of external energy, e.g., working, working plus heat, etc., is required to cause its dissociation. Why the TiNi-type alloys undergo a martensitic-like transformation with surface abrasion, heat, or both, and the relationship of this with the kinetics of the $TiNi \rightarrow Ti_2Ni + TiNi_3$ dissociation reaction remains for further study.

Metastability is common in many important metallurgical systems, e.g., quench hardened steel, precipitation hardened non-ferrous alloys and the existence of Fe_3C in steels in preference to its dissociation products of iron and graphite. As with other systems, the thorough understanding of the dissociation mechanism and metastability of the TiNi phase may possibly lead to the development of important engineering alloys.

ENGINEERING PROPERTIES OF TiNi AND TiNi-BASE ALLOYS

Concurrent with the constitution investigations of the TiNi phase in the titanium-nickel alloy system was a significant effort to obtain mechanical property and engineering data; particularly data that might be related to constitutional changes occurring in the TiNi and TiNi-base

materials. Without further discussion these data are presented below:

1. Hardness

Hardness measurements were made at temperatures ranging from as low as about -103°F (-75°C) up to 1800°F (982°C). For the hardness measurements between -103°F (-75°C) and 212°F (100°C) a modified Rockwell tester was employed. This tester was equipped with an immersion bath for either heating or cooling the anvil, specimen, and indenter. Rockwell testing was preferred because of the quickness of the test and the gross indentations made by the diamond indentor, the latter being important in measuring the "average" hardness of coarse structures.

Hot hardness measurements were performed in the proprietary tester shown in Fig. 23. This tester uses a diamond pyramid ground sapphire indenter mounted in a molybdenum holder. The indenter, anvil, and specimen are heated to a given temperature by radiation from a tungsten resistor element. The entire test assembly, including heat shields, is mounted inside an evacuated water-cooled chamber. The average gas pressure during the run is about 5 microns. Through specimen manipulation during the run, it is possible to make a complete series of hardness measurements at various temperatures without opening the heating chamber.

Table IV gives hardness data at room temperature for TiNi, Ti_2Ni, and $TiNi_3$. For these tests the TiNi alloy was of the 55.1 w/o Ni composition, which was found to be slightly nickel-rich. As a result, it can be seen in Table IV that the room temperature hardness increases with an increase in rolling temperature. The rapid cool, from rolling temperatures in excess of about 900°C, produces this hardening. The actual hardening phenomena in nickel-rich alloys will be discussed in more detail in a subsequent section of this report.

From the data of Table IV it can also be seen that while the Ti_2Ni compound alloy is quite hard (53 R_c), the $TiNi_3$ compound has a hardness (34 R_c) more like that of the TiNi alloy. Yet in spite of the much lower hardness exhibited by $TiNi_3$ it is similar to the Ti_2Ni compound in that it is brittle even at high homologous temperatures.

Fig. 24 shows a plot of hardness as a function of weight percent nickel, with the remainder of the alloy being essentially titanium. In this figure three curves are shown, these represent varying rates of cooling from a temperature range of 900 to 1050°C (1652 to 1922°F). Certain interesting facts are revealed by careful observation of the three curves. First, there is a minimum hardness composition attained in the Ni-Ti alloys

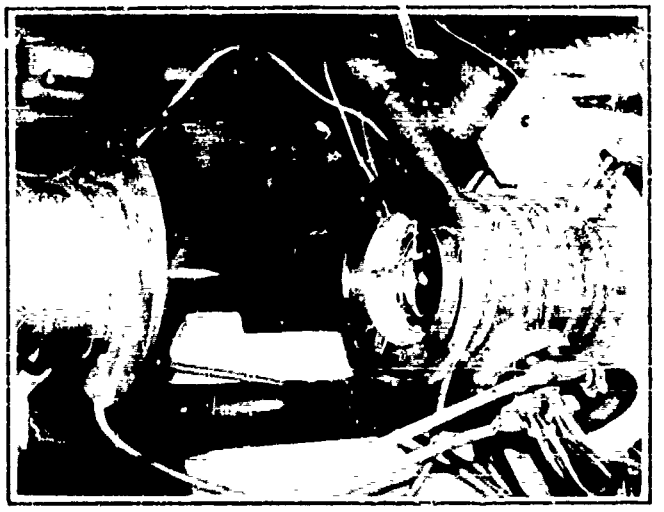

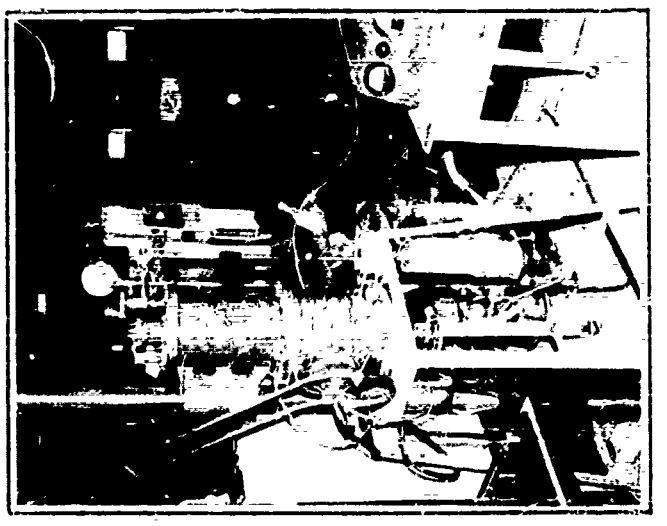

FIG. 23 TWO VIEWS OF THE HOT HARDNESS TESTER. PHOTO ON LEFT SHOWS TEST UNIT, VACUUM SYSTEM, AND POWER SUPPLY. PHOTO ON RIGHT SHOWS TESTER OPENED REVEALING SAPPHIRE INDENTER, HEAT SHIELDING AND THERMOCOUPLE LEADS.

TABLE IV

HARDNESS DATA FOR TiNi, Ti_2Ni, AND $TiNi_3$ COMPOSITIONS

Alloy Composition	Alloy Melting	Hot Rolling Temperature	Hardness	Remarks
TiNi*	Button Arc	As Cast	30 - 31 R_c	
TiNi	Button Arc	600°C	38 R_c	Hot rolled from about .3" to .1" some edge cracking
TiNi	Button Arc	700°C	38 R_c	Hot rolled from about .3" to .1"
TiNi	Button Arc	950°C	32 - 34 R_c	" " " "
TiNi	Button Arc	1000°C	39 R_c	" " " "
TiNi	Button Arc	1100°C	39 - 41 R_c	" " " "
Ti_2Ni	Button Arc	As Cast	53 R_c	
Ti_2Ni	Button Arc	950°C	---	Cracked severely during initial pass through mill
$TiNi_3$	Button Arc	As Cast	34 R_c	
$TiNi_3$	Button Arc	1050°C	---	" " " "

* 55.1 w/o Ni-Ti

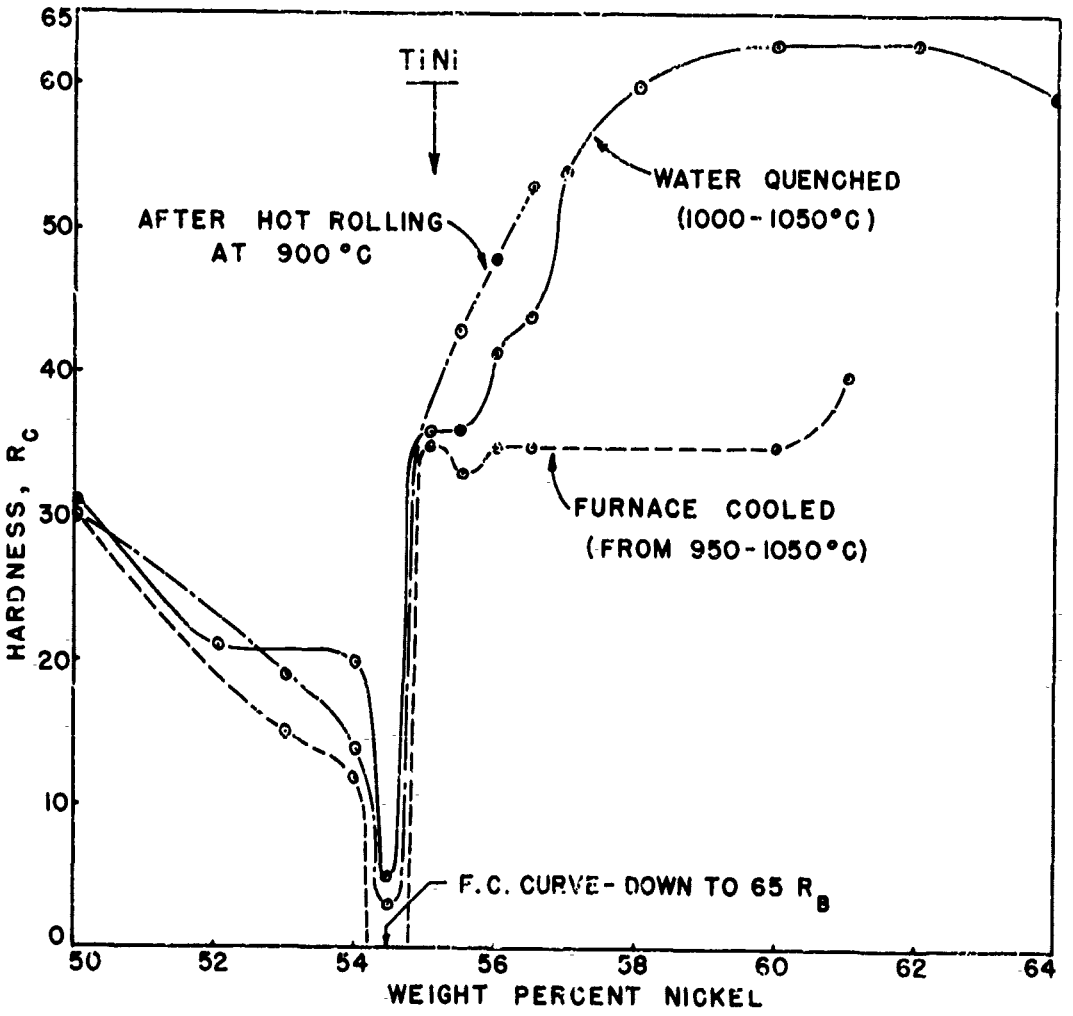

FIG. 24 HARDNESS AS A FUNCTION OF NICKEL CONTENT FOR VARIOUSLY TREATED TiNi ALLOYS

at about 54.5 w/o Ni. This made the present investigators suspicious of the 55.1 w/o Ni-Ti alloy as representing the stoichiometric composition. Subsequent X-ray diffraction studies confirmed the fact that the arc-melted 54.5 w/o Ni alloy gave a more phase-pure TiNi.

Another interesting piece of information obtained from observing Fig. 24 is that the alloys of about 55 w/o Ni and lower Ni content all yield about the same hardness regardless of the cooling rate. Alloys containing in excess of 55 w/o Ni produce a considerable hardness variation with cooling rate. Furnace cooling produces a constant hardness in the Ni-Ti alloys containing between 55 and 60 w/o Ni, while water quenching, and the rapid air cool from 900°C (1652°F) rolling temperature produces a marked increase in hardness. This hardness approaches about 62 R_c between 60 and 62 w/o Ni.

A possible explanation for the entire hardening behavior may be obtained by observing the left panel of Fig. 19. In this figure the homogeneity limits, of the tentative TiNi phase area, are approximately 53 and 57 w/o Ni below about 900°C (1652°F). In addition, there exists a retrograde solubility between the TiNi and TiNi + $TiNi_3$ phase areas in the temperature range from 900°C to 1110°C (1652°F to 2030°F). Based upon this constitution diagram, little hardness change with varying cooling rate would be expected between 53 and 57 w/o Ni. Also, some composition near stoichiometry should produce a near perfect TiNi phase. This was found to exist in the arc-melted button alloys at about 54.5 w/o Ni. An increase in Ni or Ti atoms by deviating either direction from stoichiometry, should produce a solution hardening effect - which actually occurs. In spite of the narrow composition for minimum hardness, little difficulty was encountered in melting additional alloys of the 54.5 w/o Ni composition and obtaining reproducible hardness results.

On the Ni-rich side, 55.1 w/o Ni and higher, it appears that by cooling rapidly from above about 900°C (1652°F) a disproportionate amount of Ni (probably as $TiNi_3$) remains intimately mixed as a fine dispersion in the TiNi matrix causing a drastic hardening of these Ni-rich alloys. This hardening phenomena is probably only possible because of the retrograde solid solubility between the TiNi and TiNi + $TiNi_3$ phases. Furnace cooling these same alloys containing excess nickel, allows an equilibrium coalescence of the $TiNi_3$ in a TiNi matrix and results in virtually no hardness change.

The existence of the wide gap between the "quenched" and "furnace cooled" curves of Fig. 24 (between 57 and 62 w/o Ni), made the prospect of "tempering" the quench-hardened alloys to intermediate hardnesses interesting. Through a pseudo-tempering heat treatment it was hoped that a closely controlled hardness would be possible with the associated improvement in properties - particularly toughness.

These pseudo-tempering studies were performed on the 60 w/o Ni-Ti alloy. First, suitable specimens of this alloy were quenched to about 61 R_c and following this they were heated for prolonged periods of time at temperatures from 600 to 900°C (1112 to 1652°F). Each specimen was heated at a different temperature, followed by a still air cool. Fig. 25 shows the results of these treatments. As expected, the 600°C (1112°F) tempering temperature caused only a minor drop in hardness and leveled off after about 30 minutes at about 58 R_c. The 700°C (1292°F) temperature produced a considerable drop in hardness down to about 44 R_c and also leveled off after about 30 minutes at temperature. The 800°C (1472°F) and 900°C (1652°F) tempering temperatures produced less hardness drop than was experienced at 700°C (1292°F). The unusual behavior of the 800 and 900°C tempering treatments further pointed up the influence exerted by the retrograde solid solubility change discussed earlier. From these data it was decided that for tempering temperatures in excess of about 800°C (1472°F) the rate of cooling was the principal controlling factor in the determination of the resulting hardness.

This finding was confirmed by quenching the same specimens again, then heating at various temperature levels for one hour followed by furnace cooling. These data are shown in Fig. 26 and compared with the results obtained by air cooling in still air. Now it can be seen from Fig. 26 that the tempered hardness decreases steadily as the treating temperature is increased. By employing furnace cooling the controlling factor influencing final hardness becomes the treating temperature.

Table V gives some data on the effect on hardness produced by varying the cooling rate. From these data it can be seen that widely varied intermediate hardnesses are possible by heating into the retrograde solubility temperature range followed by a controlled cooling rate.

At the time of the preparation of this report no data were available on the relationship between the pseudo-tempered hardness and other mechanical properties, e.g., impact strength, tensile strength, elongation, Young's modulus, etc. This study is currently being performed and will be reported later.

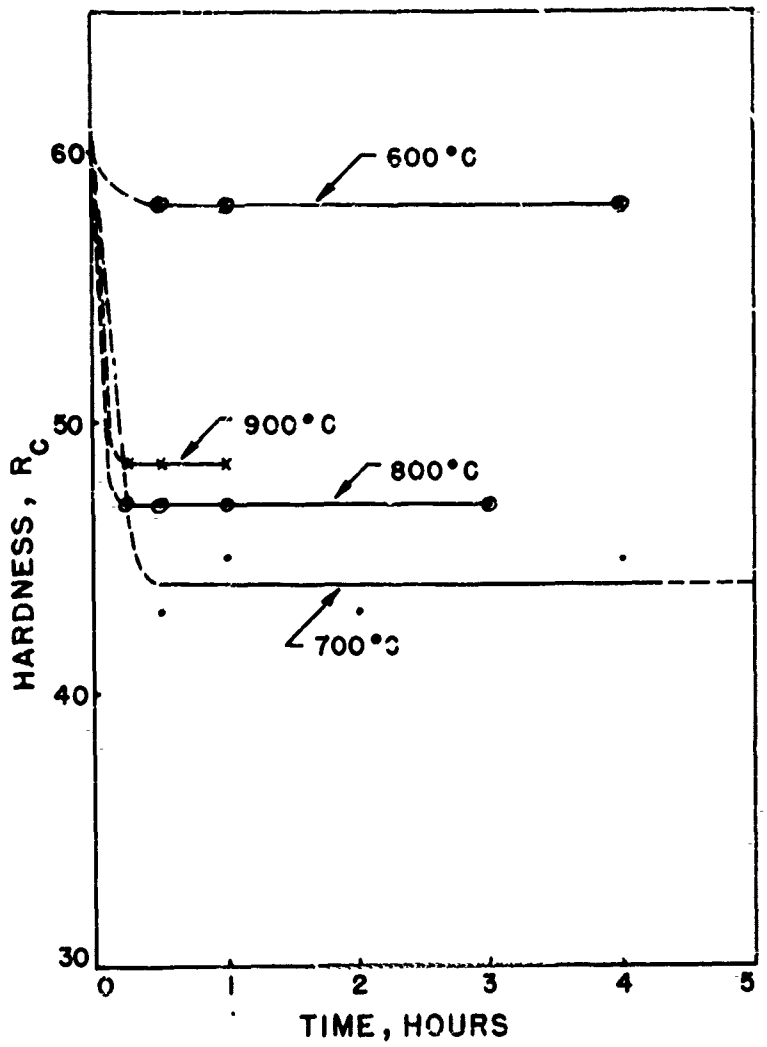

FIG. 25 HARDNESS CHANGES OCCURRING IN QUENCHED 60 % Ni-Ti ALLOY WHEN REHEATED AT TEMPERATURES FROM 600 TO 900°C.

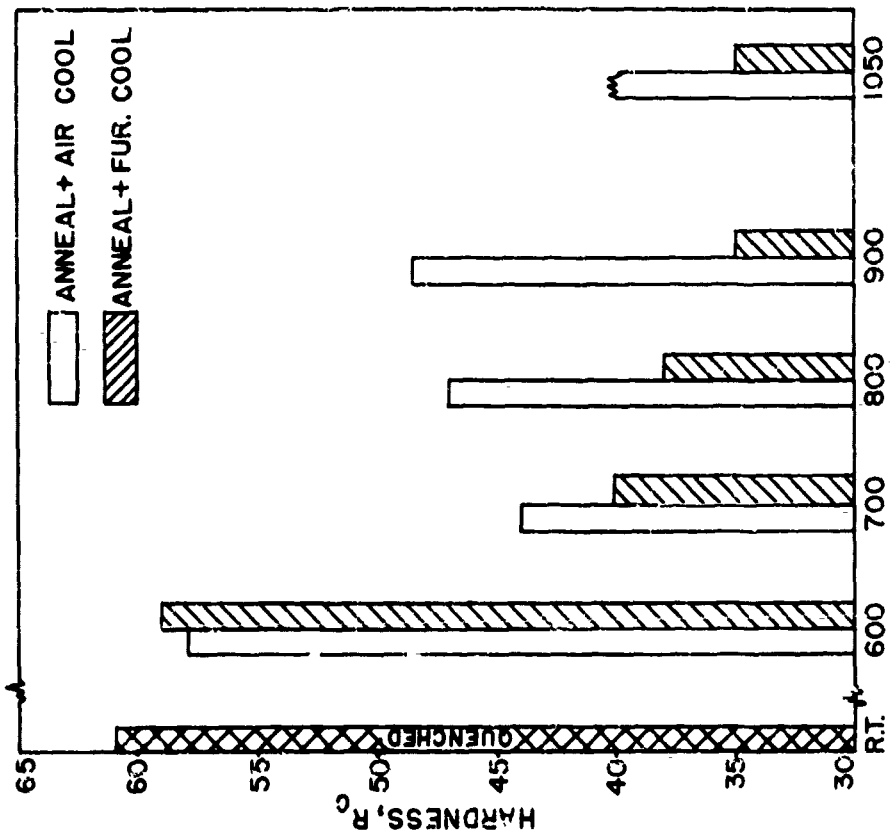

FIG. 26 SHOWS THE EFFECT OF COOLING RATE ON FINAL HARDNESS OF A 60 % Ni-Ti ALLOY GIVEN A POST-QUENCH ANNEALING TREATMENT

TABLE V

EFFECT OF COOLING RATE ON THE
RESULTING HARDNESS OF 60 w/o Ni-Ti ALLOY

Nominal Alloy Composition w/o	Thermal Treatment*	Hardness **	
		R_A	R_C (By Conv.)
60 Ni - Ti	1050°C, 20 min. H_2O Quench	82	61
60 Ni - Ti	1050°C, 20 min., Air Cool	76.5	51
60 Ni - Ti	Heated and Cooled in Stain. St. Block 1-1/2" D. x 1-1/2" - 1050°C, 90 min., cooled in vermiculite	70	39
60 Ni - Ti	H_2O Quenched from 1050°C followed by 650°C, 1/2 hour, furnace cooled	71	41

* Specimen: - 1/2" diameter cylinder about 1/2" long.

** Hardness data taken from a carefully prepared flat on the side of the cylinder.

It was decided to measure hardness near ambient temperature after the X-ray diffraction investigations revealed changes in phase-equilibria with minor temperature changes. These measurements were performed at temperatures between about -75°C (103°F) and 100°C (212°F) on a modified Rockwell tester. A summary of the hardness data obtained on six specimens, varying from 50 to 60 w/o Ni, is given in Table VI. Probably the most significant part of these data is the variation in the values of Δ Hardness$_{max}$ given in the bottom row of the table. It conclusively indicates that the major changes in hardness (and phase-equilibria) are occurring, in this temperature range, at or near the stoichiometric TiNi composition. In this same vein Fig. 27 is given to show the hardness hysteresis effects, particularly at the lower temperatures. These data corroborating the time-dependent relaxation phenomena revealed in the 54.5 w/o Ni alloy by X-ray diffraction, internal friction, and electrical resistivity measurements.

In addition to the hardness studies performed at and around room temperature, some effort was devoted to determining hardness at temperatures up to 1800°F (982°C). Using the hardness tester previously described, hot hardness measurements were made on Ti_2Ni, $TiNi_3$ and TiNi. In the case of the TiNi compound, both the 54.5 and 55.1 w/o Ni alloys, in the furnace cooled and rapid cooled condition, were studied. The hardness data for all of the above compound systems are shown in Figs. 28 and 29.

Observing the curves of the TiNi compositions (54.5 and 55.1 w/o Ni) it can be seen that in both cases the rapidly cooled specimens underwent a well defined secondary hardening phenomena at a temperature slightly below 900°F (482°C). Similarly, the same compositions when furnace cooled exhibited an almost continuous hardness decrease with temperature increase. As previously mentioned, these secondary hardening tendencies in the TiNi phase are believed to be related to the existing degree of order (superlattice) or presence of extraneous interstitial elements or phases based upon these elements. Westbrook[4], in his comprehensive review of the literature on intermetallic compounds, shows hardening peaks in Ni_3Al at higher temperatures. These he attributes to strain aging phenomena. Further, Westbrook[4] shows an increased magnitude in these peaks in Ni_3Al when the interstitial elements C, O, and N were introduced. However, the compound Ni_3Al is an A_3B type compared to the AB type of TiNi and there exists many irregular peaks in the Ni_3Al compared to the smooth, well defined single peak in TiNi. Also, it seems more than coincidence that this well defined peak should correspond so well with other physical changes in TiNi, e.g., resistivity, dilation, etc. This points strongly to order-disorder (or short-range to long-range) transformations as being responsible for the hot hardness behavior in rapidly cooled specimens. Westbrook[4] found that in the case

TABLE VI. HARDNESS DATA OBTAINED FROM Ni-Ti ALLOYS AT TEMPERATURES ABOVE AND BELOW ROOM TEMPERATURE

AVERAGE HARDNESS (R_A) OF VARIOUS ALLOY COMPOSITIONS (w/o)

Heating & Cooling Treatments	50 Ni - 50 Ti: Test Temp.,°C	F.C.*	Test Temp.	Quench*	53.5 Ni - 46.5 Ti: Test Temp.,°C	F.C.	Test Temp.	Quench	54.5 Ni - 45.5 Ti: Test Temp.,°C	F.C.	Test Temp.	Quench
Heating	25.5	67	22.5	65	26.5	70	27	61	See Graphs in Figure 24		See Graphs in Figure 24	
	38	63	39	67			33	60				
	52	69	52	67	53	73	52	61				
	62	68	66	68	62	72	65	60				
	72	63	79	67	72	72	79	60				
	85	59	93	67	85	71						
	94	69			93	71	94	59				
	102	67										
Cooling	92	68			85	71	85	59				
	79	66	79	68	74	71	79	59				
	73	67	64	67	65	71	66	59				
	65	67	54	68	51	71	52	61				
	47	67	44	68	47	69						
	38	69	39	68	39	71	39	61				
	34	69	25	68	33	70	27	62				
Cooling	23.5	69	20	69	22.5	69	25	59				
	12	67	10	69	10	67	20	60				
	-1	58	0	69	0	5	0	61				
	-10	69	-10	69	-10	6	-10	61				
	-20	69	-20	69	[illegible]	66	-70	63				
	-30	69	-30	69	-30	67	-30	62				
	-40	68	-40	69	-43.5	66	-40	62				
	-52	70	-50	69	-51	68	-50	63				
	-62	68	-60	70	[illegible]	68	-60	63				
	[illegible]	70	-71.5	69	-75	69	-71.5	64				
Heating	-55	70	-58	67	-60	69	-60	65				
	[illegible]	70	-39	70	-50	69	-50	65				
	[illegible]	70	-28	69	-37	69	-40	64				
	-20	70	-18	69	-21	69	-30	62				
	-9	70	-10	69	-10	63	-20	53				
	[illegible]	70	0	70	0	68	0	63				
	10	70	20	64	9	68	10	61				
	27	69	25	69	20	70	27.5	62				
Δ R_A max		4		4		9		6		7		20.5

Heating & Cooling Treatments	55.1 Ni - 44.9 Ti: Test Temp.,°C	F.C.	Test Temp.	Quench	56 Ni - 44 Ti: Test Temp.,°C	F.C.	Test Temp.	Quench	60 Ni - 40 Ti: Test Temp.,°C	F.C.	Test Temp.	Quench
Heating	22.5	65	25	59	23.5	69	23.5	72	27	60	24	76
	32	69	38	64			34	72	38	60	33	77
	47	71	52	66	48	74	52	73	66	59	52	77
	60	71	70	67	53	74	66	73			66	77
	73.5	70	79	63	72	73	79	73	73	60	79	77
	92	69			93	73	93	72	79	60	93	76
	103	69	95	64	107	71	105	69	100	59	110	76
Cooling	95	69	79	65	100	71	93	71	68	60	83	76
	79	69	64	66	93	71	79	71	79	59	79	75
	73	70			74	71	62.5	72	66	60	65	75
	66	70	52	66	65	71			[illegible]	60	52	75
	59	70			53	72			[illegible]	62	33	75
	45	69	38	65	44	72	39	71	37	60		
	27	63	25	52	28	70	27.5	72			23.5	70
Cooling	23.5	63	19	59	22	68	27	71	24	59	20.5	76
	10	65	10	55	10	66	10	71	10	63	10	77
	0	60	0	54	0	65	0	73	0	61	0	77
	-10	5	-10	52	-10	65	-10	73	-10	63	-10	77
	-20	55	-20	55	-20	65	-20	73	-20	62	-20	77
	-30	[illegible]	-30	53	-30	66	-30	74	-30	62	-31	77
	-40	55	-40	57	-40	66	-44	72	-40	63	-40	77
	-50	54	-51	59	-50	66	-45	74	-50	62	-50	78
	-69	59	-61	60	-70	63	-60	73	-60	65	-64	78
	-73	59	-74	62	-73	68	-70	72	-70	64	-74	78
Heating	-58	61	-60	60	-62	69	-60	74	-60	64	-60	78
	-35	62	-46	60	-52	69	-50	73	-40	64	-50	75
	-25	61	-40	59	-42	68	-40	73	-30	62	-33	77
	-16	59	-30	53	-22	68	-20	73			-20	77
	-5	62	-21	57	-2	69	-10	74	-20	[illegible]	-10	77
	12	67	-10	57	8	69	0	74			0	76
	18	70	0	57	12	69	10	73	0	63	10	77
	30	71	25	63	27	70	30	71	30	63	23	79
Δ R_A max		17		13		9		5		7		8

* F.C. = Heated 1 hour at 800°C (1472°F) in an argon atmosphere and furnace cooled.
Quench = Heated 1 hour at 800°C (1472°F) in an argon atmosphere and water quenched.

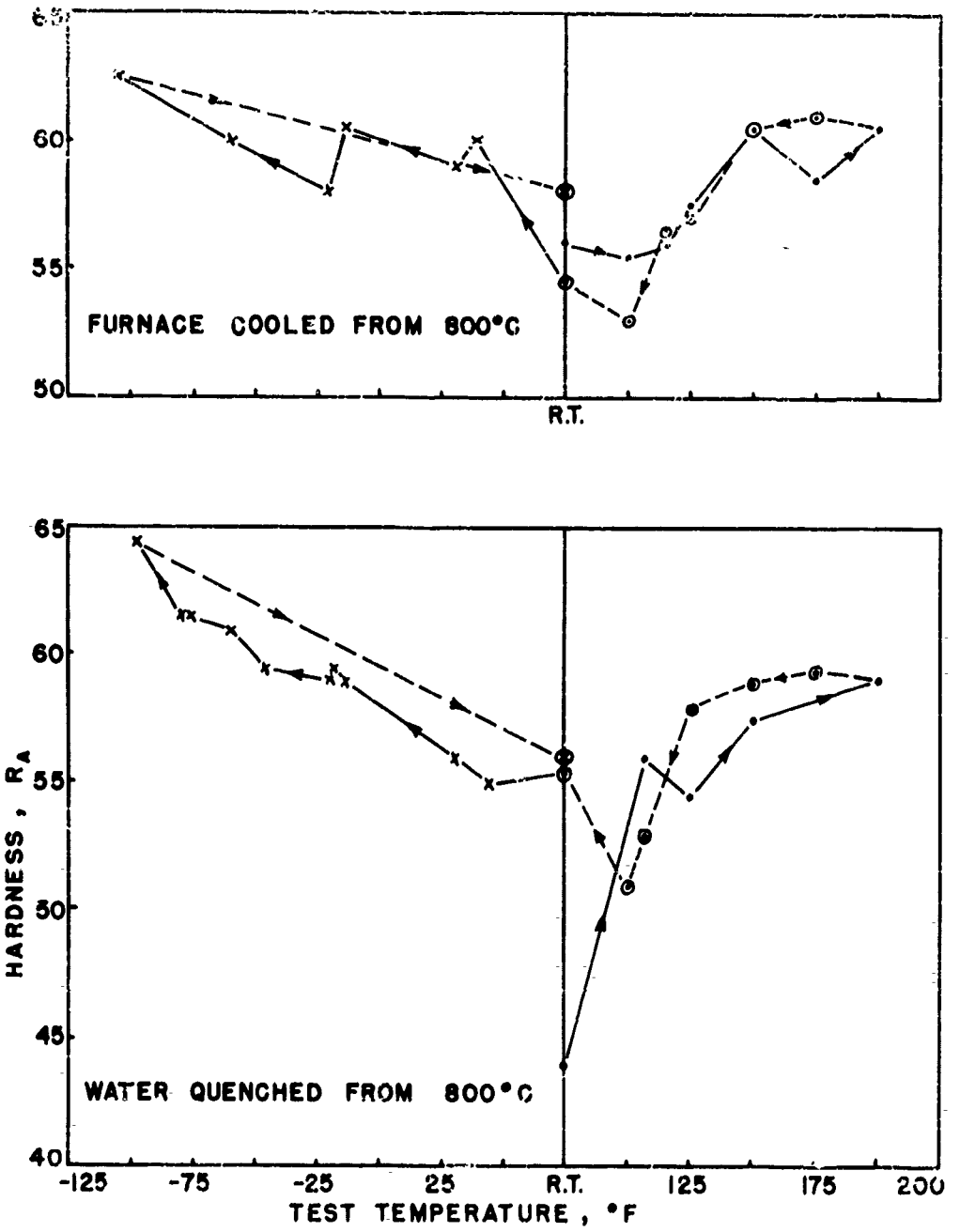

FIG. 27 CURVES OF HARDNESS AS A FUNCTION OF TEST TEMPERATURE FOR A 54.5 % Ni-Ti ALLOY GIVEN DIFFERENT INITIAL HEAT TREATMENTS.

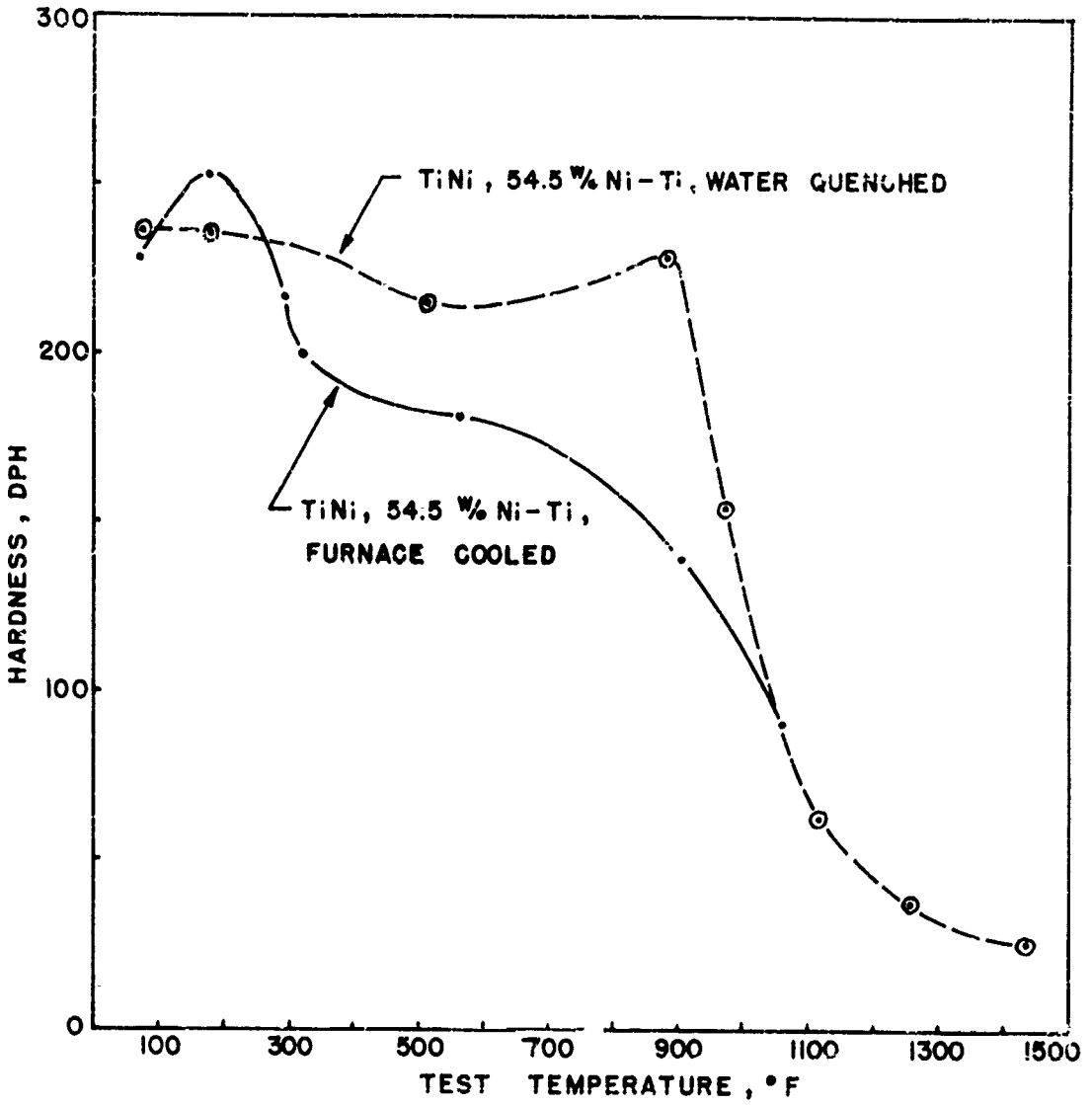

FIG. 28 HOT HARDNESS CURVES FOR WATER QUENCHED AND FURNACE COOLED 54.5 W% Ni-Ti ALLOY.

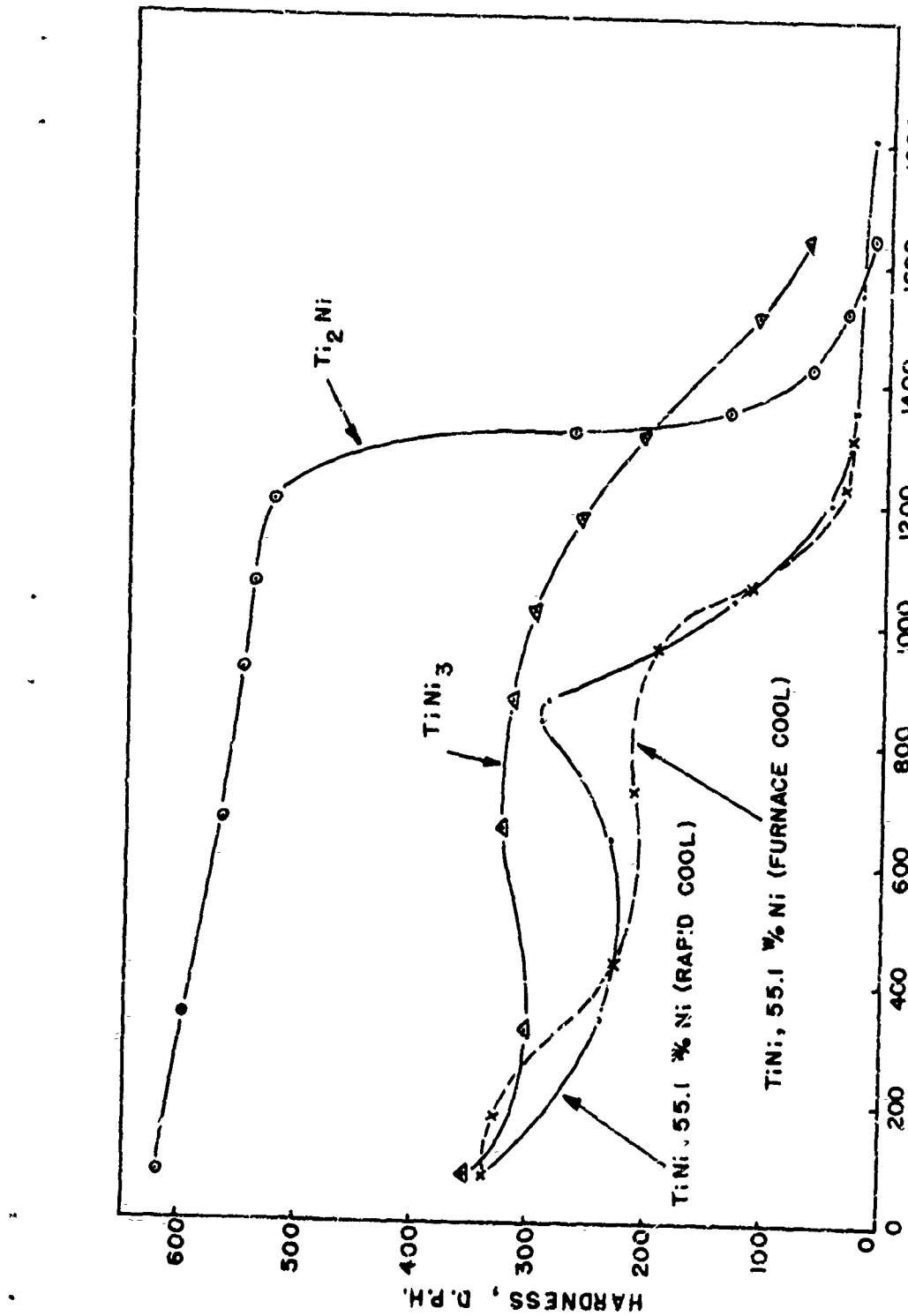

FIG. 29 SHOWING HOT HARDNESS DATA ON THE THREE INTERMEDIATE PHASES OF NICKEL-TITANIUM

of the AB type compounds AgMg and NiAl that the hardness of the stoichiometric compound was harder at very high homologous temperatures. While the non-stoichiometric alloy compositions were harder at the low homologous temperatures, he reasoned that at low fractions of the melting point, deformation proceeded primarily by slip, and any lattice defects constituted impediment to slip. While at the high homologous temperatures deformation is primarily diffusion controlled and hence a lattice imperfection, such as a vacancy defect, enhances diffusion.

Based upon Westbrook's anologies[4], it would appear that the rapidly cooled TiNi specimens were hardened by ordering transformations. This is particularly evident since the (100) superlattice line was noted in all of the room temperature X-ray diffraction scans, regardless of prior thermal treatment. Whether this forbidden (100) reflection, at ambient temperature, represents large domains of short-range order or long-range order remains in doubt. However, in the rapidly cooled TiNi specimens some atomic structural rearrangement appears to occur upon heating between about 600 to 900°F (316-482°C) that has a significant effect upon the elevated temperature slip mechanism. Further confirmation of the occurrence of this structural change was established by dilatometric measurements. A comparison of the hot hardness and differential dilation curves are shown in Fig. 30. Very real and significant slope changes are present in the dilation curve at a temperature corresponding to the peak in the rapid cooled hardness curve.

Order-disorder transformation theory[20] indicates that the order in an AB type alloy continuously changes with temperature. However, as the temperature increases the change becomes more rapid and finally becomes extremely fast, perhaps consummating in a long-range order or lattice perfection that restricts diffusion and promotes the associated increase in hardness.

Creep is related to hot hardness in that creep is a form of thermally activated plastic flow. While hardness (cold or hot) measures the resistance of a material to plastic deformation - usually by indentation. As a result, the same thermal activation that is an essential factor in creep should proportionally affect hardness measurements.

The hot hardness curves given in Figs. 28 and 29 are important from the standpoint of indicating the potential elevated temperature strength and creep properties in the essentially phase-pure Ni-Ti compounds. By observing these curves it can be seen that the expected creep rate would be high and the load carrying capacity low in TiNi above about 1200°F (649°C). Ti_2Ni should exhibit excellent elevated temperature strength

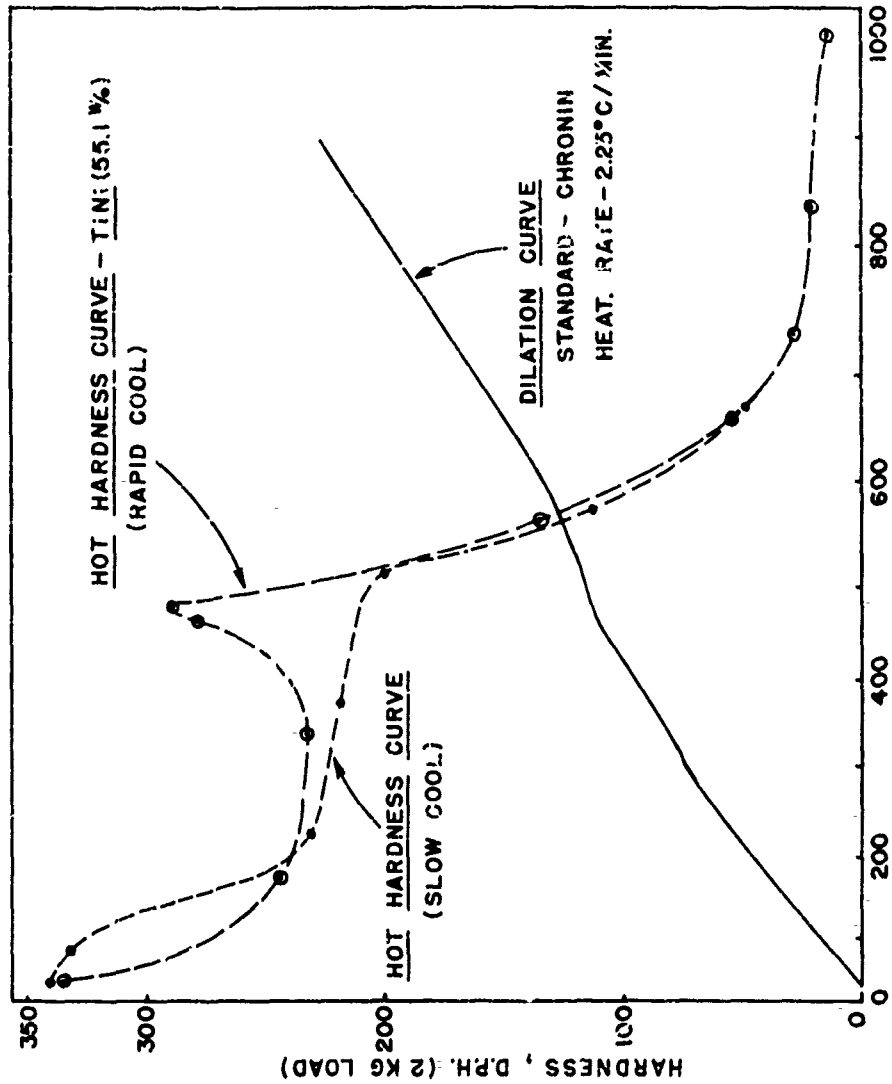

FIG. 30 SHOWS CURVES OF HOT HARDNESS AND DIFFERENTIAL DILATION PLOTTED ON THE SAME TEMPERATURE AXIS. NOTE CHANGES IN SLOPE OF THE DILATION CURVE AT A TEMPERATURE CORRESPONDING TO THE SECONDARY HARDENING PEAK.

to 1200°F (649°C) with a rapid decrease above this temperature. $TiNi_3$ should possess a lower strength than Ti_2Ni in the lower temperatures, but its maximum usable strength capabilities seem to extend up in the vicinity of 1600°F (871°C).

Though the $TiNi_3$ and Ti_2Ni appear more useful from an elevated temperature standpoint, their brittleness at all temperatures limits their usefulness as single-phase structural materials. TiNi, on the other hand, does not suffer these same brittleness problems. What then would be the elevated temperature strengthening effect of introducing one or both of these brittle phases into a ductile TiNi matrix? A partial answer may be seen in the hot hardness curves given in Fig. 31. In this figure can be seen the significant hardening and strengthening effect at elevated temperatures produced by the addition of an excess of 5 w/o Ni. The second phase responsible for the persistent increased hardness of the TiNi matrix is undoubtedly $TiNi_3$. However, again as with the almost phase-pure TiNi, the maximum useful temperature appears to be 1200°F (649°C).

2. Tensile Properties

Tensile properties were measured on both the 54.5 and 55.1 w/o Ni alloys. In every case a standard specimen measuring 0.252" diameter x 1.0" gage length was employed. The actual test sections were finish lapped in the longitudinal direction to avoid any possible transverse notches. In a few instances the test sections and radii were electropolished to minimize notch effects. No noticeable advantage was obtained from electropolishing and this step was eliminated. To avoid oxidizing the prepared sample surfaces and minimize the possible interstitial element (O, N, H) pickup vacuum or controlled atmosphere heat treating was used. Vacuum heat treating was performed in an evacuated quartz tube.

The tensile test results obtained from the two TiNi alloys are given in Table VII. By observing these data several things become apparent. These are:

a. The ductility, as indicated by the percentage elongation, can go as high as 15.5%. With the average running more in the 7 to 10% range. Some of the lower values being produced by sample failure outside the gage length. For an intermetallic compound, even employing the more flexible definition (see introduction) this is an unusually high room temperature elongation.

b. The ultimate tensile strength tends to vary between about 110,000 and 140,000 psi. There appears to be little pattern to the

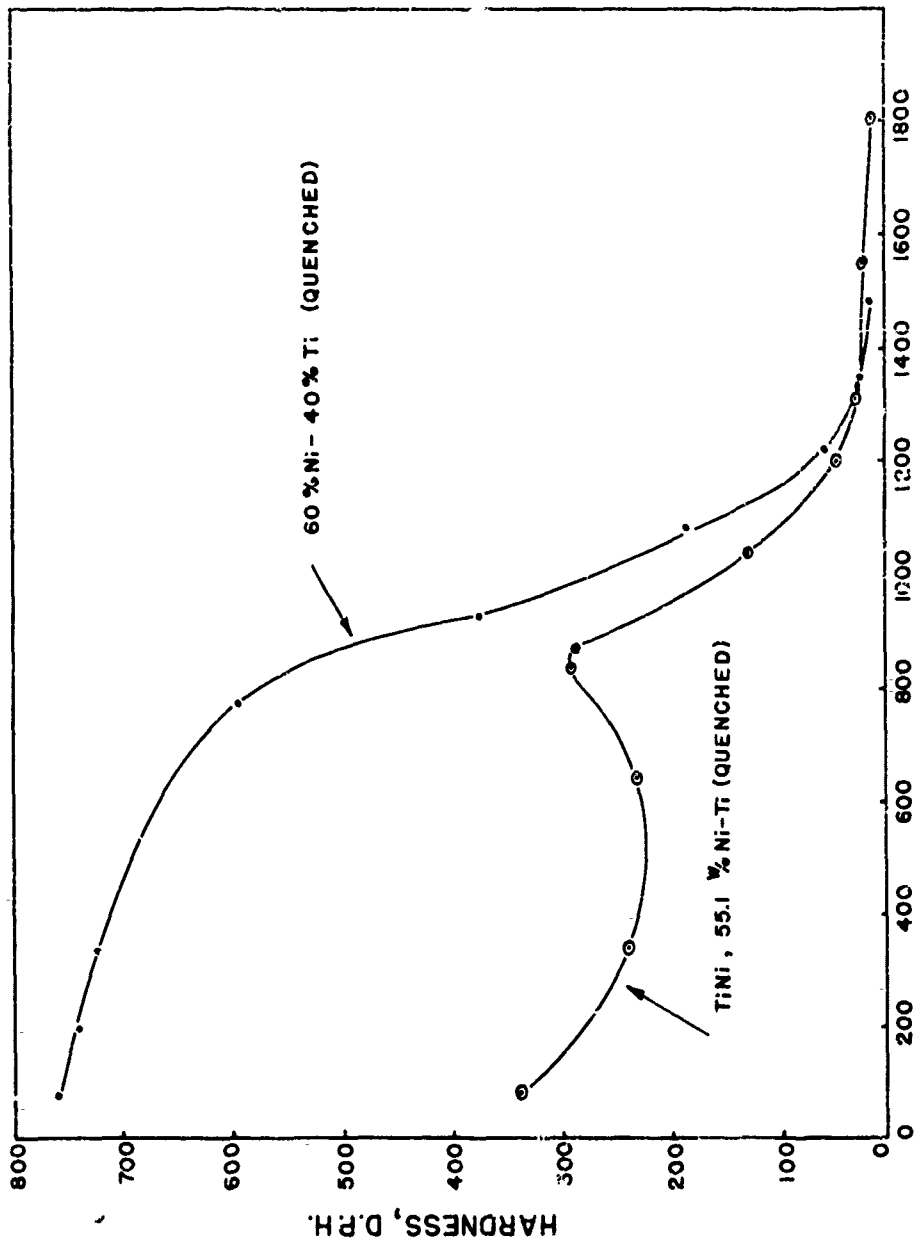

FIG. 31 SHOWING HOT HARDNESS DATA ON TiNi AND TiNi HARDENED BY $TiNi_3$

TABLE VII

TENSILE TEST D/ A**

Specimen Treatment	Ultimate Tensile Str., lbs/in²	Yield Strength lbs/in²	Elongation %	Reduction in Area %	Modulus of Elasticity, psi	Remarks
54.5 w/o Ni-Ti Alloy (room temperature)						
800°C 1 hour, furnace cooled*	112,100	40,000	8.1	--	11.6×10^6	Broke outside gage length
800°C 1 hour, water quench*	123,800	40,700	15.5	16.0	11.8×10^6	
54.5 w/o Ni-Ti Alloy (185 to 192°F test temperature)						
800°C 1 hour, furnace cooled*	110,500	46,800	3.6	--	11.1×10^6	Broke outside gage length
800°C 1 hour, water quench*	115,300	55,100	10.9	13.0	11.2×10^6	
55.1 w/o Ni-Ti Alloy (room temperature)						
Hot swaged at 900°C, air cooled	125,000	81,400	8.1	--	11.2×10^6	
1000°C 30 min., furnace cooled+	116,700	56,200	7.2	--	9.7×10^6	Hard. = 26 R_c
1000°C 30 min., furnace cooled+	114,200	33,600	3.2	--	10.4×10^6	Broke outside gage length Hard. = 24 R_c
1000°C 30 min., furnace cooled+	140,500	36,200	9.9	--	---	Hard. = 24 R_c
1000°C 30 min., water quench+	82,320	71,400	3.5	--	10.2×10^6	Hard. = 33 R_c
1000°C 30 min., water quench+	84,400	62,250	4.5	--	11.8×10^6	Hard. = 31 R_c

* Heat treatment performed in an argon atmosphere.
\+ Specimen sealed in an evacuated quartz tube during heat treatment.
** Tensile specimen size 0.252" dia. x 1.000" gage length.

relationship between heat treatment, composition, and ultimate tensile strength.

c. The yield strength, on the other hand, varies considerably with composition and heat treatment. The 55.1 w/o Ni alloy showing the greater spread in this property. This slightly Ni-rich alloy, with its increased extraneous phases (particularly $TiNi_3$) exhibits higher yield strengths in the rapidly cooled condition.

d. Modulus of elasticity on the average is fairly constant, regardless of composition or heat treatment, at slightly above 11. x 10^6 psi.

e. Little change occurs in the 54.5 w/o Ni alloy when the test temperature is raised to 185 to 192°F (85 to 89°C).

In general, it appears that the presence of minor quantities of a second phase(s) serves mainly to increase the yield strength level. However, more conclusive experimental evidence on the influence of these minor phases on mechanical properties is needed. Future plans of the present investigators call for cooling tensile specimens of the 54.5 w/o Ni alloy to sub-ambient temperatures followed by rapid warming to room temperature and immediate testing. Through this sub-ambient treatment it will be possible to dissociate some of the TiNi into Ti_2Ni and/or $TiNi_3$ (see Fig. 6). The quantity of the extraneous phase(s) can be controlled by the cooling temperature and time. The long relaxation times at room temperature for the transformation back to TiNi phase should allow sufficient tensile testing time.

3. Impact Properties

For these tests very carefully prepared unnotched square cross-section bars were used. The specimen surfaces were hand lapped in the longitudinal direction to minimize transverse scratches. The Charpy impact tests were performed in a standard Riehle machine. The resulting data are given in Table VIII.

Again, as in the case of the tensile elongation, the present investigators were pleased with the unusually high impact strengths as compared with most intermetallic compounds. For both of the TiNi alloys the minimum value was 23 ft-lbs even on the undersize specimens (0.296" sq). In both the 54.5 and 55.1 w/o Ni alloys the impact strength was enhanced by cooling the specimen to a test temperature of -112°F (-80°C) prior to testing. This is again undoubtedly related to the change in phase-equilibria and will require additional investigation to explain the phenomena. From

TABLE VIII

IMPACT DATA FOR TiNi COMPOSITION ALLOYS*
GIVEN PRIOR THERMAL TREATMENTS AND AT VARIOUS TEST TEMPERATURES

Nominal Alloy Composition	Specimen Section Size	Conditions of Test	Charpy Impact ft-lbs
54.5 w/o Ni-Ti†	0.296" x 0.296"	Test Temperature: 75°F (R.T.)	28
54.5 w/o Ni-Ti†	0.296" x 0.296"	Test Temperature: 125°F	32
54.5 w/o Ni-Ti†	0.296" x 0.296"	Test Temperature: 200°F	29.5
54.5 w/o Ni-Ti†	0.296" x 0.296"	Test Temperature: -112°F	40
54.5 w/o Ni-Ti†	0.296" x 0.296"	Cooled to -112°F, Warmed in R.T. water, stabilized 15 min. in R.T. air	23
54.5 w/o Ni-Ti†	0.296" x 0.296"	Cooled to -112°F, Warmed in R.T. water, stabilized 15 min. in R.T. air, plus heat to a test temperature of 160°F	25
55.1 w/o Ni-Ti††	0.297" x 0.297"	Test Temperature: 75°F (R.T.)	24
55.1 w/o Ni-Ti††	0.297" x 0.297"	Test Temperature: 200°F	28
55.1 w/o Ni-Ti††	0.297" x 0.297"	Test Temperature: -112°F	43

* Unnotched square cross-section bars were employed.
† Specimens prepared from hot swaged (900°C) bars.
†† Specimens prepared from hot rolled (900°C) plate.

Table VIII it can also be seen that heating to a test temperature of 200°F (93°C) improved the impact strength only slightly.

4. Recrystallization and Grain Growth

If a metal or alloy is deformed below its recrystallization temperature it is said to be "cold worked." In this condition the grains are no longer polygon shaped but instead are elongated in the direction of working. Under a process of "recrystallization" the atoms present in the material rearrange themselves into an entirely new set of crystals. This rearrangement starts from very small nuclei which grow until all of the cold worked material is consumed. The resulting process lowers the free energy of the system. When recrystallization is complete and the recrystallization temperature is exceeded some of the new grains further increase in size at the expense of their neighbors. The driving force behind this phenomena being once again a reduction in the free energy of the system.

Studies to determine the recrystallization temperature and grain growth behavior were undertaken since it was possible to cold work (by rolling) the TiNi alloy below its recrystallization temperature. These studies resulted in the graphical data given in Figs. 32 and 33. Fig 32 shows the effect on hardness of heating cold reduced specimens (4.95 to 21.75%) one hour at various temperatures. As might be expected the initial room temperature hardnesses increased proportionally with the degree of cold reduction. All the specimens in Fig. 32, with the possible exception of the 21.75% cold reduced specimen, increased in hardness with heating one hour at 400°C (752°F). Then the hardness of all of the specimens dropped drastically at about 600°C (1112°F). This sharp hardness drop indicating the TiNi recrystallization temperature. Metallographic examination of the same specimens confirmed the 600°C (1112°F) recrystallization temperature.

Fig. 33 shows the grain growth effects of one hour at two heating temperatures, 800°C and 1000°C (1472°F and 1832°F). Normal grain growth behavior prevails in this alloy in that the grain growth tendency is greatest in the specimens given the least cold reduction. The inset in this figure shows a photomicrograph of a 13.4% cold reduced specimen after heating at 800°C (1472°F). In many cases much effort was required to reveal the grain boundaries, as shown in this photomicrograph, by chemical etching.

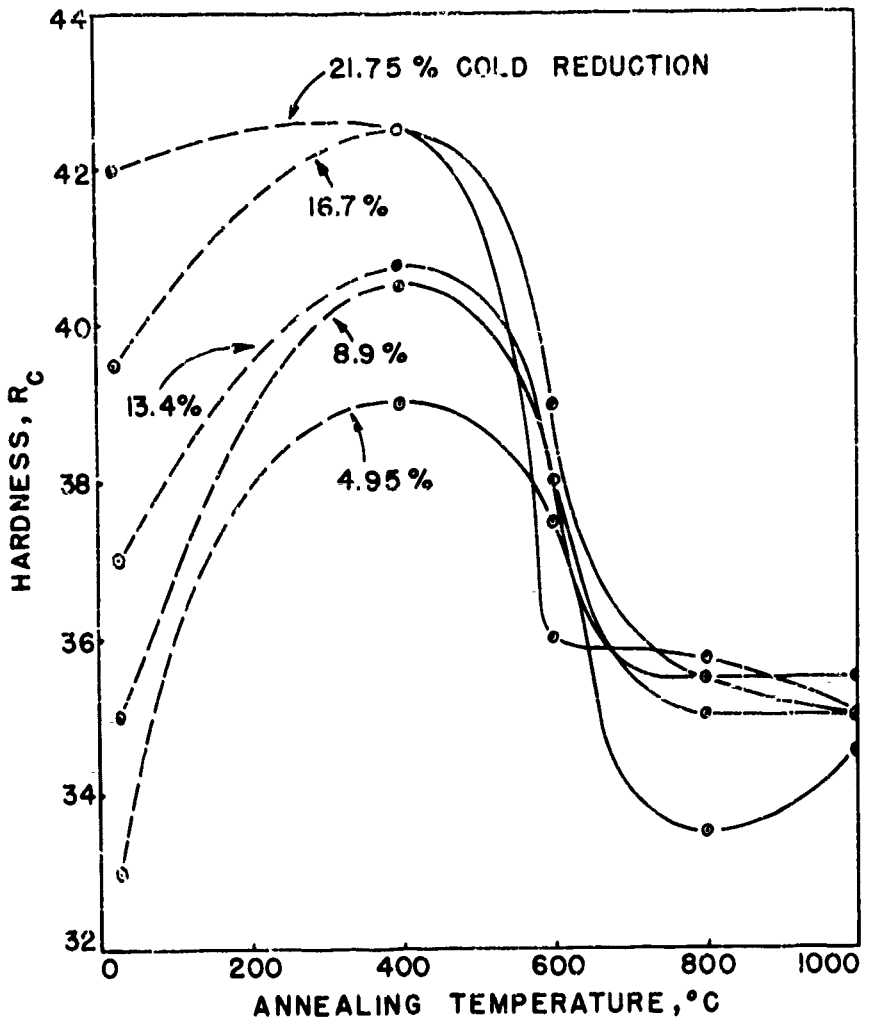

FIG. 32 HARDNESS CHANGES OCCURRING IN COLD REDUCED TiNi COMPOSITION SPECIMENS HEATED 1 HOUR AT INCREASING TEMPERATURES

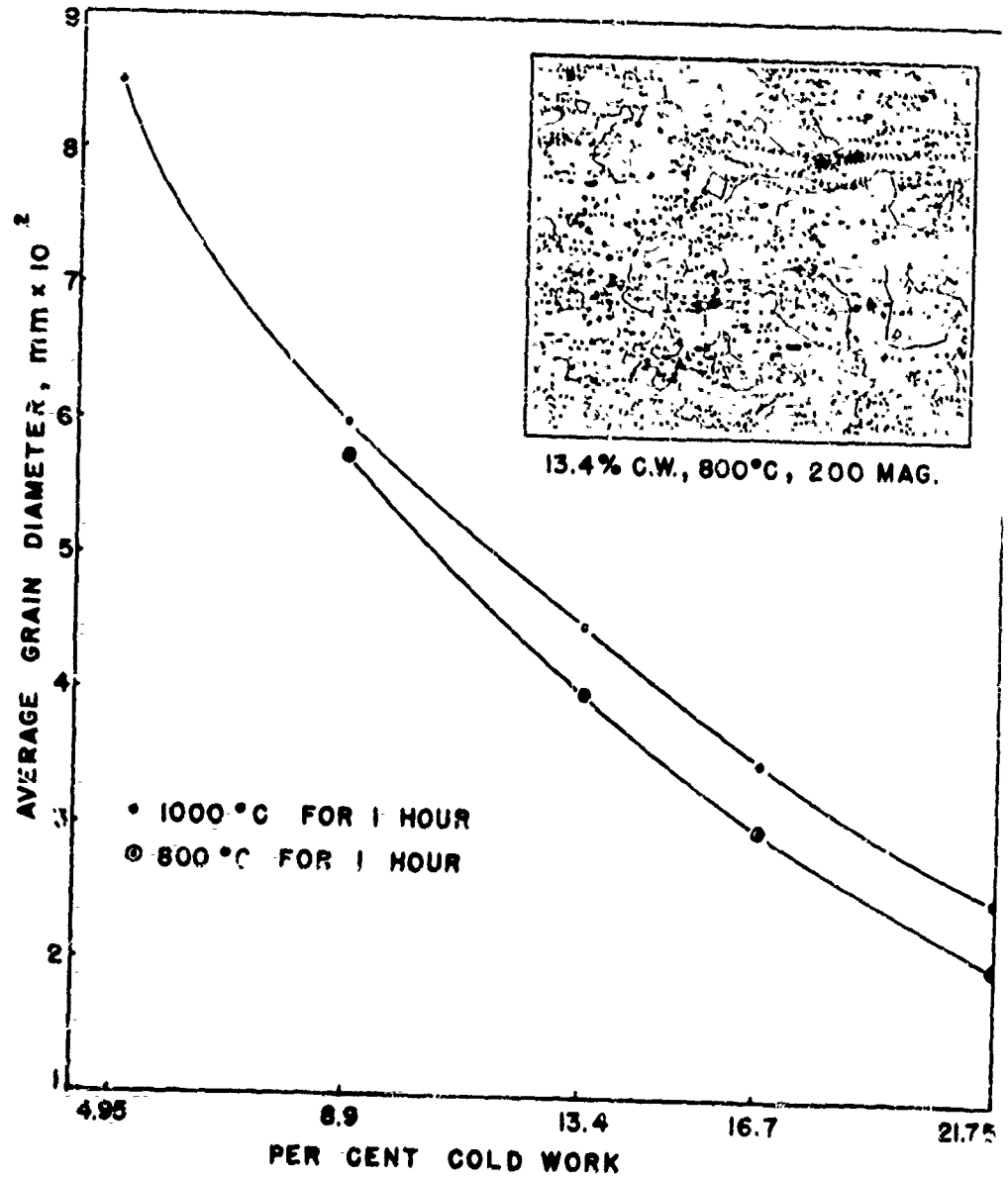

FIG. 33 CURVES SHOWING EFFECTS OF HEATING 1 HOUR AT 800 AND 1000 °C ON THE GRAIN SIZE OF VARIOUSLY COLD WORKED TiNi ALLOY

5. Welding

Joining is an extremely important consideration in present day structural materials. To have some idea of the welding capability of the TiNi material a preliminary welding experiment was performed. This experiment consisted of butt welding together two chamfered 1/8" thick hot rolled plates of TiNi. Heliarc welding was chosen because of the high titanium content of the alloy. A feeder rod of hot swaged TiNi was fed into the joint and arc plasma during the welding operation. The resulting weld and its structure are shown in Fig. 34. Little difficulty was encountered in making the joint. The weld section appeared to be free of cracks and porosity. The fusion zone of the weld was characterized, for the most part, by a fine dendritic structure, this being typical of the cast structure of the alloy. A comparison of the hot worked base structure and the fine dendritic structure in the transition zone can be seen in the upper photomicrograph. The higher magnification photomicrograph, at the lower left of Fig. 34, shows angular and star-shaped particles of extraneous phases. Since their appearance is quite unlike the excess phases (Ti_2Ni and $TiNi_3$) shown in Fig. 18, it must be concluded that these are interstitial phases (based on N, O, H) formed during welding. Controlled atmosphere welding may be needed to eliminate these from future welds. No mechanical property tests have been made on the initial test weld. However, based upon the properties observed in arc-cast TiNi material, the weld section should be quite strong and tough. Cursory examination of the magnetic properties of the weld section indicate that it is equally as paramagnetic as the base pieces. Further work is planned on investigating both the mechanical and magnetic properties of TiNi welds because of the importance in non-magnetic ordnance applications.

6. Environmental Attack

Specimens of the TiNi composition were exposed to various common corrosive media and to elevated temperature oxidation attack. In the former, preliminary corrosion tests were conducted in salt spray, sea water, normal air atmosphere, and normal handling. The results of these tests are given in Table IX. In each case the attack was negligible and only in the salt spray tests was a perceptible whitish surface film formed where the specimen was held. The passivity of this alloy to corrosive attack is further characterized by the difficulty encountered in finding suitable etchants to attack the metallographic specimens.

Oxidation tests were performed in air at 600°C (1112°F), 800°C (1472°F) and 1000°C (1832°F). The carefully prepared specimens had Pt wires spot-welded to them and this was shaped into the form of a hook.

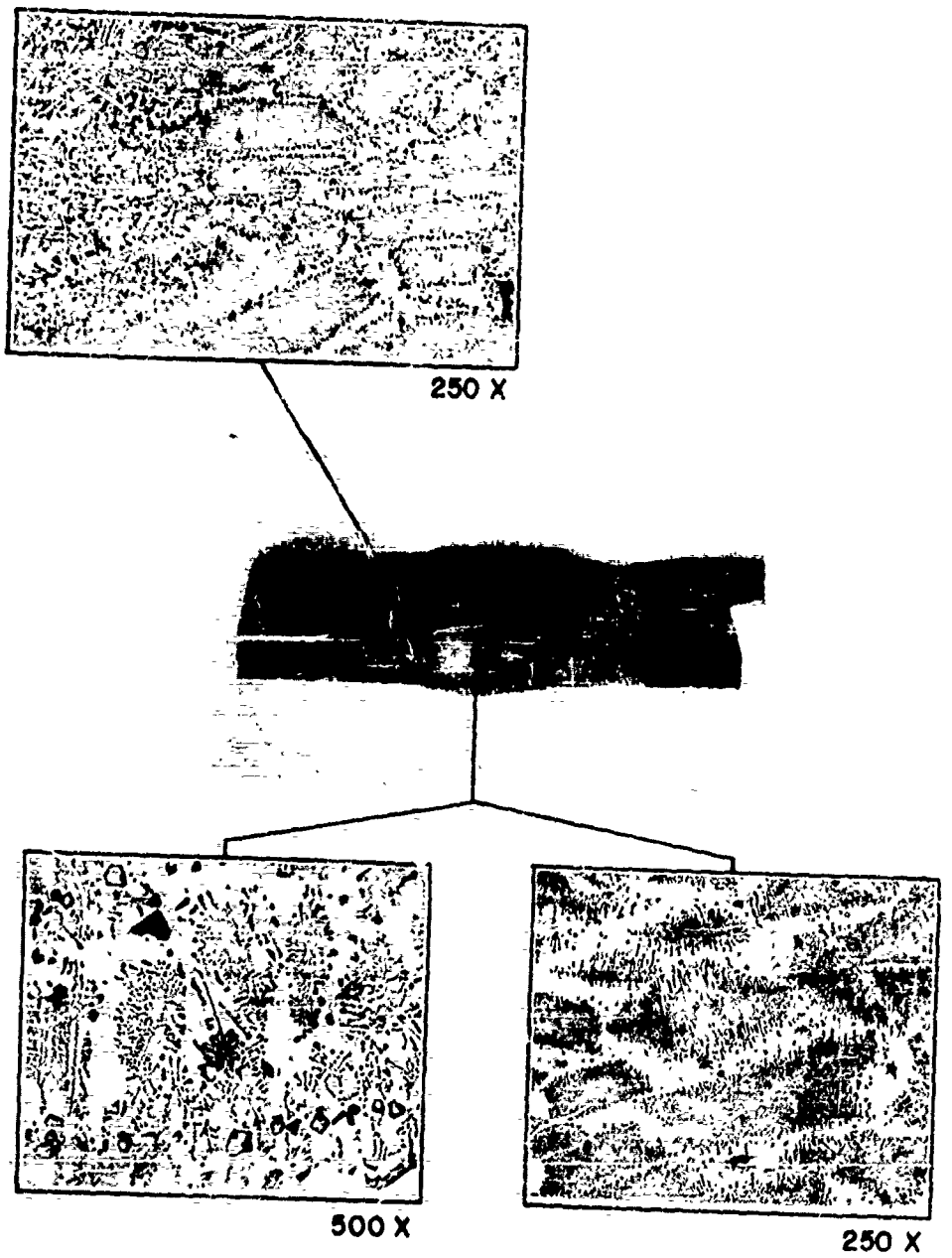

FIG. 34 SHOWING HELIARC WELDED TiNi ALLOY PLATES (2 PHOTOMICROGRAPHS OF PORTIONS OF WELD SECTION ARE ALSO SHOWN.

TABLE IX

CORROSION PROPERTIES OF THE TiNi (55.1 w/o Ni-Ti) ALLOY

CORROSIVE MEDIA	RESULTING ATTACK
Salt Spray - 20% soln., 95°F, for 96 hours	Faint whitish surface deposit on back edge of specimen
Sea Water - 192 hours	Nil
Normal Air Atmosphere	Nil
Normal Handling	Nil

Then the weighed specimens were hung on a ceramic rod over a stainless steel catch pan. In this way, it was possible to record the weight gain due to oxidation even if the oxide coating spalled off. The results of these tests are shown in Fig. 35. At 600°C (1112°F) the initial oxide coating was fairly thin and adherent and the rate of oxide buildup was almost negligible after the first two hours. At 800°C (1472°F) some oxide coating spalling occurred and after the first two hours oxidation proceeded steadily. At 1000°C (1832°F) the rate of oxidation was rapid from the beginning and oxide spalling was profuse.

7. Ternary Alloying

The possibility of strengthening the TiNi material, through solution or precipitation strengthening, was investigated. The addition elements chosen were silicon and aluminum. The effects of varying additions of these two elements are given in Table X. From this table it can be seen that the higher additions (4 w/o) produce a considerable hardening effect. This is probably due to the formation of other intermetallic compounds of the aluminide and silicide type. "Solution treating" was tried in each case but only the 2 w/o Si - TiNi alloy showed any tendency to respond.

8. Hard Facing

After discovering the hardening effect of aluminum on TiNi, an experiment in hard facing was tried. In this experiment pure Al was arc-melted into the top surface of a TiNi button. The button was cut in half exposing the cross-section of the fusion interface. The Al-rich hard facing was found to be too brittle and fragile to study. However, a knoop hardness traverse was made near the interface section. This is shown along with the microstructure in Fig. 36. Following the hardness indentations it can be seen that the weld interface is rather sharp, going from 23 R_c to 55 R_c. This condition is somewhat undesirable for the intended application. Melting a TiNi + 10 w/o Al alloy on a TiNi button also resulted in a sharp hardness transition. Perhaps some widening of the interface transition zone could be accomplished by a post-melting heat treatment to promote diffusion of the aluminum.

From this experiment another interesting observation is possible. The TiNi base material has a hardness of 23 R_c which is lower than the 30 to 35 R_c hardness experienced normally in this 55.1 w/o Ni alloy. One possible explanation for this behavior may be traced to a general lowering of the nickel content in this bordering area. The excess nickel diffusing to the interface and leaving an alloy composition approaching 54.5 w/o Ni with its associated lower hardness (See Fig. 24).

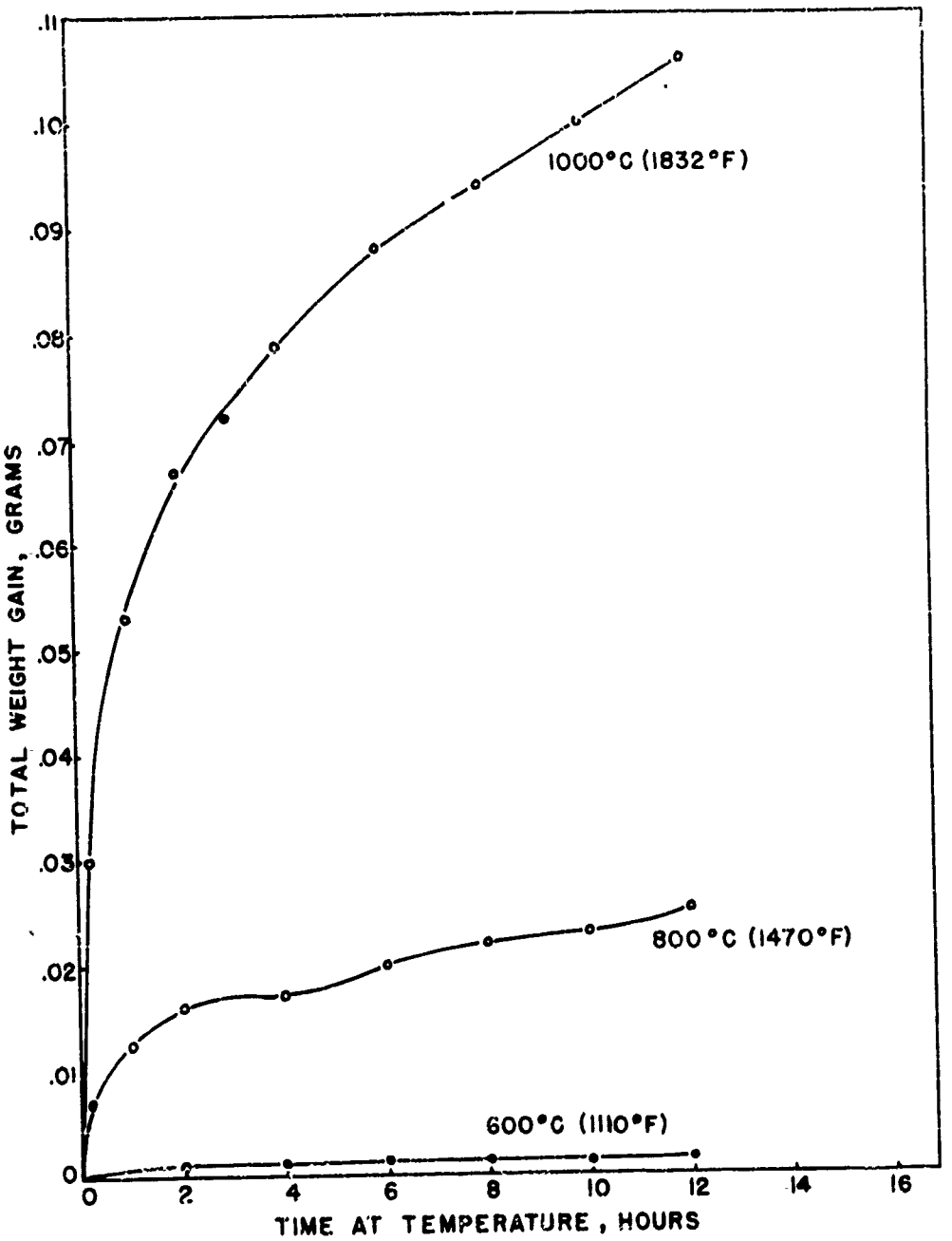

FIG. 35 RATE OF OXIDATION OF TiNi AT DIFFERENT TEMPERATURES. INITIAL WEIGHT OF SPECIMENS, APPROXIMATELY 6.5 GRAMS.

TABLE X

HARDNESS DATA OBTAINED ON TiNi-BASE ALLOYS* IN THE "AS-CAST" AND "SOLUTION TREATED" CONDITIONS

Charge Composition Weight, %	Hardness, R_c	
	"As Cast"	"Solution Treated" (900°C, 1/2 hr. Water Quenched)
TiNi + 2% Si	37	27
TiNi + 4% Si	43	43
TiNi + 2% Al	34.5	33
TiNi + 4% Al	55	55

* Hardness of TiNi material (55.1 w/o Ni) around 31 to 34 R_c

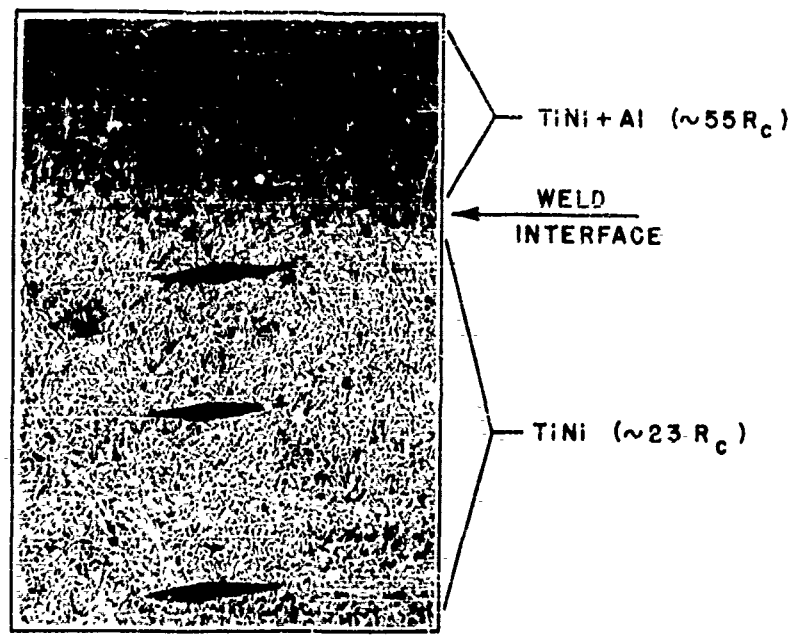

FIG. 36 PHOTOMICROGRAPH SHOWING THE TiNi BASE MATERIAL (BOTTOM) WITH AN OVERLAY OF ALUMINUM WELDED ON THE TOP. NOTE THE INCREASE IN HARDNESS IN THE FUSED AREA (TiNi+Al). ALL KNOOP HARDNESS INDENTATIONS WERE MADE USING 1.0 KG INDENTER LOAD.

CONCLUSIONS

1. The TiNi phase has been found to exist at room temperature.

2. Stoichiometric TiNi composition alloys usually have minor quantities of the phases Ti_2Ni and/or $TiNi_3$ present at room temperature.

3. Alloys which exist as TiNi or predominantly TiNi exhibit ductility and impact resistance at room temperature and below.

4. The difficulty in obtaining a completely TiNi material indicates the narrowness of the TiNi homogeneity range at lower temperatures.

5. The mechanical vibration damping properties of the TiNi alloy (54.5 w/o Ni) appear to be directly related to the TiNi phase purity. High TiNi phase purity yields a low damping characteristic while the presence of minor impurity phase(s) promote high damping.

6. The TiNi phase equilibria, and in turn the damping-to-non-damping transition temperatures, are affected by hot working and the presence of minor quantities of iron. Hot working promotes the formation of minor impurity phases and results in raising the transition temperature. While iron, present in quantities up to about 0.09 w/o, tends to stabilize the TiNi phase to lower temperatures and results in lowering the damping transition temperature.

7. TiNi alloys, because of their fine cast grain size, possess unusual ductility and toughness even in the arc-cast condition.

8. Nickel-rich TiNi alloys, containing about 60 to 62 w/o Ni, are hardenable by a quenching treatment.

9. Slow cooling alloys containing from 55 to 60 w/o Ni produces a uniform hardness of about 35 R_C (the TiNi matrix hardness).

10. Intermediate hardness levels, between quenching and slow cooling, are possible in the nickel-rich alloys by performing pseudo-tempering treatments on the quenched material.

11. Permeability and susceptibility measurements show TiNi and nickel-rich TiNi alloys to be paramagnetic. This low permeability value (< 1.002) remains unchanged by working, heat treatment and substantial temperature

variation.

12. Hot hardness curves for rapidly cooled TiNi alloys show a "secondary hardening peak" which seems to be related to an ordering change.

13. Based upon hot hardness and oxidation resistance the TiNi alloys appear to be suitable for elevated temperature application up to 1200°F (649°C).

14. The nickel-rich TiNi alloys (rapidly cooled) have superior hot hardness in the lower temperature range.

15. Based upon both quantitative and qualitative data the corrosion and abrasion resistance of TiNi alloys is excellent.

POSSIBLE FUTURE WORK ON THE TiNi TYPE ALLOYS

The following itemized list gives in a general way areas which the present investigators feel should be investigated more thoroughly. This list includes:

1. Additional comprehensive study into the kinetics of the phase transformations, particularly the $TiNi \rightleftharpoons Ti_2Ni + TiNi_3$ at temperatures around ambient.

2. Investigate thoroughly the mechanism of the TiNi dissociation into Ti_2Ni and $TiNi_3$ during polishing and/or deep etching. A possible experimental approach might be internal friction studies on variously polished and etched wire specimens.

3. High temperature X-ray diffraction studies on TiNi-type alloys, room temperature up to about 1100°C (2012°F), to understand better the phase-equilibria and order-disorder transformations at the higher temperatures.

4. Also study order-disorder transformations as a function of temperature by using the specific heat method given by Lipson[20]. The range of particular interest being around 800 to 900°F (427 to 482°C).

5. Investigate further into a possible transpiration-type cooling which may be produced by the partial fusion of Ti-rich TiNi alloys.

6. Completely determine the mechanical properties of the 60 Ni - 40 Ti alloy after quench-hardening and after various pseudo-tempering treatments.

7. Determine the hardenability factor for quench-hardened 60 Ni - 40 Ti alloy. Sectioned large quenched rounds appear to be the simplest method of getting quantitative data on this parameter.

8. Conduct further studies into the effects of alloying elements when added to the TiNi composition alloy.

9. Study the effects of the extraneous phase(s) of Ti_2Ni and/or $TiNi_3$ on the mechanical properties of the TiNi alloy. This can be accomplished by cooling TiNi (54.5 w/o Ni) tensile specimens below ambient temperature, even as low as -196°C (Liquid N), warm quickly to room temperature and measure the tensile properties. Monitor precipitated extraneous phases by X-ray diffraction (see Fig. 6).

10. Investigate carefully controlled TiNi welded sections to determine the mechanical and magnetic properties attained in the weld and surrounding areas.

11. Continue studies into the corrosion resistance of TiNi-type alloys to common corroding media.

Some of the above suggested investigations on the TiNi-type alloys are currently being performed at the U. S. Naval Ordnance Laboratory and will be subsequently reported.

POSSIBLE APPLICATIONS

The predominantly TiNi phase material and the TiNi-base alloys (containing up to about 7 w/o excess Ni) possess many desirable inherent properties. Based upon these properties and characteristics, Table XI gives a list of possible applications as a function of some of the properties required.

TABLE XI. POSSIBLE APPLICATIONS FOR TiNi AND TiNi-BASE ALLOYS

POSSIBLE APPLICATIONS	PROPERTIES AND CHARACTERISTICS OF TiNi AND TiNi-BASE ALLOYS												
	Paramagnetic ($\mu < 1.002$)	Corrosion Resistance	Lower Density	Hardening Capability	Temperature-Sensitive Damping	Room Temp. and Elevated Temp. Strength and Hardness	Room Temp. Ductility and Toughness	Improved Impact Strength at Lower Temps.	Oxidation Resistance	Abrasion Resistance	Lustrous Surface after Polishing and Buffing	Ease of Welding (heli.c)	Ease of Hot Forging and Working
Non-magnetic tools for mine disposal work	X	X		X		X	X					X	X
Sensing devices	X				X								
Underwater Ordnance, e.g., mine cases, mine components, etc.	X	X				X	X			X		X	
Elevated temperature components, up to 1000°F (538°C)						X	X		X			X	X
Chemical handling equipment		X				X	X			X		X	X
Space and aircraft components			X			X	X	X	X			X	X
Magnetic-mine craft parts, sweeping and servicing	X	X	X			X	X					X	X
Stainless cutlery		X		X						X	X		
Decorative and jewelry uses, e.g., auto trim, non-magnetic watch parts, etc.		X					X			X	X	X	X

REFERENCES

1. Metals Handbook, American Society for Metals, Cleveland, Ohio, 8th Edition, 1961

2. Structure of Metals, C. S. Barrett, McGraw-Hill, New York, 1952

3. Atomic Theory for Students of Metallurgy, William Hume-Rothery, The Institute of Metals, London, 1948

4. Mechanical Properties of Intermetallic Compounds, Edited by J. H. Westbrook, Wiley & Sons, Inc., 1959

5. W. A. Maxwell and E. M. Grala, "Investigations of Nickel-Aluminum Alloys Containing from 14 to 34 Percent Aluminum," NACA Tech. Note 3259, Aug. 1954

6. E. M. Grala, "Investigation of the NiAl Phase of Nickel-Aluminum Alloys," NACA Tech. Note 3828, Jan. 1957

7. R. L. Wachtell and W. H. Herz, "An Investigation of Various Properties of NiAl, " WADC Tech. Report 52-291, Part I (1952), Part II (1954), Part III (1955)

8. R. D. Grinthal, "New High Temperature Intermetallic Materials," WADC Tech. Report 53-190, Part V, (1956), Part VI, (1958)

9. Constitution of Binary Alloys, Max Hansen, McGraw-Hill Book Co., 2nd Edition, 1958

10. P. Duwez and J. L. Taylor, Trans. AIME, 188 1950, 1173-1176

11. D. M. Poole and W. Hume-Rothery, J. Inst. Metals, 83, 1955, 473-480

12. H. Margolin, E. Ence, and J. P. Nielsen, Trans. AIME, 197, 1953, 243-247

13. T. V. Philip and P. A. Beck, Trans. AIME, 209, 1957, 1269-1271

14. P. Pietrokowsky and F. G. Youngkin, J. Appl. Physics, Vol. 31, No. 10, Oct. 1960, pgs 1763-1766

15. H. G. Van Bueren, "Imperfections in Crystals," North-Holland

Publishing Co., Amsterdam, 1960

16. Bruce Chalmers, "Physical Metallurgy," John Wiley and Sons, Inc., 1959

17. C. Sachs and K. R. Van Horn, "Practical Metallurgy," American Society for Metals, Cleveland, 1947

18. J. K. Stanley, "Metallurgy and Magnetism," American Society for Metals, Cleveland, 1948

19. A. H. Cottrell, "Theoretical Structural Metallurgy," Edward Arnold Ltd., London, 1957

20. H. Lipson, "Progress in Metal Physics (2)," Chapter 1, Butterworths Scientific Publications, 1950

21. G. R. Purdy and J. G. Parr, "A Study of the Titanium-Nickel System Between Ti_2Ni and TiNi," Transactions AIME, Vol. 221, June 1961, pg 636

ACKNOWLEDGMENT

The authors wish to express their gratitude to Mr. J. V. Gilfrich for X-ray diffraction studies and their interpretation. In addition, the authors wish to acknowledge the assistance of Mr. C. E. Sutton for the construction of special equipment and for measurements of various properties, and Mr. H. E. Eberly for alloy melting and fabrication.

APPENDIX

I. X-ray Diffraction Techniques

1. Room Temperature Studies

Fifteen gram alloy buttons approximately one-inch in diameter, melted and prepared as stated in Section II of Appendix, were used in these investigations. X-ray reflections were obtained from the prepared flat arc-cast bottoms of the buttons. For this investigation alloy buttons containing from 50 to 60 w/o Ni remainder Ti were used. In each case the prepared specimen was placed directly in the sample holder with the flat side up and at the center of the diffractometer focusing circle. A diffractometer scan was made from 10° to 50° (2θ) using Mo K_{α} radiation to determine which phase or phases (TiNi, Ti_2Ni or $TiNi_3$) were present. Based upon the peak height of the strongest lines, as measured by a Krypton Geiger tube, a fairly accurate quantitative determination of the amounts of each phase could be made. The measured phase quantity also took into account the preferred orientation present in the cast specimens.

Samples which had TiNi phase present were further studied to determine the lattice parameter of this phase and ascertain the effects of excess Ni or Ti on the lattice parameter. It was hoped through a study of this type to establish the boundaries of the TiNi phase region. To this end each significant peak was scanned at a slow speed using Fe K_{α} radiation (to displace peaks toward higher 2θ angles) and a lattice parameter determined for each peak. The average of these lattice parameters for each sample, or a value obtained by extrapolating ($\sin^2 \theta$ to $\theta = 90°$) was plotted against weight percent Ni.

The lattice parameter obtained for TiNi of 3.015 Å agreed with previous investigators. However, scatter in the lattice parameter data for non-stoichiometric alloys, rich in Ti or Ni, made precise location of the

TiNi phase boundaries uncertain. As a result, these data were not included in this report. Other metallurgical investigations, e.g., metallography, internal friction, hardness, etc., reported in this report show the metastable nature of the TiNi phase and help to show why the lattice parameter data could not reveal the precise TiNi phase boundaries.

2. Studies Above and Below Room Temperature

The same equipment was used for this investigation that was used for the room temperature studies. This included a standard Norelco diffraction unit equipped with a Krypton Geiger tube and molybdenum X-ray tube. Molybdenum K_{α} radiation was used throughout these studies.

A special sample holder was constructed of copper through which the heating or cooling medium (liquid or gas) could be pumped. This holder was attached to the diffractometer in the same manner as the standard flat Norelco sample holder. A hole was milled in the radiation shield for the inlet and outlet tubing which conducts the temperature controlling medium.

The sample, as before, was a 15 gram arc-melted button of the 54.5 w/o Ni composition. This button was ground to a width of 3/4 inches and a thickness about 0.200 inches making it possible for the specimen to fit the copper sample holder and place the specimen surface at the center of the focusing circle. Finally, a thermocouple was placed in contact with the sample surface at a point out of the X-ray beam. With this thermocouple, specimen temperatures were monitored throughout the runs.

In running at temperatures up to about 85°C no problems were encountered. Heated water, at a constant temperature, was used as the heating medium. Cooling down to 3°C was accomplished by circulating ice water through the system. Temperatures below about 3°C were produced by circulating alcohol cooled by dry ice or nitrogen gas cooled by liquid nitrogen. In addition, for all runs made below room temperature dry precooled nitrogen gas was directed over the sample surface to prevent either moisture or frost from forming. Using the above research setup the diffractometer scans shown in Fig. 6 were accomplished.

II. Alloy Melting and Sample Preparation

In order to investigate fully the titanium-nickel intermetallic compounds of TiNi, Ti_2Ni and $TiNi_3$, suitable alloys of closely controlled chemical composition and homogeneity had to be prepared. In view of the high titanium content, arc-melting in a water-cooled copper hearth or crucible was the most suitable method. This melting technique, employed by other

investigators[12] to prepare alloys for constitution studies, was found to produce inhomogeneities. However, in this investigation care was taken to produce chemically homogeneous melts by melting small specimens (usually buttons between 15 and 90 grams), using sufficient power to maintain almost the entire button molten, and multiple melting of each specimen.

Employing the arc-melting furnace shown in Fig. 37, the titanium-nickel alloys around the TiNi composition, arc-melted without difficulty. Losses, due to vaporization of the component metals, were found by checking weight to be negligible. All X-ray diffraction samples, for constitution studies, were made small (about 15 gram buttons) to insure chemical homogeneity. When larger melts were required for mechanical property specimens, these were produced in a two-step process. First, well mixed buttons of the desired composition were thoroughly melted and alloyed by non-consumable arc-melting. These buttons were then arc-cut into smaller segments and charged a few at a time to a water-cooled copper crucible measuring about 2 1/2" in diameter x 2 1/2" deep. The charged segments of button melts were then non-consumably melted. Following this, new segments were charged and completely fused into the previously melted portion of the ingot. In this manner it was possible to produce a monolithic ingot weighing about 1 1/2 pounds which was homogeneous in composition and free of any seams. The upper left photomicrograph of Fig. 18 shows a typical TiNi arc-cast material, while Figs. 19 and 20 show the arc-cast Ti_2Ni and $TiNi_3$ structures respectively.

As was mentioned earlier in the report, the TiNi and TiNi-base alloy compositions in most cases were found to be sufficiently ductile to be capable of being hot and cold worked directly from the arc-cast structure. As a result, almost all specimens employed in this investigation were arc-cast, hot rolled or hot swaged between 700°C and 1050°C, cold rolled where necessary at room temperature, machined and ground to final specimen dimensions. Fig. 18 shows effects upon an "as cast" 55.1 w/o Ni alloy when rolled hot and cold. Hot rolling at 700°C, which is about 100°C above the recrystallization temperature (see Fig. 32) has the effect of eliminating the cast dendritic structure while promoting the coalescence of particles of a second phase. Hot rolling at 1100°C, which is near the solidus temperature for this alloy composition, causes the complete elimination of the dendritic structure and coalesces the second phase particles in a fairly uniform distribution. X-ray diffraction studies confirm the existence of the second phase(s) in an alloy of this composition

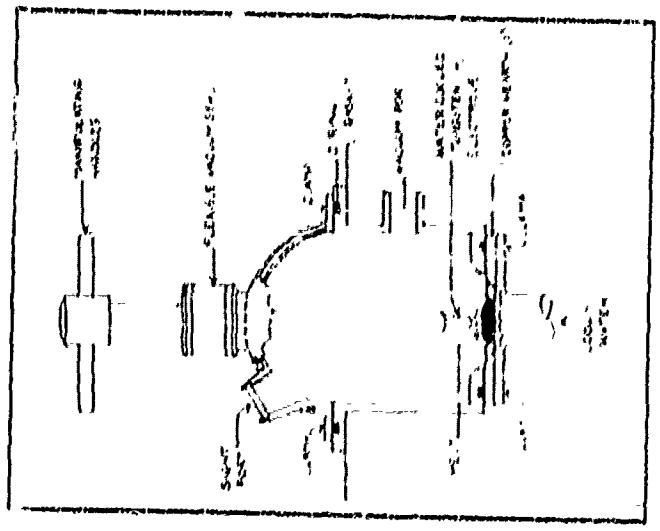

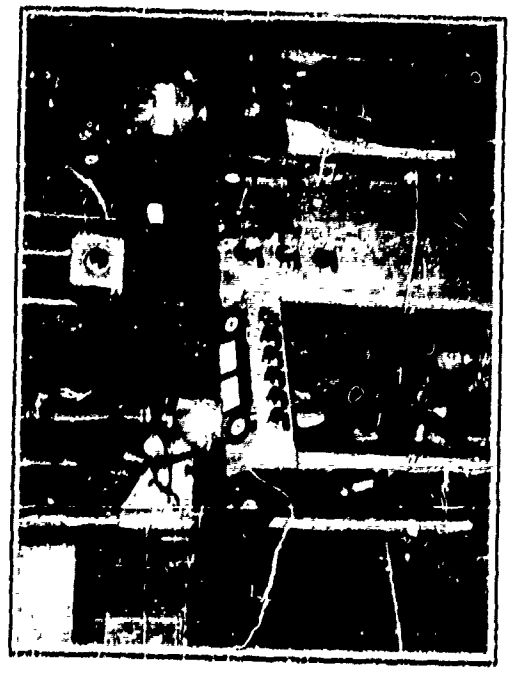

FIG. 37 PHOTO AT LEFT SHOWS THE ARC- MELTING FURNACE INCLUDING CONTROL CONSOLE, HIGH FREQUENCY STARTER, VACUUM GAUGE, AND D.C POWER SUPPLY. AT RIGHT IS A SCHEMATIC VIEW OF MELTING CHAMBER EQUIPPED TO PERFORM NON-CONSUMABLE BUTTON MELTING.

Alloys close to the stoichiometric TiNi composition (52 to 56 w/o Ni) hot worked readily between about 900 to 1050°C. Slightly lower rolling temperatures were required for the titanium rich alloys (52 to 54 w/o Ni) because of the lower solidus temperature for these alloys. When the nickel content is increased in excess of 57 w/o hot working problems arise. As mentioned previously, there exists a retro-grade solid solubility change between the TiNi phase area and the TiNi + $TiNi_3$ two-phase area between 900°C and the solidus line, which occurs at about 1115°C. As a result, Ni-Ti alloys containing about 57 w/o or more Ni, heated above 900°C, undergo changes in the quantity of the existing phases. This change in the quantity of TiNi and $TiNi_3$ is dependent upon the heating temperature. Hot rolling investigations were performed on 57 and 60 w/o Ni alloys under various conditions, taking into consideration the above solid solubility changes. The results of these investigations are shown in Figs. 38 and 39. It can be seen from these figures that the best results were obtained either by rolling at 900°C or precipitating from solution the excess nickel, probably as $TiNi_3$, prior to rolling at 850°C. In the latter case the excess $TiNi_3$ probably was precipitated as innocuous particles in a TiNi matrix. Though this TiNi matrix is on the nickel-rich side it still permits hot deformation. In the case of the 60 Ni - 40 Ti alloy most cracking occurs during the initial passes through the mill. This problem may in part be eliminated in the future by breaking down the arc-cast structure by hot extrusion.

Following hot rolling it was found that the principally TiNi alloys could be cold rolled at room temperature. The bottom right photomicrograph of Fig. 18 shows the typical rolling texture obtained by rolling TiNi below the recrystallization temperature.

The various specimens employed in the physical, mechanical, and constitution studies were alloyed, cast, hot and cold worked as stated above. In the case of the X-ray specimens, these were prepared as 15 to 20 gram buttons to provide chemical homogeneity. The bottom sides of these arc-melted buttons were ground and diamond abrasive polished. Most of the X-ray samples were satisfactory "as polished" or after being given a light etch. Heavy etching with the HNO_3 + HF solution caused a partial dissociation of the TiNi phase into Ti_2Ni and $TiNi_3$. This is explained more completely in the X-ray diffraction section of this report.

Initially, the TiNi and TiNi-base alloys were difficult to machine by conventional techniques. This was found to be due to the high hardness (29 to 35 R_c) coupled with the rapid work hardening of the machined surfaces. Figs. 2 and 3 show the martensite-like layer that is formed during polishing. With continued machining studies it was found that turning and milling could be accomplished by employing sharp carbide tools. During machining care

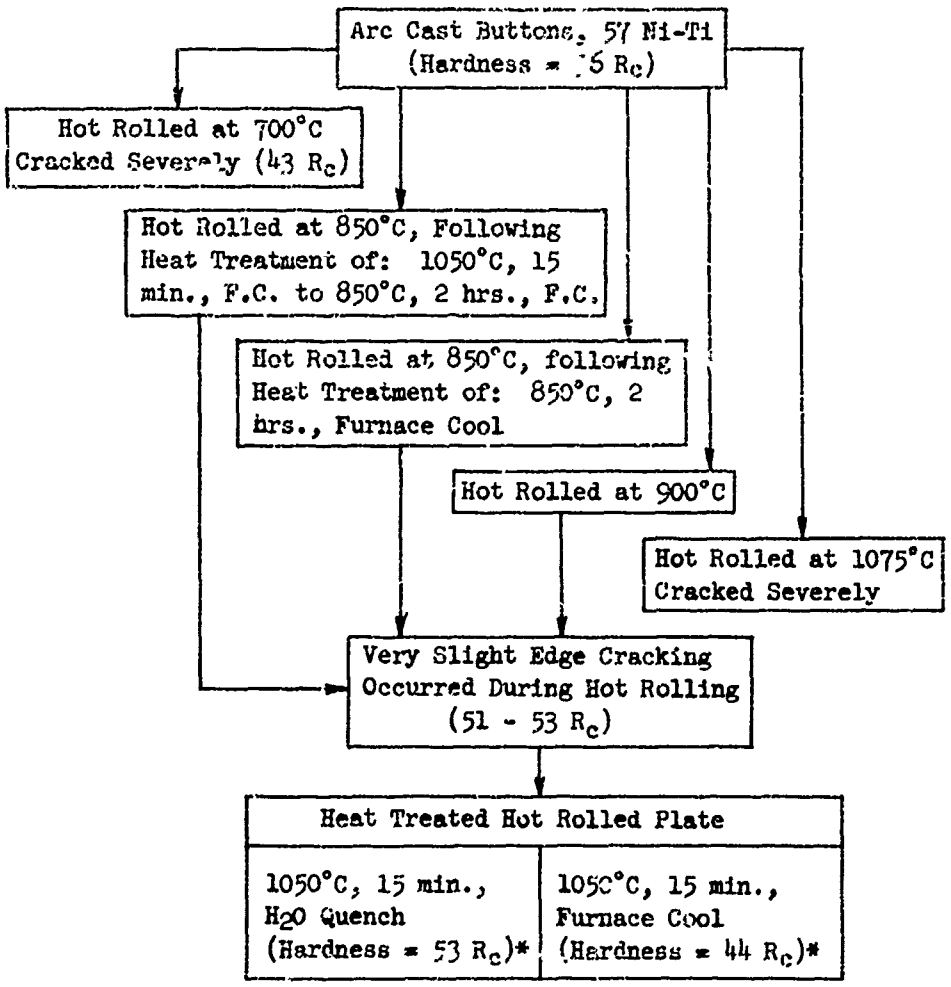

* Results from heat treatment of hot rolled plate less predictable than the 60 Ni-Ti alloy. Audible clicking noise from this alloy when major load is applied to hardness indenter.

Figure 38. Hot Rolling Studies to Determine Hot Working Characteristics of Arc-Melted 57 w/o Ni-Ti Alloy

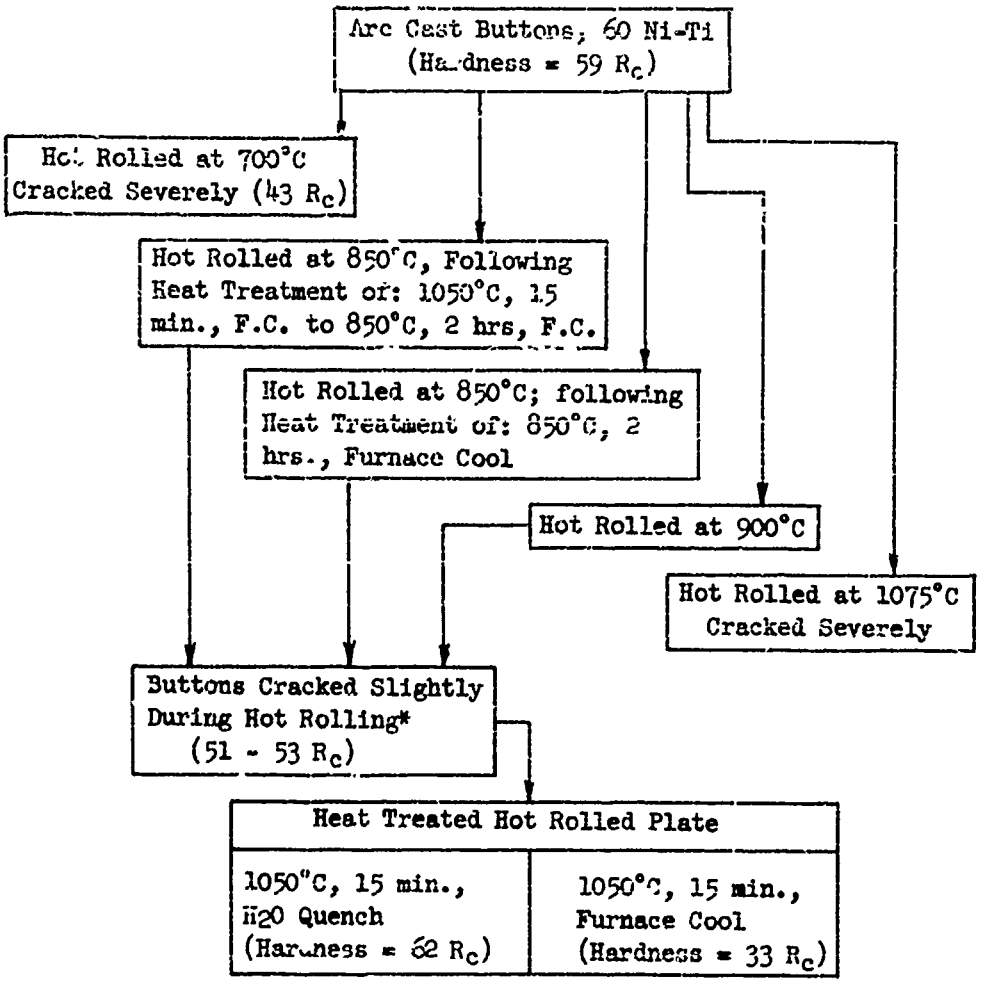

* Most of cracking occurring during initial passes through mill

Figure 39. Hot Rolling Studies to Determine Hot Working Characteristics of Arc-Melted 60 w/o Ni-Ti Alloy

must be exercised to avoid "glazing" the surface with a dull tool. If these local work-hardened areas form on the machined surface serious machining problems are encountered during the following cuts.

Sawing, using a tool steel saw blade, was very unsatisfactory. The cut surface work-hardened almost immediately preventing further cutting. Cutting the TiNi alloy into segments was accomplished by using a resin bonded cut-off wheel and a copious supply of water coolant. The cut surfaces were free of any apparent heat checks.

Grinding surfaces of X-ray and mechanical test specimens was performed without incident. Water cooling was used during grinding. In the case of the mechanical test specimens the ground surfaces were finish lapped readily to a mirror-like finish.

Wire drawing was accomplished on the 54.5 and 55.1 w/o Ni alloys. The starter material for wire drawing was a hot swaged rod about 0.115 inches in diameter. Any oxide surface coating was removed by sanding with emery cloth. The wire was annealed between diameters of 0.115 and 0.035 inches, following each die pass, by passing an electric current through the wire until a dull red heat was obtained. This annealing was essential because of the rapid rate of work hardening in these alloys. From 0.035 to smaller diameters two passes were made before annealing was required. A thick soap solution was used as a die lubricant.

III. Electrical Resistivity Measurements

1. Near Room Temperature

The samples employed for measuring electrical resistivity in this report were, in every case, hot rolled and slit strips about 0.010" thick x 0.125" to 0.186" wide x about 5.5" (≈ 14 cm) long. The surfaces of the specimens were carefully prepared to provide the optimum electrical contact. The potential leads were fastened by pressure at a distance of 10 cm apart. The current leads were similarly fastened to the strip outside the potential leads. A small current of about 7 milliamps was passed through the specimen for short durations to prevent resistance heating of the specimen.

Resistivity was measured by using a standard method which incorporated a highly sensitive type K-3 potentiometer into the measuring circuit. The high sensitivity of this potentiometer was needed in order to measure the small resistivity changes experienced with small temperature

variations. The actual resistivity was calculated from the equation:

$$\rho = \frac{RA}{\ell}$$

where ρ = electrical resistivity, ohm-cm

R = electrical resistance between potential leads, ohms

A = cross-sectional area of specimen, cm^2

ℓ = distance between potential leads, cm

The test temperature was carefully monitored by appropriate chromel-alumel thermocouples. To induce temperatures below room temperature the entire device, including sample and holder, was placed in a refrigerator. Constant temperature, around the level desired, was attained in the sample prior to measuring the voltage drop. The same system was applied to measurements made slightly above room temperature (up to about 210°F). In the latter case a controlled low temperature oven was used as a heat source. Again, as in the sub-ambient temperature measurements, the strip specimen was allowed to stabilize at a given temperature prior to making any voltage drop readings.

For these studies, where the temperature varied between about -70°F and 210°F, no effort was made to control the testing atmosphere. Thus the atmosphere used was an air atmosphere with naturally varying humidity.

2. Elevated Temperature Measurements

Electrical resistivity measurements were made at elevated temperatures up to 900°C by placing the strip specimens, with spot-welded current and potential leads, in a controlled atmosphere system. The overall system consisted of a long quartz tube sealed on one end and fitted on the other end with a vacuum-tight brass header. The brass header contained the vacuum tight electrical connections and suitable valves for evacuating the tube and header and reintroducing dry helium or argon gas. After evacuating the flushing with the inert gas several times the tube and header are filled with the inert gas and the gas was made to flow at a very low rate through the chamber during the run.

The actual voltage-drop measurements were made on the same K-3 potentiometer and circuitry as employed for the lower temperature studies.

Spot welding was required in order to fasten the platinum current and potential leads onto the specimen and maintain them in close contact with the specimen up to 900°C. The resulting TiNi-Pt couple produced voltages at various temperatures that had to be considered in the measurement of the actual voltage-drop of the specimen. An example of the magnitude of this generated EMF as a function of test temperature for a TiNi-Pt couple can be seen in Fig. 40. Table III shows the TiNi-Pt couple compensations employed to obtain the actual voltage-drop in a 55.1 w/o Ni alloy strip at various temperatures.

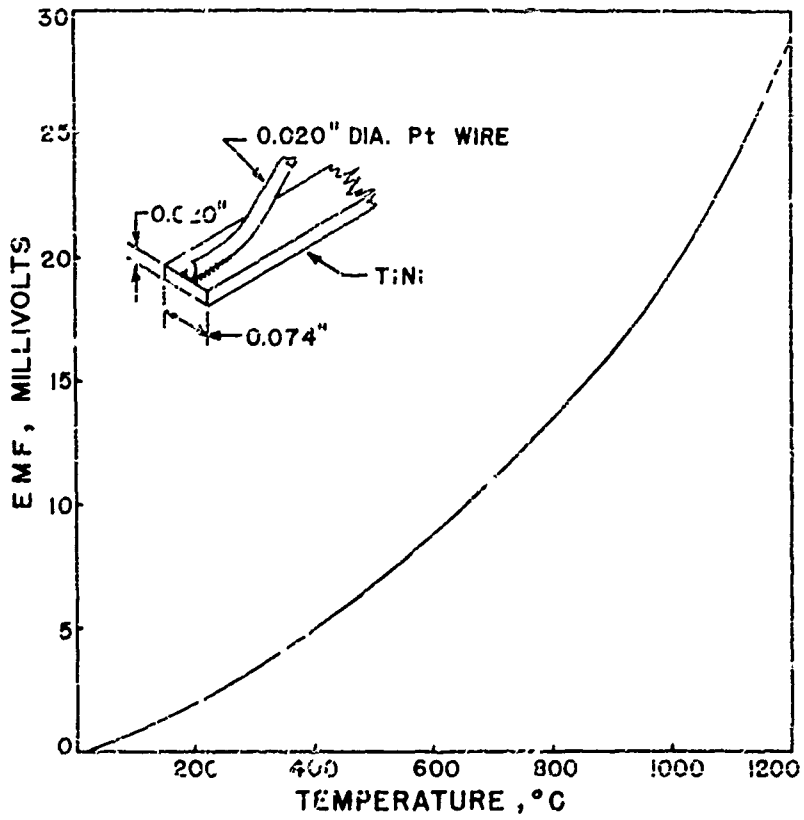

FIG. 40 CURVE SHOWING EMF GENERATED AT VARIOUS TEMPERATURES IN THE TiNi - Pt COUPLE SHOWN IN THE INSET

DISTRIBUTION

	Copies
Chief, Bureau of Naval Weapons	
Code RRMA (N. E. Promisel)	1
Code RRMA-2 (T. Kearns)	1
Code RRMA-22 (H. J. Boertzel)	1
Code RRMA-23 (T. Hamill)	1
Code RRMA-24 (R. M. Custafson)	1
Code RUME-332 (W. E. Gaines)	1
Code RUME-343 (G. M.Studds)	1
Code RUDC-4 (C. C. Holstrom)	1
Code RUDC-44 (LCdr. R. L. Miller)	1
Library (DLI)	1
Chief, Bureau of Ships	
Code 337 (G. Sorkin)	1
Code 69181 (J. Kerr, Jr.)	1
Code 634B (F. Early)	1
Code 362B (L. Stoffert)	1
Technical Library	1
Armed Services Technical Information Agency	10
Arlington Hall	
Arlington, Virginia	
Office of Naval Research	
Washington 25, D. C.	
Attn: E. I. Salkowitz, Rm. 2516, T-3	1
Director, Naval Research Laboratory	
Technical Library	1
B. F. Brown	1
Leland A. DePue	1
R. A. Huber	1
E. J. Chapin	1
Chief of Naval Operations	
Washington 25, D. C.	
Library	1
New Developments & Op. Eval. Div.	1

Officer in Charge, Naval Air Development Center
Johnsville, Pennsylvania
Attn: W. S. Lee 1
J. Martin 1
Library 1

Commanding Officer, U. S. Army Signal
Research & Development Lab.
Fort Monmouth, New Jersey
Attn: Eberhard Both 1
Library 1

Director, National Bureau of Standards
Washington, D. C.
Attn: Library 1
I. S. Cooter 1
T. G. Digges 1

Office of Technical Services 100
Department of Commerce
Washington 25, D. C.
Dorothy W. Graf 10

Defense Metals Information Center 1
Battelle Memorial Institute
Columbus 1, Ohio

Director, David Taylor Model Basin
Washington 7, D. C.
Attn: A. R. Willner 1

Naval Engineering Experimental Station
Annapolis, Maryland
Attn: W. C. Stewart 1

Office of Naval Material
Washington 25, D. C.
Attn: W.D. Barlow 1

Special Projects Office
Bureau of Naval Weapons
Attn: H. Bernstein 1

National Academy of Sciences
Materials Advisory Board
Washington 25, D. C.
Attn: J. R. Lane — 1

National Aeronautical and Space Agency
1512 H Street, N.W.
Washington 25, D. C.
Attn: H. Hessing — 1
E. E. Stauss — 1
A. Piltch, Code 330 — 1

National Aeronautical and Space Agency
Structures Research Laboratory
Langley Research Center
Langley Field, Virginia — 1

Commander, Ordnance Materials Research Office
Watertown Arsenal
Watertown 72, Mass. — 1

Naval Air Material Laboratory
Philadelphia, Pennsylvania
Attn: J. F. Bowen, Air Materials Lab. — 1

Naval Air Missile Test Center
Point Mugu, California
Attn: Library — 1

Naval Ordnance Laboratory
Corona, California
Attn: Library — 1

U. S. Bureau of Mines
Dept. of Interior
Washington 25, D.C.
Attn: E. T. Hayes — 1

Commander, Wright Air Development Center
Air Research & Dev. Command
U. S. Air Force
Wright-Patterson Air Force Base, Ohio
Attn: Library — 1

Naval Ordnance Laboratory, White Oak, Md. (NOL technical report 61-75)
THE PROPERTIES OF TiNi AND ASSOCIATED PHASES (U), by W.J. Buehler and R.C. Wiley. 3 Aug. 1961. 91p. tables., diagrs. Projects PR-7, RRMA 02009/212 1/R007 06 001, RUUC-3-E-231/212 1/F008-12-002. UNCLASSIFIED

Investigations were made into the phase equilibria, physical and mechanical properties of the ductile intermetallic compound TiNi and associated compounds Ti_2Ni and $TiNi_3$. Measurements of internal friction, electrical resistivity, hardness, impact strength, oxidation and corrosion resistance, magnetic permeability and susceptibility, dilation, etc., were made on the TiNi and TiNi-base alloys. These data are presented along with discussion relating the property data with the existing phase equilibria. Information on hardenable Ni-rich alloys, with hardnesses up to 62 R_c, is given.

1. Titanium-nickel alloys
2. Nitrinols
I. Title
II. Buehler, William J.
III. Wiley, Raymond C., jt. author
IV. Project
V. Project
VI. Project

Abstract card is unclassified

Naval Ordnance Laboratory, White Oak, Md. (NOL technical report 61-75)
THE PROPERTIES OF TiNi AND ASSOCIATED PHASES (U), by W.J. Buehler and R.C. Wiley. 3 Aug. 1961. 91p. tables., diagrs. Projects PR-7, RRMA 02009/212 1/R007 06 001, RUUC-3-E-231/212 1/F008-12-002. UNCLASSIFIED

Investigations were made into the phase equilibria, physical and mechanical properties of the ductile intermetallic compound TiNi and associated compounds Ti_2Ni and $TiNi_3$. Measurements of internal friction, electrical resistivity, hardness, impact strength, oxidation and corrosion resistance, magnetic permeability and susceptibility, dilation, etc., were made on the TiNi and TiNi-base alloys. These data are presented along with discussion relating the property data with the existing phase equilibria. Information on hardenable Ni-rich alloys, with hardnesses up to 62 R_c, is given.

1. Titanium-nickel alloys
2. Nitrinols
I. Title
II. Buehler, William J.
III. Wiley, Raymond C., jt. author
IV. Project
V. Project
VI. Project

Abstract card is unclassified

Naval Ordnance Laboratory, White Oak, Md. (NOL technical report 61-75) THE PROPERTIES OF TiNi AND ASSOCIATED PHASES (U), by W.J. Buehler and R.C. Wiley. 3 Aug. 1961. 91p. tables., diagrs. Projects PR-7, RRMA 02009/212 1/R007 06 001, RUUO-3-E-23 /212 1/F008-12-002. UNCLASSIFIED

Investigations were made into the phase equilibria, physical and mechanical properties of the ductile intermetallic compound TiNi and associated compounds Ti_2Ni and $TiNi_3$. Measurements of internal friction, electrical resistivity, hardness, impact strength, oxidation and corrosion resistance, magnetic permeability and susceptibility, dilation, etc., were made on the TiNi and TiNi-base alloys. These data are presented along with discussion relating the property data with the existing phase equilibria. Information on hardenable Ni-rich alloys, with hardnesses up to 62 R_c, is given.

1. Titanium-nickel alloys
2. Nitrinols
I. Title
II. Buehler, William J.
III. Wiley, Raymond C., jt. author
IV. Project
V. Project
VI. Project

Abstract card is unclassified

Naval Ordnance Laboratory, White Oak, Md. (NOL technical report 61-75) THE PROPERTIES OF TiNi AND ASSOCIATED PHASES (U), by W.J. Buehler and R.C. Wiley. 3 Aug. 1961. 91p. tables., diagrs. Project PR-7, RRMA 02009/212 1/R007 06 001, RUUO-3-E-231/212 1/F008-12-002. UNCLASSIFIED

Investigations were made into the phase equilibria, physical and mechanical properties of the ductile intermetallic compound TiNi and associated compounds Ti_2Ni and $TiNi_3$. Measurements of internal friction, electrical resistivity, hardness, impact strength, oxidation and corrosion resistance, magnetic permeability and susceptibility, dilation, etc., were made on the TiNi and TiNi-base alloys. These data are presented along with discussion relating the property data with the existing phase equilibria. Information on hardenable Ni-rich alloys, with hardnesses up to 62 R_c, is given.

1. Titanium-nickel alloys
2. Nitrinols
I. Title
II. Buehler, William J.
III. Wiley, Raymond C., jt. author
IV. Project
V. Project
VI. Project

Abstract card is unclassified

Naval Ordnance Laboratory, White Oak, Md. (NOL technical report 61-75) THE PROPERTIES OF TiNi AND ASSOCIATED PHASES (U), by W.J. Buehler and R.C. Wiley. 3 Aug. 1961. 91p. tables., diagrs. Projects PR-7, RRMA 02009/212 1/R007 06 001, RUUO-3-E-231/212 1/F008-12-002. UNCLASSIFIED

Investigations were made into the phase equilibria, physical and mechanical properties of the ductile intermetallic compound TiNi and associated compounds Ti_2Ni and $TiNi_3$. Measurements of internal friction, electrical resistivity, hardness, impact strength, oxidation and corrosion resistance, magnetic permeability and susceptibility, dilation, etc., were made on the TiNi and TiNi-base alloys. These data are presented along with discussion relating the property data with the existing phase equilibria. Information on hardenable Ni-rich alloys, with hardnesses up to 62 R_c, is given.

1. Titanium-nickel alloys
2. Nitrinols
I. Title
II. Buehler, William J.
III. Wiley, Raymond C., jt. author
IV. Project
V. Project
VI. Project

Abstract card is unclassified